An Acousto-Ultrasonic System for the Evaluation of Composite Materials

by

Michael T. Kiernan

Thesis submitted to the Faculty of the

Virginia Polytechnic Institute and State University

in partial fulfillment of the requirements for the degree of

Master of Science

in

Engineering Mechanics

APPROVED:

J. C. Duke, Jr., Chairman

E. G. Henneke, II

M. P. Singh

September 1986

Blacksburg, Virginia

An Acousto-Ultrasonic System for the Evaluation of Composite Materials

by

Michael T. Kiernan

J. C. Duke, Jr., Chairman

Engineering Mechanics

(ABSTRACT)

A presentation is given of an acousto-ultrasonic system for the evaluation of composite materials. First, a brief statement will be made on the acousto-ultrasonic technique and its relative worth compared to other nondestructive testing techniques as applied to composite materials. The following two chapters describe the system instrumentation and system software, respectively. Next, comments are given regarding the implementation of the system for research on graphite/epoxy laminates, with additional remarks concerning efforts to evaluate aluminum/graphite tubes with the system. This includes physical descriptions of the composite systems. Subsequently, results are presented comparing parameters and forms of presentation which can be employed to relate results. Finally, conclusions are made on the application of the acousto-ultrasonic system to nondestructive testing of composite materials, with specific results on its application to graphite/epoxy plates. More specifically, comments are made on the variation of SWF factors with azimuthal angle on the graphite/epoxy plates, the identification of specific frequency peaks, and the relationships these may have to certain modes of vibration and material properties. For example, a low frequency mode was found to vary in a manner reminiscent of E_x and to show characteristics of an extensional Lamb wave. In general, results are presented and discussed in order to show how the system can be implemented to gain physical information on composite materials, such as the property of anisotropy.

Acknowledgements

The author would like to express his thanks to the following people for their contributions:

1. Dr. J. C. Duke, Jr. for providing the opportunity to work on the Stress Wave Factor project and for his guidance and technical assistance during the course of the research

2. Dr. J. C. Duke, Jr., Dr. E. G. Henneke, II and Dr. M. P. Singh for graciously serving on his committee

3. and NASA Lewis for providing financial support for the research

4. The members of the Materials Research Group for various forms of support

5. , , and for providing both technical assistance and lending an extra hand in the laboratory

6. , , , , and for their technical assistance

7. My parents for providing me with the opportunity to pursue higher education through both their moral and financial support

Table of Contents

Introduction 1

System Description 12

Introduction 12

Basic System Configuration 12

Pulser 16

Transducers 19

Preamplifier 21

Computer and Data Acquisition System 22

System Software 24

Introduction 24

Analysis 26

Computer Program 36

System Implementation 52

Introduction 52

Application to Al/Gr Tubes 54
Description of Al/Gr Tubes 54
Experimental Procedure for Al/Gr Tubes 56
Application for Graphite/Epoxy Plates 60
Experimental Procedure for Graphite/Epoxy Plates 60
Phase One Experiments 60
Phase Two Experiments 69
Phase Three Experiments 69

Results 71
Al/Gr Tube Results 71
Graphite/Epoxy Plate Results 79
Description of Graphite/Epoxy Results 79
Results of Phase One 79
SWFs Versus Azimuthal Angle Results for Phase One and Two 84
Results For Phase Three 112
Summary 112

Discussion of Results 120
Introduction 120
Aluminum/Graphite Tube Conclusions 121
Graphite/Epoxy 122
Phase One 122
Variation of Output with Azimuthal Angle for Phase One and Two 124
Effect of Delamination on Results 127

Conclusions 129
Conclusions on the Specific System and its Applications 129

Conclusions on System and Method 132

Appendix A. SWF Values for Mechanically Loaded and Virgin Tubes **134**

Appendix B. Comparison of Theoretical and Experimental Wave Velocities **136**

Appendix C. Program Listing **138**

References **151**

Vita **153**

List of Illustrations

Figure 1. Diagram of original SWF configuration 6
Figure 2. SWF as a failure location predictor 7
Figure 3. SWF as a fatigue damage indicator 9
Figure 4. Change in Spectrum as a result of fatigue damage 10
Figure 5. Picture of present system 13
Figure 6. Picture of spacing fixture 15
Figure 7. Power spectrum for low damping pulse setting 17
Figure 8. Power spectrum for high damping pulse setting 18
Figure 9. Transducer transfer function 20
Figure 10. Definition of parameter D 30
Figure 11. Example frequency spectrum 32
Figure 12. Calculation of SWF parameters 34
Figure 13. Block diagram of software 37
Figure 14. Input spectrum for low damping 42
Figure 15. Output spectrum for low damping 43
Figure 16. Transfer function for low damping 44
Figure 17. Input spectrum for high damping 45
Figure 18. Output spectrum for high damping 46
Figure 19. Transfer function for high damping 47
Figure 20. Power spectrum for relatively undamaged specimen 48
Figure 21. Power Spectrum for heavily damaged specimen 49

Figure 22. Coherence function for undamaged specimen spectrum over damaged specimen spectrum 50

Figure 23. Picture of tube 55

Figure 24. Fixture for length wise acousto-ultrasonic application 57

Figure 25. Fixture for Circumferential acousto-ultrasonic application 59

Figure 26. Definition of azimuthal angle on gr/ep plates 61

Figure 27. Plot of E_x as a function of azimuthal angle 63

Figure 28. Plot of Q_{11} as a function of azimuthal angle 64

Figure 29. Plot of ν_{xy} as a function of azimuthal angle 65

Figure 30. Plot of $\mu_{xy,x}$ as a function of azimuthal angle 66

Figure 31. Plot of G_{xy} as a function of azimuthal angle 67

Figure 32. Virgin tube a)Region with clad overlay b)Region without clad overlay 72

Figure 33. Loaded tube a)Region with clad overlay b)Region without clad overlay 73

Figure 34. SWF1 versus circumferential region for lengthwise SWF of loaded tube 75

Figure 35. SWF2 versus circumferential region for lengthwise SWF of unloaded tube 76

Figure 36. SWF2 versus circumferential region for circumferential SWF of unloaded tube . . 77

Figure 37. SWF1 versus length region for lengthwise SWF of unloaded tube 78

Figure 38. Spectrum for 4-ply zero degree laminate 80

Figure 39. Spectrum for 8-ply zero degree laminate 81

Figure 40. Spectrum for end part of the wave train from 8-ply zero degree laminate 82

Figure 41. Spectrum as seen with receiving transducer on bottom of laminate 83

Figure 42. Output spectrum for ten MHz sending transducer 85

Figure 43. Output spectrum with no pressure applied in area between transducers 86

Figure 44. Output spectrum with pressure applied in area between transducers 87

Figure 45. [0,0,0,0] time/voltage plot 0 degree direction 88

Figure 46. [0,0,0,0] spectrum for zero degree direction 89

Figure 47. [0,0,0,0] time/voltage for twenty degree direction 90

Figure 48. [0,0,0,0] spectrum for twenty degree direction 91

Figure 49. [0,0,0,0] time/voltage for ninety degree direction 92

Figure 50. [0,0,0,0] spectrum for ninety degree direction 93
Figure 51. [0,0,0,0] SWF1 unfiltered as a function of azimuthal angle 95
Figure 52. [0,0,0,0] SWF1 filtered as a function of azimuthal angle 96
Figure 53. [0,0,0,0] SWF1 filtered as a function of azimuthal angle 97
Figure 54. [0,0,0,0] SWF2 unfiltered as a function of azimuthal angle 98
Figure 55. [0,0,0,0] SWF3/SWF4 unfiltered as a function of azimuthal angle 99
Figure 56. [90,0,0,90] time/voltage for zero degree direction 100
Figure 57. [90,0,0,90] spectrum for zero degree direction 101
Figure 58. [90,0,0,90] time/voltage for fifteen degree direction 102
Figure 59. [90,0,0,90] spectrum for fifteen degree direction 103
Figure 60. [90,0,0,90] time/voltage for 75 degree direction 104
Figure 61. [90,0,0,90] spectrum for 75 degree direction 105
Figure 62. [90,0,0,90] time/voltage for ninety degree direction 106
Figure 63. [90,0,0,90] spectrum for ninety degree direction 107
Figure 64. [90,0,0,90] SWF1 unfiltered as a function of azimuthal angle 108
Figure 65. [90,0,0,90] SWF1 filtered as a function of azimuthal angle 109
Figure 66. [90,0,0,90] SWF2 unfiltered as a function of azimuthal angle 110
Figure 67. [90,0,0,90] SWF3/SWF4 unfiltered as a function of azimuthal angle 111
Figure 68. [45,0,0,45] SWF1 unfiltered as a function of azimuthal angle 113
Figure 69. [45,0,0,45] SWF1 filtered as a function of azimuthal angle 114
Figure 70. [45,0,0,45] SWF2 unfiltered as a function of azimuthal angle 115
Figure 71. Delaminated SWF1 unfiltered as a function of azimuthal angle 116
Figure 72. Delaminated SWF1 filtered as a function of azimuthal angle 117
Figure 73. Delaminated SWF2 unfiltered as a function of azimuthal angle 118
Figure 74. Delaminated SWF3/SWF4 unfiltered as a function of azimuthal angle 119

Introduction

To meet the stringent design demands of expanding technology, there exists an urgent need for improved structural materials. Examples of where improvements can occur are:

1. Strength to weight ratio

2. Stiffness to weight ratio

3. Fatigue resistance

4. Thermal expansion properties

5. Overall design tailorability [ref. 1].

One avenue being pursued to realize the aforementioned improvements is to develope composite materials. Composite materials combine two or sometimes more materials together on a relatively macroscopic scale to achieve the improvements in structural materials demanded by technology. However, the added complication of combining the constituent materials in sometimes one step processes can introduce deleterious, yet not immediately detectable variations in the composite material. As an added concern, a high degree of reliability is essential for high technology applica-

tions, such as spacecraft, space structures and aircraft. Basically, high technology applications demand many of the characteristics realized in composite materials, yet require a degree of reliability beyond that of current processing techniques and predictive modeling methods. In addition, the complex energy absorbtion and damage mechanisms in composite materials yield complex internal damage states for loaded or impacted structural material and as a result greatly complicate the problem of damage detection. Thus, to fully exploit the virtues of composite materials for the high technology applications for which they are suited, there exists a need for reliable and well understood methods of damage detection which lead to useful interpretations.

Presently, a number of methods, known as nondestructive testing techniques, are being utilized to detect damage in composite materials. These techniques differ in a variety of ways, resulting in various advantages and disadvantages for a given technique. Basically, these techniques involve noting the relationship between various aspects of material behavior and the material state. Often, several techniques must be combined in order to obtain all the information desired on the amount of damage present in a material and the overall material state.

For example, one method often used in the laboratory is radiography. In general for composite materials, radiography involves the injection of a penetrant which is opaque to x-rays into the material prior to exposing the material and film to x-rays. Thus, the penetrant will flow into cracks, causing them to show up as unexposed areas on the radiograph. One advantage of the method is the high resolution of microdamage which is visible in radiographs. Additionally, the method yields results which are directly related to damage at various thicknesses, since the x-ray interacts with all material through the thickness. Consequently, direct interpretations can be made of certain results. For example, matrix cracks in a transverse ply would show up as lines in the transverse direction, making the mode of damage immediately identifiable. However, subtle problems can arise when one tries to extract exact information and a quantitative description of the damage which is evidenced in the radiographs. For instance, cracks in transverse plies and delaminations may be clearly revealed in a radiograph, but it is extremely difficult in many instances to say in exactly which ply the damage is present. Moreover, it is not immediately clear how the recognized damage is going

to interact mechanically, especially without any real information regarding depth and orientation. Although, stereo-radiography does provide a means for obtaining information on the depth of damage. Additionally, the information is not quantitative and thus does not provide an easy means for making comparison to models for use in situations where an accept or reject decision must be made. Another problem with the method is that of practical implementation for applications where access to two sides is not available. Also, the method often requires access to a free edge for the application of the penetrant, since the method relies on the flow of the penetrant through a system of cracks in the material. In general, radiography provides a high resolution indication of damage, but is not quantitatively related to a material's mechanical properties.

Another useful technique for assessing material state is the monitoring of material modulus or stiffness [ref. 2]. This obviously provides direct information on material state, since stiffness is a material property which is affected by damage. However, some methods of stiffness measurement are pointwise and thus only provide information for one material location. Additionally, application of strain gages and extensometers can be difficult in certain instances, especially when measurements are to be made in several locations. Other stiffness measurements are done over a relatively large gage length and are thus an integrated effect of damage over the gage length. Hence, stiffness measurement is useful since it is a material property, but is often only one piece of information, for a given gage and involves either obtaining the combined effects of various damage zones over a large area or obtaining the more specific state of a small region.

A variety of thermographic techniques are available which exploit thermoelastic, viscoelastic and other heat producing mechanisms to obtain surface strain fields in loaded materials [ref. 3]. These methods offer the attraction of yielding more or less quantitative information on the full field behavior of the material. An advantage of these methods is the fact that they actually are related to basic mechanical properties of the material. Ultimately, variations in these properties may be correlated to damage. One limitation is that the material must be loaded in a carefully prescribed manner in order for successful application of the method. Moreover, results are often more dependent on what is occurring in surface plies and although affected by internal damage, results may

not be as sensitive to internal damage. The system in many cases requires recalibration for various applications and is difficult to implement in applications where other heating mechanisms exist. Basically, in certain instances thermographic/mechanical methods provide a good full field method for interrogating materials, but often only indicate how damage affects strain fields in the surface plies and are difficult to implement in certain situations.

Various ultrasonic methods exist for evaluating the state of composite materials. In general, these involve a pulsed stress wave that is transmitted through the material and subsequently received by either the sending transducer upon reflection from a back surface or by another transducer on the back face of the material. In either case, the stress wave interacts with all the material through the thickness and thus yields a result which integrates the influence of all the material through the thickness. Specifically, the stress wave will propagate directly at a flaw internal to a material, being attenuated, reflected and transmitted as the characteristics of the flaw mechanically dictate. Thus, the stress wave is directly affected by the damage in the material. Usually, either time of travel measurements are made in order to calculate phase velocities or attenuation measurements are made in order to determine how much the material dissipates energy. The phase velocities can be used to determine the moduli of the material. As mentioned, the moduli are important material parameters and have been shown to change as a result of damage. The attenuation of stress waves is utilized in a variety of applications. One major implementation of an attenuation method is the c-scan, where stress waves are propagated through a material, reflected from the bottom surface of the object, propagated back through the material and are received by the sending transducer. By selectively gating the signal and looking at relative signal amplitudes, an indication of through-the-thickness material state can be obtained. In the case of a c-scan, this is done at discrete points over the material face to determine areas of possible damage. Also, by looking at various places in the signal a possible indication of a pulse due to a reflection off of a delamination or crack may be witnessed. A basic attraction of all ultrasonic methods is that they interact with the material in a mechanical way and thus directly relate to the mechanical state of the material. One problem with the pulse echo and through transmission techniques mentioned is that they may mostly interrogate

the object perpendicular to the load carrying directions. However, recent work by Stiffler et. al. incorporates the measurement of phase velocity measurements for Lamb waves as a means of measuring in plane moduli [ref. 4]. Thus, a variety of ultrasonic methods exist for assessing composite material with the main advantage being that they are a result of the actual mechanical behavior of the material.

A relatively new ultrasonic method being studied is the stress wave factor (SWF) or acousto-ultrasonic technique. The method as suggested by Vary of NASA/Lewis involves the introduction of stress waves at one point on a material surface and detection at another point. Basically, the hypothesis being that if a region transmits the disturbance well, then the region will also transmit stress due to load well and thus will have less stress concentration upon loading and subsequently be less prone to fracture. Alternately, a region that does not propagate the disturbance well will not adequately transfer stress and as a consequence be more susceptible to failure. As a result, a quantitative parameter can be obtained to assess the quality of a composite material in the directions of applied loads.

Originally, the method was implemented on thin tensile specimens and involved using a counting scheme where a timed counter took voltage readings and counted excursions above an established threshold. This was done for a set time interval T, where the excitation was being pulsed at a rate P (see Figure 1).
Basically, the calculated SWF value is a relative measure of the detected signal's root mean square or energy level. Therefore, the SWF value is a measure of the material's ability to transfer energy and enacting preceding arguments is a measure of a material's resistance to fracture. In support of this, tests have been performed on thin tensile specimens to compare failure location with relative SWF values along the length. In general, results of the tests seem to indicate that the SWF value could be used to predict failure location (see Figure 2) [ref. 5].

To compare the method to the previously mentioned stiffness measurement method, testing was conducted by Govada et. al. where both stiffness and SWF were monitored at various numbers of

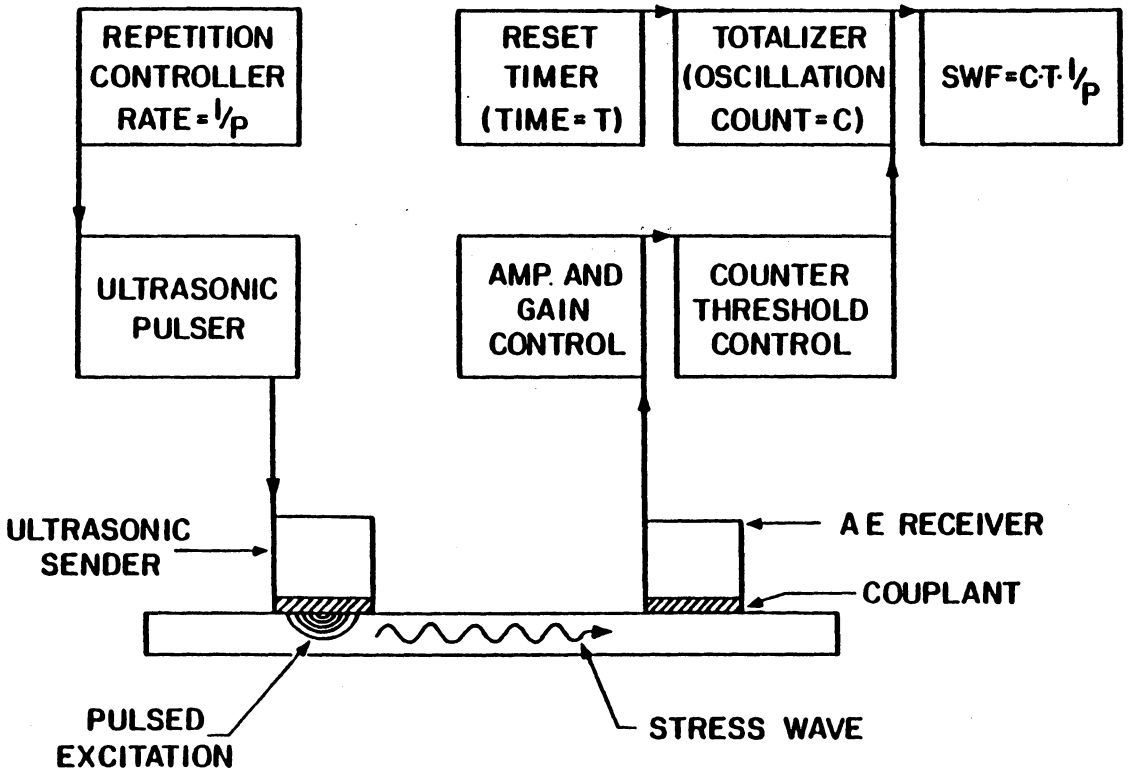

Figure 1. Diagram of original SWF configuration

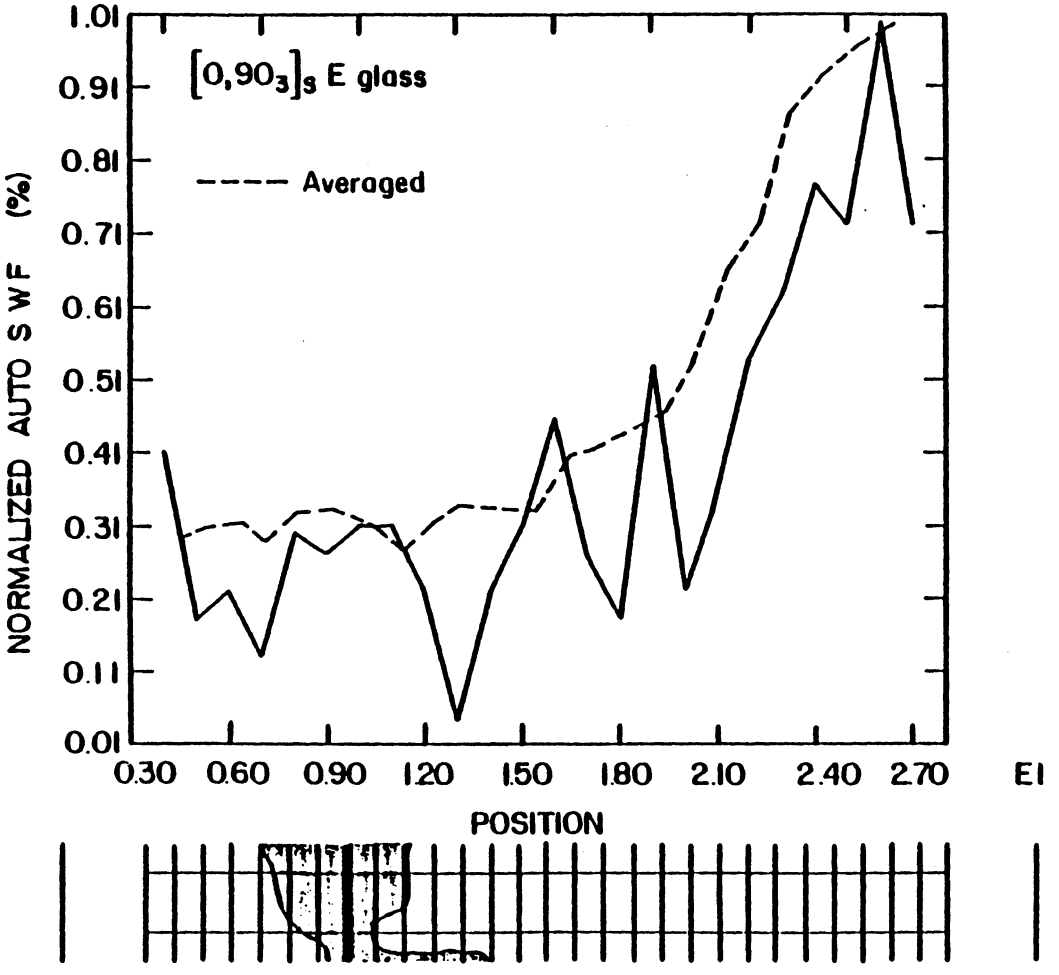

Figure 2. SWF as a failure location predictor

fatigue load cycles. As Figure 3 indicates, the measurement of SWF compared quite nicely as an indicator of damage during the fatigue process [ref. 5].

The desire to extract more detailed information from the stress wave factor method led to the implementation of Fourier analysis to describe the time signal. Initially, the power spectrum can be viewed so as to gain a basic idea of what frequency peaks exist. In addition, more elaborate forms of analysis may be employed to extract even more specific information. For instance, Williams et. al. have utilized homomorphic signal processing to separate different reflection patterns in an acousto-ultrasonic signal [ref. 6]. This involves selectively gating the time signal and then performing the FFT. Next, a log operator is applied to the absolute value of the spectrum in order to deconvolve two reflection signals. Then an inverse FFT is performed, along with a cepstrum window to effectively filter out one component of the reflection pattern. Subsequently, an FFT can be performed, followed by an inverse log operator to obtain a magnitude spectrum of a specific reflection spectrum. Hence, a means exists for obtaining information on an exact portion of the material for an exact mode of wave propagation. However, the problem must be well modeled for proper choice of gating and window parameters, as well as correct interpretation of results. As a means of directly parameterizing information in the power spectrum, Talreja [ref. 7] suggested using shape parameters to simply quantify the Fourier analysis results. A later chapter will discuss the theory and some of the exact details of this analysis.

An example of how the observed spectrum can change over the course of fatigue cycling can be seen in Figure 4. The first two spectra are for earlier in the fatigue life, while the bottom spectrum is for late in the fatigue life.

Notice the decay of the large amplitude peak, which existed in the earlier two spectra, to smaller separate peaks in the spectrum for the higher number of cycles. Hence, one may conjecture that the method is sensitive to more than just attenuation of amplitude. Additionally, Fourier analysis yields resonance peaks which may be employed to derive physical meaning from the output. Specifically, Stiffler suggests from his work on using Lamb waves to measure plate moduli, that Lamb waves could be the mode of stress wave transfer for the acousto-ultrasonic method [ref. 4].

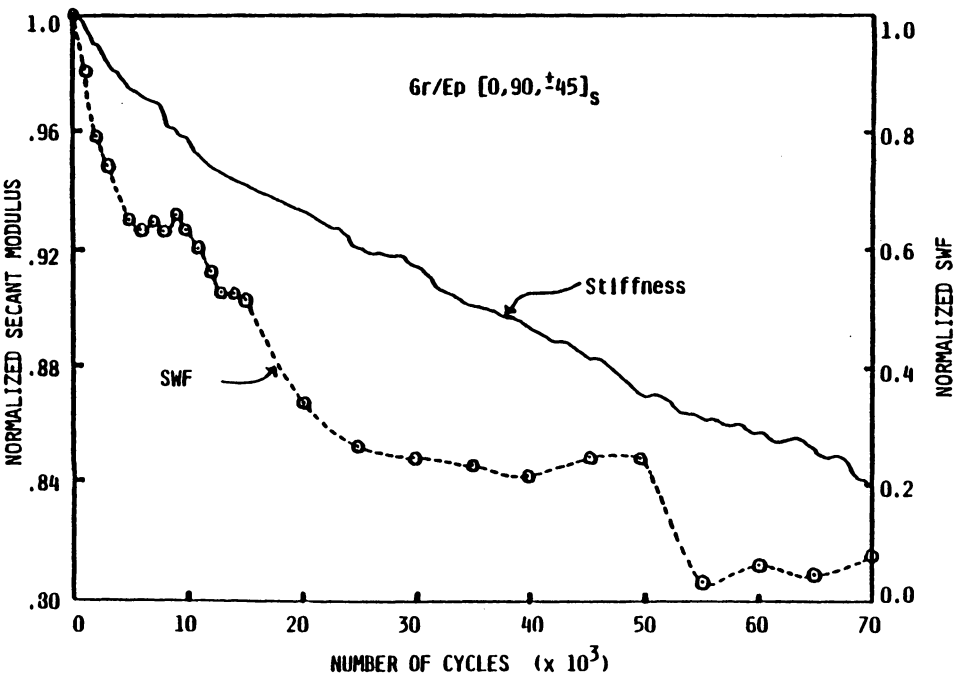

Figure 3. SWF as a fatigue damage indicator

a)

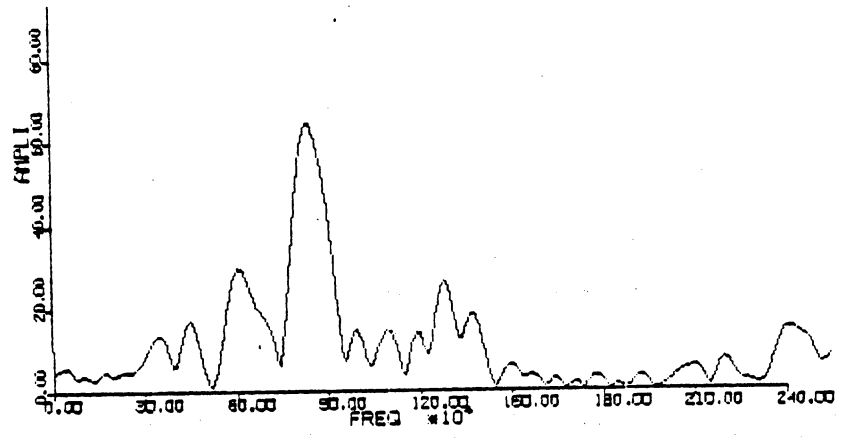

b)

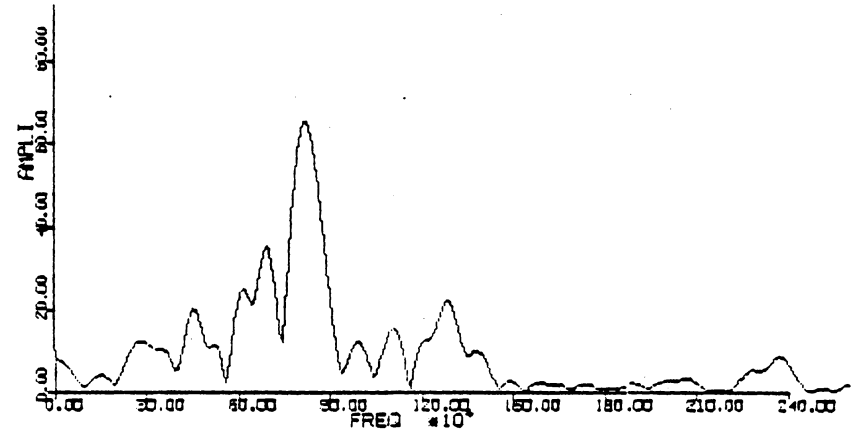

c)

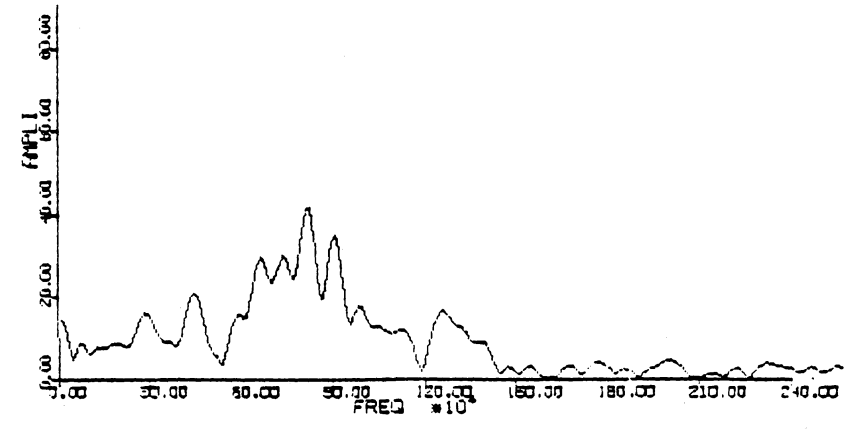

Figure 4. **Change in Spectrum as a result of fatigue damage:** a)Early in fatigue life b)Middle of fatigue life c)Late in fatigue life

To summarise, the first chapter introduced the need for composite materials and the need for non-destructively evaluating them, specifically introducing the acousto-ultrasonic technique and its relative niche in the scheme of composite material evaluation.

System Description

Introduction

As with any nondestructive technique, meaningful results are dependent on the implementation of a system which is constructed of well characterized components. Ideally, a system should be characterized in a manner such that its output is in the form of material parameters or in other words is system independent. This chapter will discuss the various components in an acousto-ultrasonic system and describe in detail the present system.

Basic System Configuration

The present system is composed of several components, Figure 5,

each performing a vital function for proper implementation of the acousto-ultrasonic technique.

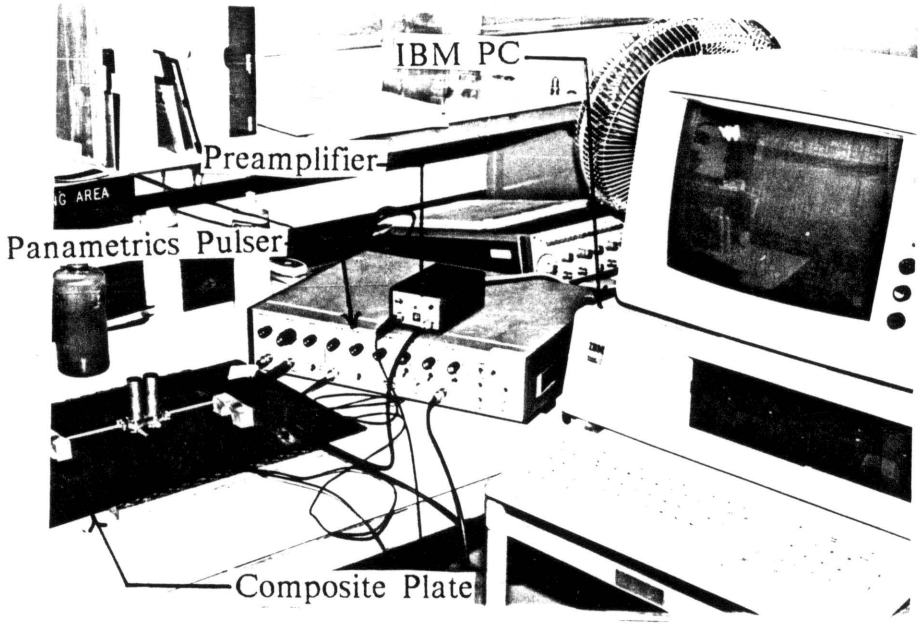

Figure 5. Picture of present system

First, a pulsing/receiving unit (Panametrics 5052 Ultrasonic Analyzer) is used to produce a wide band pulse to excite the initial disturbance. The electric pulse is transformed to a mechanical disturbance via a piezoelectric transducer (ie. the sending transducer). An ultrasonic couplant, applied between the transducer and the material, reduces the acoustic impedance mismatch and improves the transmission of the disturbance to the material. However, future systems could utilize more advance methods of excitation, such as laser pulses or particle impingement [ref. 8]. Next, the disturbance is detected, after transmission through the material, by the receiving transducer. The receiving transducer works in a inverse manner to that of the sending transducer and converts the received mechanical disturbance to a voltage signal. Once again, future systems could implement more advance detection methods, such as capacitance transducers [ref. 9] and laser interferometry [ref. 10]. The resulting electric signal is preamplified (Panametrics 5660 Ultrasonic Preamp) and returned to the pulsing/receiving unit. The voltage signal can then be gated, attenuated or amplified further as required for A to D conversion or other forms of signal processing. In general, the spacing between transducers is arbitrary. The present system uses a spacing distance of one inch. Although, no particular reason existed for this distance, it appears that it is a sufficient distance to excite plate resonances and still receive a reasonably strong signal. In order to maintain a fixed distance and consistent placement of transducers on material faces, a transducer spacing fixture, Figure 6, is incorporated into the present system.

Furthermore, the fixture utilizes alignment marks and pointers, for use with fudiciary marks to allow for exact orientation of transducers. For more complex material geometries, additional coupling blocks or waveguides must be incorporated into the system.

Finally, the signal is digitally recorded by an IBM PC with a PC DAS data aquisition board marketed by General Research Corporation [ref. 11]. The board performs data capture, storage and display of the signal by converting the screen to a virtual oscilloscope. Fundamentally, all components are essential to the system and should be well understood in order to achieve reliable results and maximum information. More importantly, each component operates on the signal and should thus be considered when one attempts to attach physical significance to the system output.

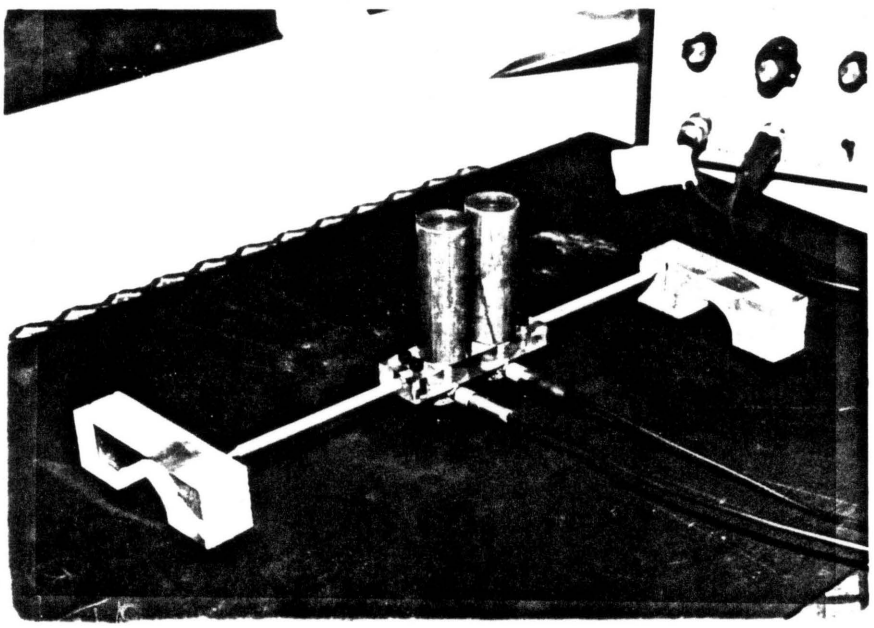

Figure 6. Picture of spacing fixture

Pulser

Initially, consideration should be focused on the spectrum of the pulse source as it is the origin of the excitation. The source of the pulse for the present acousto-ultrasonic system is the Panametrics Model 5052 Ultrasonic Analyzer. The pulser is externally triggered by the PC DAS system to send a high energy wide band pulse to the sending transducer as dictated by the energy and damping dial settings [ref. 21]. The energy can be set at 25, 50, 75 or 100% of full energy and the damping can be set from 25 to 500 ohms resistance in parallel with the sending transducer. Although, the dial settings control the overall nature of the electrical pulse the complete circuit modifies the output and is affected by the characteristics of the transducer. More specifically, the transducer will offer an impedance to the input pulse. However, in general, increased energy and damping settings lead to higher amplitudes and increased pulse widths for the input pulse. For example, notice the effect of changing dial settings on the output spectrum for two consecutive acousto-ultrasonic measurements made without moving transducers in Figure 7 and Figure 8.

Note the relative suppression of the low frequency for the low damping setting for the pulsing circuitry (smaller pulse width). The increased pulse width results in a greater low frequency content and subsequently a greater low frequency output. It should be noted that a total understanding of how the input excites mechanical disturbances would be necessary to make specific comments on exactly how the input frequency content affects the frequency content of the detected signal. The study of this issue is an objective to be pursued using the present system.

Transducers

Secondly, consideration should be focused on the conversion of the original pulse to a mechanical signal via the transducer. The present system uses Panametrics V105, 5 MHz transducers. These

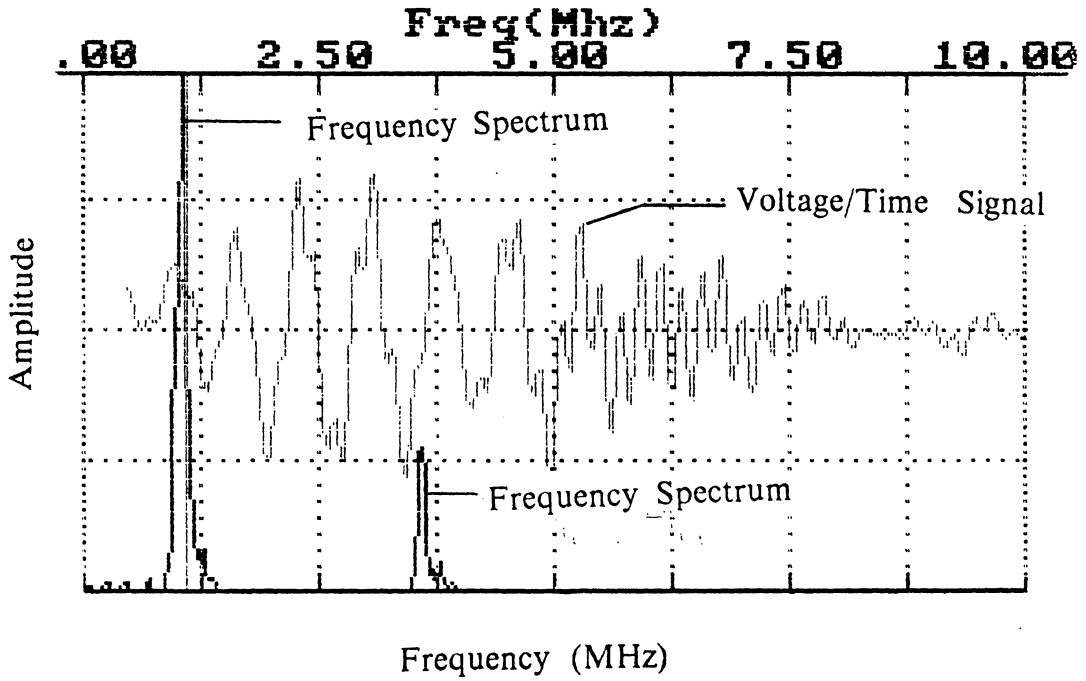

Figure 7. Power spectrum for low damping pulse setting

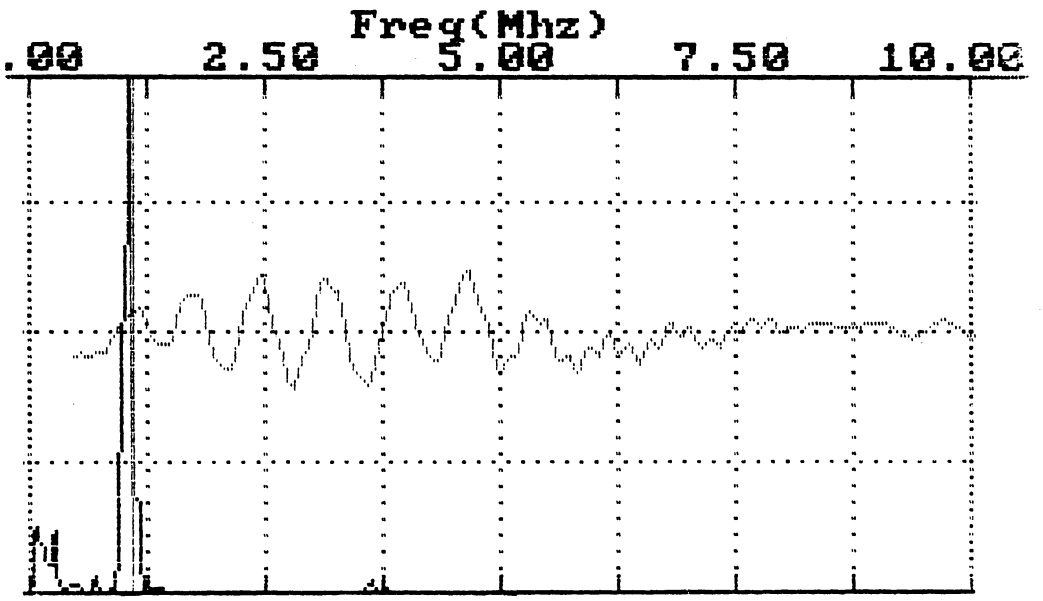

Figure 8. Power spectrum for high damping pulse setting

transducers are piezoelectric and constructed so that the face has a predominately out-of-plane motion. A variety of methods have been suggested for finding a transducer's transfer function. For instance, Hsu et. al. [ref. 12] have suggested using a step force input on an aluminum block as a means for obtaining a transfer function for the transducer. Also, McBride and Hutchison suggested using a helium gas jet as a source for calibrating transducers [ref. 13]. A first step toward calibrating the present transducers was taken by simply using a pulse echo scheme on an aluminum block, Figure 9. However, this signal was generated by the previously mentioned pulser and hence is really a representation of the combined effect of the pulser and transducer.

Additionally, work was done to try to calibrate face motion of the transducer using a laser interferometer system. However, these tests did not yield acceptable results. A later section will cover how software has been developed to try to account for the transducer's transfer function. Furthermore, a following section will describe a test that was conducted using a different sending transducer to determine the exact character of the effect of the sending transducer on the system output. Ideally, an input source should cause a prescribed displacement as a known function of position and time. Hence, if the material is unchanged and the sensor is the same then the output signal should be totally reproducible. The present system contains a variety of weaknesses in this regard. First, the piezo-electric transducers presently being used are not well enough characterized to prescribe these variables or to even understand if they are constant. Additionally, the effect of the layer of couplant between the transducer and material surface is not very well characterized, but is most likely not constant. As a note, tests conducted with a laser interferometer system revealed variation in the amplitude of displacement as a function of position on the transducer face. In general, transducers are a major component in an acousto-ultrasonic system and attention should be given to their effects on output.

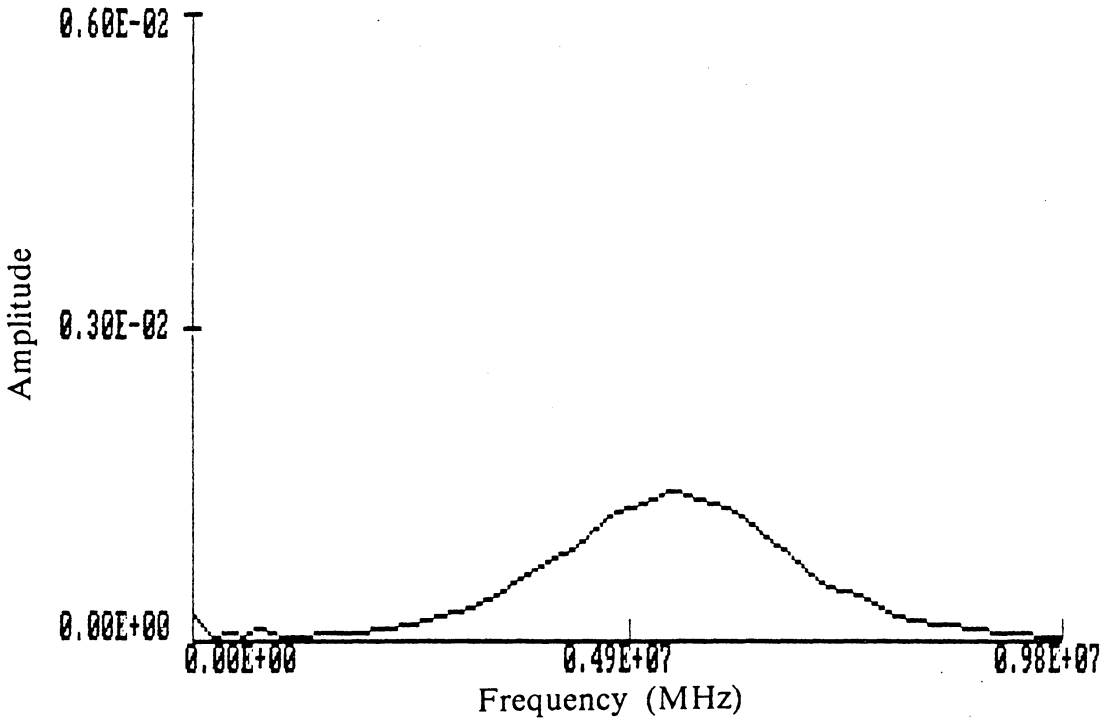

Figure 9. Transducer transfer function

Preamplifier

The purpose of the preamplifier is simply to amplify the signal, as received from the receiving transducer, to an acceptable level for gating components and data aquisition. The presently used preamplifier is capable of amplifying the signal either 40 or 60 dB.. Although the circuitry for the amplifier has an associated transfer function, it is designed to be independent of frequency and linear in voltage for the range where it is employed. One way to include the effects of the preamplifier would be to account for the amplified voltage in the analysis, if a means existed for relating original voltages to any specific physical quantities (ie. surface displacement). In the present system, there is too little understanding of the transducer and couplant combination to place any specific physical meaning on exact voltages. However, as these things become better understood and transducer technology is advanced, it should be possible to relate voltages to physical quantities and so the effect of any component which amplifies the signal should be taken into account. The present system has the capability of doing this in the transfer function routine of the software. For example, a calibrated laser interferometer detection system could be combined with a well characterized sending source and the signal could be related to actual displacements. But, it would perhaps be convenient to vary amplification levels to be in the proper range of data acquisition components, for differing applications, while still retaining the physical meaning of the original voltage. Thus, although the present system does not necessitate the incorporation of this component's effect in the analysis, these effects are noted and software does include the capability to account for amplification in future systems.

Computer and Data Acquisition System

The final component in the system is the computer/data acquisition system. First, this component performs the function of receiving the signal and digitizing it for ensuing observations and calculations. Once the signal is digitized, it is sent to the computer screen for essentially real time viewing. Using keyboard control the signal can be frozen on screen, stored and Fourier analyzed. Additionally, various parameters can be input through use of the keyboard. One example is the sampling rate for the A to D converter. Beyond this the computer can access the signal from the storage disk at later times to perform further analysis and display results on the screen or printer. For use with the present system, the PC DAS system sends a trigger signal to the pulser. Immediately after sending the trigger signal, the PC DAS system takes voltage readings from the A/D converter at the prescribed sampling rate. The base rate of sampling is twenty megahertz. But, submultiple rates of 1/2 to 1/128 can be chosen. In addition, by use of equivalent time sampling, sampling rates of 40, 80 and 160 megahertz may be achieved. The sampling interval, which is simply the reciprocal of the sampling rate, is defined as Δ and should be of a value such that

$$f_h \leq 1/2\Delta$$

where, f_h is the highest frequency of interest in the signal. In otherwords, the sampling rate should be twice that of the highest frequency in the signal. This frequency limit, $f_m = 1/2\Delta$, is known as the Nyquist frequency. The PC DAS system acquires 4096 points which it stores in local buffer memory. The system echoes the memory to the PC screen so that the time/voltage data may be viewed. After obtaining 4096 points a new trigger signal is sent to the pulser and the process is repeated. However, a mode exists for taking the signal from repeated retriggers and averaging each of the 4096 data points. In this mode each of the 4096 points is the result of from 2 to 128 voltages being averaged. The user has the capability of choosing the number of averages beginning with 2 and the possibility of all succesive multiplications of 2 up to 128. These average values are then placed in memory and echoed on the screen as the most recent signal. Thus, after the 4096 points

are sampled the specified number of times, the average values are obtained and the process can be repeated. At any time the present signal may be frozen in memory. Subsequently, the 4096 data points may be gated. Additionally, a normalized power spectrum may be obtained via key board control. Also, the points in the chosen gate may be stored on disk along with sampling and gating information for further analysis. Basically, the data acquisition system can capture and store the signal and the computer can later be used to calculate parameters and produce plots.

System Software

Introduction

After capturing the signal digitally, the information inherently carried in the signal must be transformed into parameters which are physically descriptive of the material state. Ideally, the parameters should be related to modes of wave transfer, which in turn are dependent on the properties of the composite material. In a composite material, the quality of bonds and constituent material state govern these properties. Ultimately, a set of parameters should exist which can immediately be related to material integrity and the resulting composite material properties. To learn as much as possible concerning the modes of wave transfer and the effect which damage has on these modes, software allows for the abilitiy to look at prescribed parts of the time domain and perform a Fourier analysis to see what wave modes or peak frequencies are present. With knowlege of where in the wave train a particular peak frequency appears, an estimate can be made of the phase velocity corresponding to the mode of wave propagation. As will be shown, a narrow band analysis may be applied to just the frequency spectrum of the gated portion of the time signal to determine the relative amount of energy transfer in that portion of the time signal. Also, additional parameters (SWF parameters) may be calculated to determine other physically significant quantities such as the

center frequency of the power spectrum (SWF2). This indicates the average frequency at which the energy is being transferred. Another SWF parameter can be calculated that estimates the ratio of maxima peaks to zero crossings in the time domain signal (SWF3/SWF4). Moreover, digital filtering may be applied to the narrow band analysis approach to calculate SWF parameters, so that the amount of energy transfer in a particular frequency range may be obtained. Specifically, this can be done for a particular peak in the frequency range to determine how much relative energy is being propagated via that mode. Thus, a quantitative parameter may be obtained which yields a very specific piece of information concerning the energy transfer rate for a single mode of wave transfer in a particular portion of the wave train.

As mentioned in the previous chapter, eventually the software should contain the capability of eliminating the effects of all system components, thus yielding a material parameter. For this reason, the present system does include a means for calculating a transfer function in order to cancel the effects of system components if they are well characterized. Basically, this involves dividing the Fourier coefficients from the received signal by the Fourier coefficients of the input signal and multiplying by an amplification factor. In addition, this software routine can be employed to calculate a coherence function by dividing the Fourier coefficients of the signal for an undamaged composite by the Fourier coefficients of a damaged composite or vice versa. Thus, it is the purpose of this chapter to describe the system software which has been developed to extract physical significance from the signal through descriptive parameters which quantify information.

The present system is not limited to a particular application, but instead is tailored to be used for basic research of the method. As a result, flexibility has been emphasized rather than efficiency. For specific applications, the software can easily be altered to yield more immediate results by eliminating user controlled data manipulations and output selections. In particular, almost all data manipulations and output schemes are carried out by subroutines, which are called from main control routines. In the present system, this routine allows for many user input choices, however for particular applications this could be replaced by a routine with embedded choices.

The capabilities for the system will be discussed and in particular the procedures for establishing:

- Estimated phase velocities
- Voltage/time plots
- The frequency spectrum using the FFT
- The SWF parameters (filtered and unfiltered)
- The transfer function of the system
- The coherence function for two signals
- The plot of SWF parameters versus other parameters

Analysis

This section will detail the means by which the data stored on disk and user entered information are transformed to the various parameters and plots. The data stored on disk include:

- Voltages for points in the chosen gate (V_i)
- Time for gate start
- Sampling interval (Δt)
- Number of data points (n).

The user must input:

- Control information
- Ranges for plot axes
- New time for gate start (TP)
- Distance between transducers (D)
- Filter parameters.

With this information the user may obtain:

- A plot of voltage/time data
- An estimate of the phase speed (V)
- Plot of power spectrum
- Phase/frequency plot
- SWF parameters from received signal (filtered and unfiltered)
- Plot of transfer function power spectrum
- Plot of coherence function power spectrum
- SWF parameters from transfer function (filtered and unfiltered)
- SWF parameters from coherence function

- Plot of SWF parameters versus other parameters (e. g. azimuthal angle)

Note that values obtained for output calculations may be stored on disk for use with other software. For example, SWF parameters may vary as a function of some other variable, for instance azimuthal angle (see Figure 26 in chapter on System Implementation). Thus, SWF parameters may be stored for each angle and later additional software can be used to plot any SWF parameter as a function of azimuthal angle.

Once the digitized signals have been stored, attention must be given to analyzing the signal and generating an output which is physically related to the state of the material. As with any time related signal, certain information of importance is immediately available in the time domain while other information is more easily interpretable in the frequency domain. In general, a total representation of a signal involves consideration of both domains. Analysis considers where, after the pulse trigger, information in the time signal occurs and provides a means of selecting a portion of the time signal (gating) for Fourier analysis. As a result, consideration can be given to both information in the time domain and the frequency domain. An adjustment in length and gate start location can be applied to the time signal, so that frequency information can be obtained for a known portion of the wave train. Subsequently, this information can be analyzed with knowledge of pulse, trigger and gating information to produce a variety of quantitative parameters which may then be related to the material state.

The gating procedure involves taking one portion of the signal intact and zeroing all other parts before performing the Fourier analysis. Caution should be given to looking at a large enough portion of the signal so that low frequency information is not misrepresented. In general, the length of the gate should excede the period associated with any frequency information of interest. In the present system, a moving gate can be applied to the signal so that information can be obtained concerning the phase speed of various wave modes and where relative amounts of energy for each mode occur in the time signal. More specifically, the present system considers the initial triggering time, gating values, sampling rates and transducer separation distance to extract estimates of phase

velocities. An estimate for the phase velocity is determined by finding where in the time domain a certain frequency content appears, using Fourier analysis, and then accounting for transducer separation distance D (D is equal to one inch for the present system) and finding placement in the time signal TP as mentioned above and calculating phase velocity by the equation V = D/TP (Figure 10).

Also, judicious gating coupled with various other methods of analysis, that will subsequently be introduced, will allow a wealth of information to be gathered from a single signal.

Another function, included in the system software, is the ability to zero average the time data in order to subtract out the effect of DC biasing in the signal. The algorithm, quite simply, encompasses summing all the voltage readings and then dividing this number by the number of voltages, yielding the average voltage for the signal. The average value can then be subtracted from each voltage reading to yield a zero average voltage for the signal, resulting in the subtraction of the DC bias from the signal. Mathematically,

$$V_a = \sum_{i=1}^{n} V(i)/n$$

$$V_f(i) = V(i) - V_a$$

where, $V(i)$ are the original voltages, V_a is the DC bias and $V_f(i)$ are the unbiased voltages.

In addition, capabilities for plotting out the time versus voltage graph allows for visual inspection of system time domain results so that general trends can be noted. As with all plots, the user can control the range on the X axis and the scale on the Y axis, where the beginning value for the X-axis is the user defined gate start. User manipulation of voltage plots allows for a variety of comparisons to be made between different signals or for a user to obtain a maximum range to observe more subtle signal characteristics.

The program offers the additional capability of adding zero values for voltage readings in order to change the number of points in the $V(i)$ array before calculation of the FFT. First, this can be used

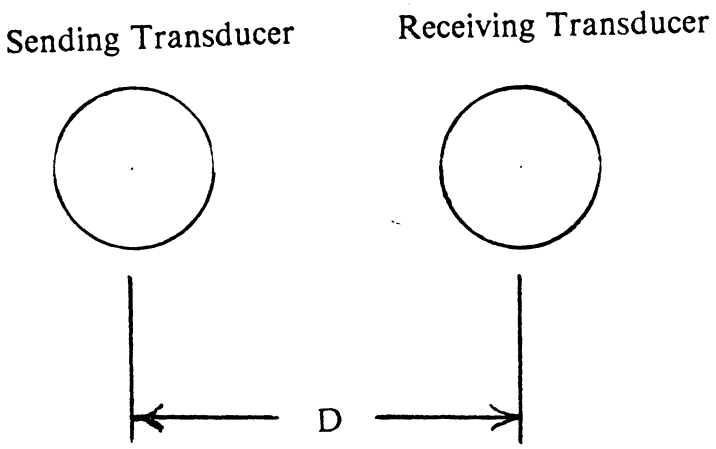

Figure 10. Definition of parameter D

to increase the frequency resolution Δf for the Fourier analysis (see ref. 14). Furthermore, the FFT algorithm requires that the number of array values be a power of two and for this reason the program automatically adds zero valued array points to meet this requirement.

Further information can be acquired by running an FFT on the stored time signal to produce amplitude/frequency information, where the amplitude is a relative indication of the energy content at the given frequency. Thus, information can be obtained on signal frequency content by looking at FFT results. For example, in Figure 11 the peak at one MHz indicates that the material may be vibrating at one MHz or that at least some vibration mode causes a one MHz voltage variation. Most assuredly, simple examination of the amplitude/frequency plot reveals useful information. Additionally, this information can be combined with time domain and gating information to generate more specific conclusions, such as the previously mentioned phase velocities. More quantitatively, the units of the amplitude are volts squared seconds. Hence, integration over the frequency range will yield a volts squared result. In fact, theory shows that this is the mean square of the voltage signal [ref. 14]. For the digitized signal, the integration is replaced by a summation of amplitudes multiplied by the frequency differential. The frequency differential being defined by:

$$\Delta f = \frac{1}{n\Delta t}$$

where, n is the number of time samples and Δt is the time sample interval between voltage readings. Physically, this is an indication of the energy transferred through the material and therefore is related to the original SWF as instituted by Vary. One advantage of the narrow band analysis is the avoidance of setting a threshold voltage, thus alleviating an extraneous variable. One disadvantage of the narrow band analysis is the extra data processing time associated with the software. Additionally, one can look at the amplitude and area under specific peaks to obtain an indication of the amount of energy being transferred at that frequency. This can be done by applying the summation only over the domain corresponding to the frequency peak of interest, while just treating other frequencies as having zero amplitudes, in essence filtering the signal. Mathematically this may be expressed as:

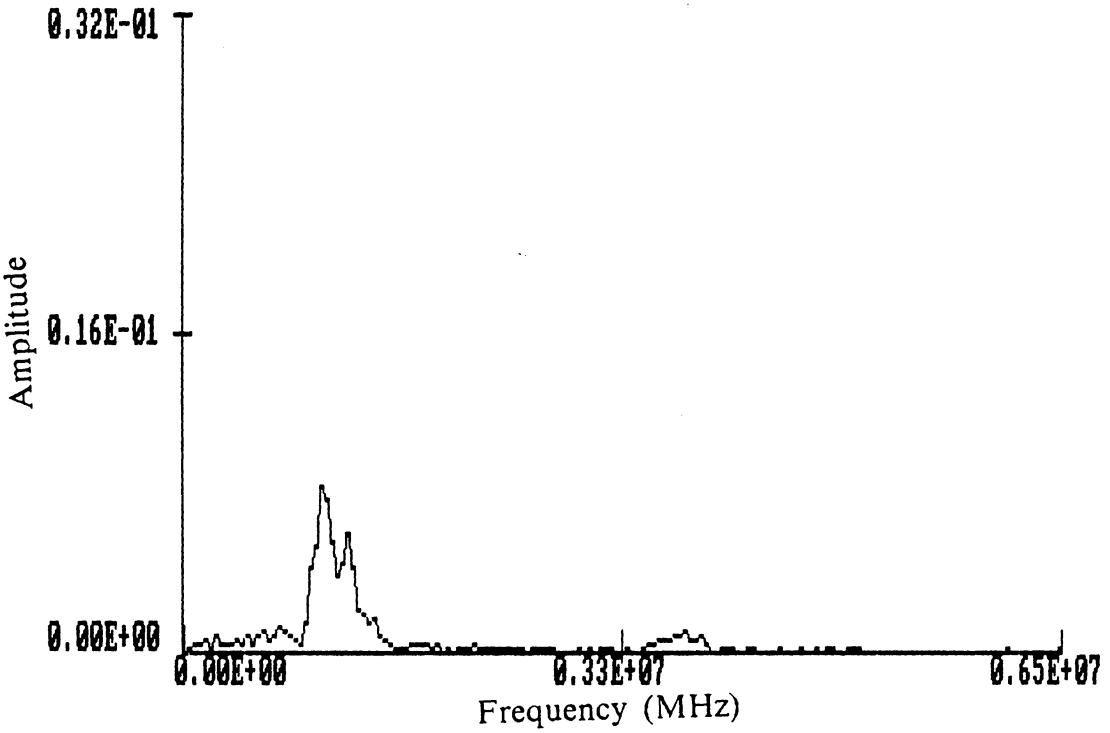

Figure 11. Example frequency spectrum

$$SWF1(filt) = \int_{f_1}^{f_2} S(f)df$$

where, f_1 is the low frequency in the applied filter and f_2 is the high frequency in the filter. In the present software, a boxcar filter is used. Simply put, all spectral values for frequencies lower than f_1 and greater than f_2 are set equal to zero, while all spectral values corresponding to frequencies between f_1 and f_2 remain at their original values. Hence, integration or summation for purposes of SWF parameters can be applied only in the domain between f_1 and f_2. In other words, one can get an SWF value for specific modes of wave propagation (ie. frequency peaks). Furthermore, this procedure can be performed at different regions in the time domain so as to find how the energy transfer capabilities of various modes vary as a function of time. Thus, specific parameters can be produced from the frequency spectrum to yield information concerning particular modes of wave transfer.

More extensively, a method as suggested by Talreja [ref. 7] is being implemented to calculate shape parameters from the frequency spectrum. Essentially, this involves taking various moments of the frequency spectrum about the amplitude axis. In other words, the method consists of taking the formula for the area under the curve and multiplying by the frequency (f) raised to the n power inside the summation, or for the continuous domain, inside the integral. Thus, the zero moment corresponds to the area under the curve or the signal mean square voltage. A general description of the theory for the continuous domain is given in Figure 12.

Notice, that SWF1 is defined as the zero moment and thus is simply an indication of energy transfer. Also, the SWF2 parameter is the centroid of the frequency spectrum and therefore is an indication of the amount of energy content in the high frequency range relative to that in the low frequency range. In other words, a signal with a high amount of energy being transferred at high frequencies will have a higher central frequency and thus have a higher SWF2. SWF3/SWF4 is defined as the fourth moment divided by the second moment. This may be related theoretically to the ratio of signal maxima to the number of zero crossings. Hence, a small amplitude high frequency component in a high amplitude low frequency signal would produce a high SWF3/SWF4.

NARROW BAND ANALYSIS

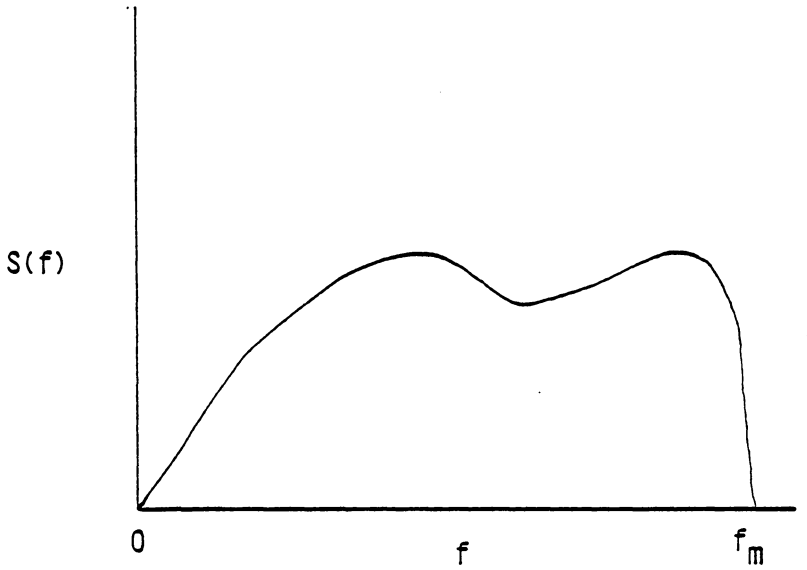

S(f) - Amplitude of spectral density

f - Frequency

$M_n = \int_0^{f_m} S(f)\, f^n\, df$ n-th moment

$M_0 = \int_0^{f_m} S(f)\, df$ 0-th moment (Area under curve)

SWF1 = $(M_0)^{\frac{1}{2}}$ - Proportional to energy transfer

SWF2 = M_1/M_0 - Frequency (f) corresponding to centroid

SWF3 = $(M_2/M_0)^{\frac{1}{2}}$ - Frequency of mean crossings

SWF4 = $(M_4/M_2)^{\frac{1}{2}}$ - Frequency of maxima

SWF3/SWF4 - Distortion factor

Figure 12. Calculation of SWF parameters

This is often termed a distortion factor, since it would be an indication of the amount of high frequency noise in a predominately lower frequency signal. Basically, the software utilizes these parameters to produce quantitative parameters from an acousto-ultrasonic signal.

As stated, a software subprogram has been developed to calculate transfer functions and coherence functions by dividing the Fourier coefficients of one signal by those of another signal. In the case of the transfer function, the Fourier coefficients for the received signal $Y(f)$ and $\overline{Y}(f)$ are used with the Fourier coefficients of the input signal $X(f)$ and $\overline{X}(f)$ by the formula:

$$H(f) = S_{xy}(f)/S_{xx}(f)$$

where,

$$S_{xy}(f) = \overline{X}(f)Y(f)$$

$$S_{xx}(f) = X(f)\overline{X}(f)$$

and the over bar designates the complex conjugate. Thus by accounting for the frequency dependency of the energy input, an indication may be obtained as to the true dependency of material vibration on frequency, independent of system input. Also, a multiplication factor is introduced to account for signal amplification. Generally, the transfer function is a first step toward obtaining a material parameter from the acousto-ultrasonic signal which is independent of the acousto-ultrasonic system. The coherence function is calculated by the same routine, where the Y spectrum is for an undamaged specimen and the X spectrum is for a damaged specimen. Hence, a deviation in the coherence function from unity indicates that a difference in frequency spectra exists. This acts to amplify any signal deviation, while in a sense filtering out information concerning spectrum similarities. Therefore, if the effect of damage is to diminish the amplitude of a wave mode which is initially of low amplitude, the coherence function provides a means for illuminating the change. Additionally, the coherence function provides an excellent method for discerning differences in signals which have complicated frequency spectra.

Essentially, the software utilizes basic features of digital signal processing to extract as much information from the acousto-ultrasonic signal as possible. This includes looking at the voltage time domain, calculating FFTs on gated and ungated signals, and calculating shape parameters from the frequency spectrum.

Computer Program

As mentioned, in order to efficiently extract information which is contained in the signal from the acousto-ultrasonic technique, user friendly software has been developed. The program incorporates the form of analysis mentioned above to perform calculation of various results and parameters of physical significance. Furthermore, the computer screen and printer are utilized to graphically present results. Thus, this section will relate how the final component of the system (the computer and software) culminates the purpose of the system by presenting useful parameters and graphs.

The program utilized was constructed to allow for a maximum of user input for the purpose of research and thus has a good deal of user controlled branching. However, most primary functions are performed in subroutines and hence could be combined with other software to perform calculations without as much user input. A block diagram of the program can be seen in Figure 13. Basically, the program contains two major control routines from which the user can input information and control can be sent to auxilliary subroutines to carry out primary procedures. The first routine involves control of time domain and FFT calculations, while the second routine involves calculation of either a transfer function or coherence function. Hence, the second routine involves consideration of the Fourier coefficients of two different signals which have been previously stored.

The first control routine:

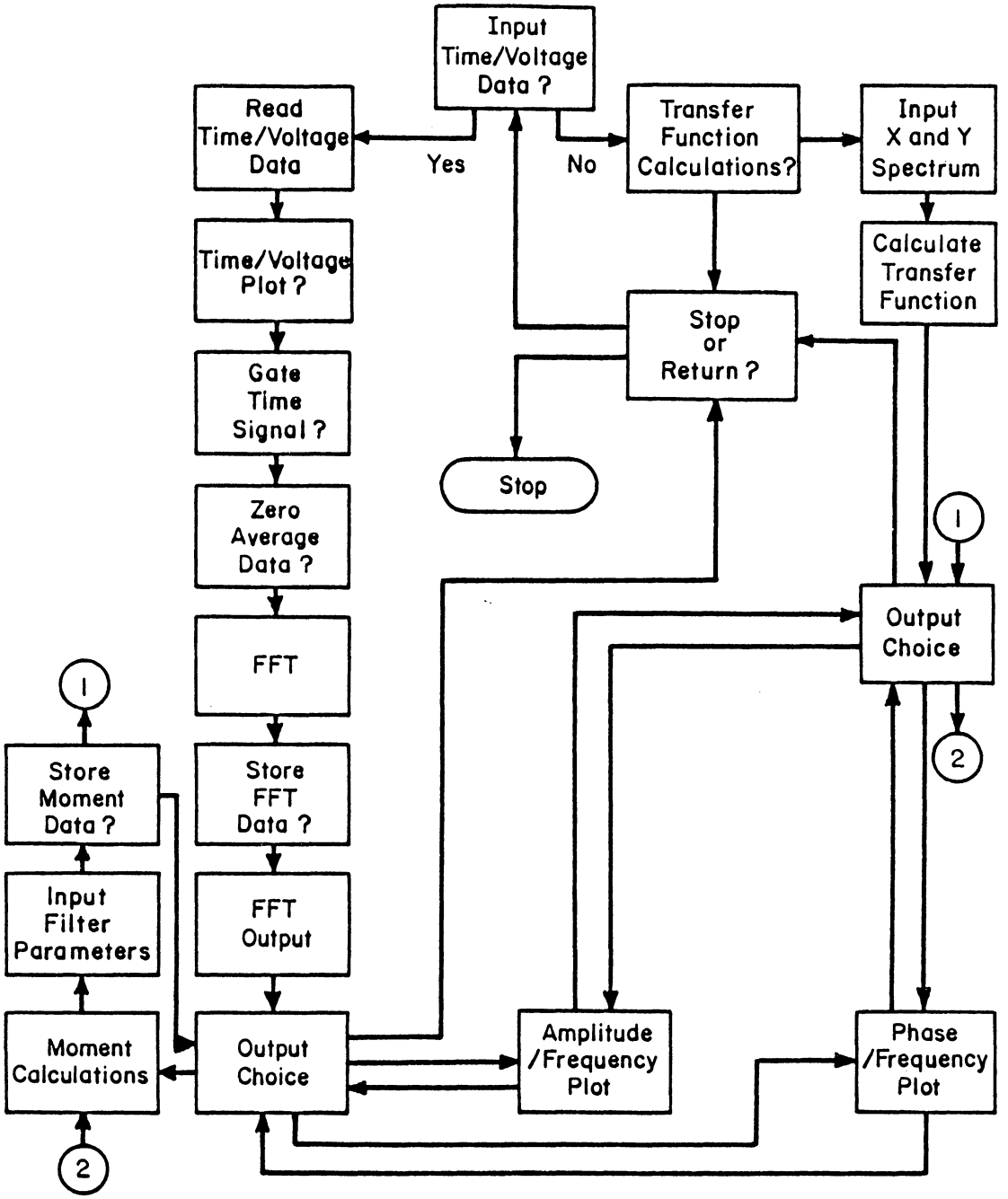

Figure 13. Block diagram of software

- Reads a data file
- Calculates phase velocities
- Generates voltage versus frequency plots (via plotting subroutine)
- Contains gating control for the time signal
- Sends control to D. C. offset routine
- Sends control to routine to adjust number of array values (add zeroes)
- Sends control to FFT subroutine for calculation of Fourier coefficients
- Plots amplitude versus frequency (via plotting subroutine)
- Plots phase angle versus frequency (via plotting routine)
- Calculates SWF parameters (filtered and unfiltered)
- Stores FFT data and SWF parameters on disk for later use

The second control routine:

- Calculates either the transfer or coherence function
- Plots transfer or coherence function amplitude as a function of frequency (via plotting subroutine)
- Plots transfer or coherence function phase angle as a function of frequency (via plotting subroutine)

- Calculates SWF parameters (filtered and unfiltered) from transfer/coherence function

- Stores SWF parameters

The program begins by presenting the user with a menu of three choices for further program control. Number one is the time domain-FFT control routine. The second choice is the transfer function and coherence function routine. Lastly, control can be sent to the post FFT portion of the first routine. In this case the user must input the name of a data file which contains the Fourier coefficients for a previously analyzed signal. Thus, both the second control routine and the post FFT section (choice number three) require that an FFT has been previously calculated and stored on disk, by using the first part of the time domain-FFT control section.

A request to transfer to the time domain-FFT section is followed with a prompt for the name of the file for the received signal. Upon receiving this input, the program accesses the voltage/time data from a disk. The program also retrieves information on gating parameters and sampling rate to be used for ensuing calculations and plots. Next, the user is given the option of plotting voltage versus time with user scaled axes. The user may also gate and zero average the time signal, as described in the preceding section. Additionally, there exists an option for the user to estimate a phase velocity using the beginning of the presently applied gate as an estimation of the time of arrival. The program also offers the option of choosing the wave arrival time (TP). This gives the user the ability to estimate where in the time domain certain wave modes appear and using this to calculate the phase velocity for a particlar wave mode. Specifically, the gate could be moved progressively forward until a certain frequency peak occurs. Then that beginning gate time can be used as an estimate of the time of travel for the wave mode. Note the estimation of where in the time domain a mode arrives can be done through a gating and Fourier analysis scheme utilizing system software.

Upon completion of the phase velocity calculations, the user is offered the option of adding zeroes to the time signal for use in calculating the FFT, resulting in decreased spacing between spectral estimates. This allows for a user to match the number of Fourier coefficients for different data sets,

a requirement for calculation of a transfer function or coherence function. If necessary, immediately before calculation of the FFT extra zeroes are added to make the number of data points a power of 2, as required by the FFT routine. After calculation of the FFT, the user is given the option of storing the modified voltage/time data and the FFT data. Next, a menu of output displays is provided. These include amplitude/frequency plots, phase/frequency plots and SWF parameter calculations. Both plots can be obtained via a common plotting routine which allows the user to control the scale on both the X and Y axes. A choice to calculate the SWF parameters is followed by an option to digitally filter the data, ie. gate the spectrum. This is done with a box car filter which simply zeroes all amplitudes corresponding to frequency components not in the filter range and keeps all amplitudes corresponding to frequencies inside the filter unchanged. The software calculates SWF1, SWF2 and SWF3/SWF4 if the spectrum is unfiltered and just SWF1 if the spectrum is filtered. The resulting calculation is displayed on the screen, and may be stored on disk for later use (e.g. plots of SWF parameters versus some other variable).

The control section for the transfer function and coherence function first asks if a transfer function or coherence function is being calculated. Next, the user must enter the file name for the input (X) and output (Y) Fourier coefficients. Subsequently, the software will calculate all resulting spectral densities. Presently, the software utilizes only S_{xx}, $S_{yy}$and S_{xy} , which as was stated in the previous section can be used to determine the ratio of amplitudes for two signals as a function of frequency. In the case of the transfer function, it is simply a means of normalizing the output with reference to the input in order to find a frequency spectrum that represents the material and is independent of the input. This transfer function or normalized spectrum can then be analyzed in the same manner as the regular output spectrum. The coherence function simply normalizes the output signal for an undamaged specimen to that of a damaged specimen or vice versa and performs similar analysis on the resulting spectrum. In both cases, the so called output signal is normalized with respect to what is termed the input signal. Presently, software is written so that the FFT of the excitation from the sending transducer must have used the same sampling interval as the FFT of the signal from the receiving transducer. Once the transfer function has been calculated control can

be sent to an analysis section which is used for the regular amplitude frequency analysis and will be explained subsequently.

A series showing the attempted use of the transfer function to account for dial settings can be seen in figures 14-19.
Although, the transfer function was different for the two cases at the high and low frequency ends and the amplitudes are slightly different, application of the transfer function did set the peak in the 3.1-3.5 MHz range to a similar ratio of the one MHz peak.

The ability of the coherence function to highlight damage in composite materials can be seen in figures 20-22.
The first spectrum is for a relatively undamaged fatigue specimen,while the second is for a specimen near the end of fatigue life. Figure 22 shows the resulting coherence function for the undamaged specimen's spectrum over the damaged specimen's spectrum. Notice that the major amplitude for the coherence function occurs at around 5 MHz, while separate frequency spectra show relatively little at 5 MHz. Although this same information is present in the separate spectra, the coherence function acts to extract this information from the separate spectra. Other coherence function calculations substantiate the relative increase in the 5 MHz peak as a function of fatigue life, if the spectrum of the specimen subjected to fewer load cycles is treated as $Y(f)$ and the spectrum of the specimen subjected to a higher number of load cycles as $X(f)$. This simply indicates a progressive decrease in the 5 MHz signal's amplitude with damage. In other words, progressive damage which occurred in the specimen acted to inhibit the mode of vibration that showed up at 5 MHz.

Basically, a transfer function routine has been included in the hope of providing a method for calculating system independent parameters and a coherence function for highlighting specific changes which occur in an acousto-ultrasonic signal due to damage.

Once the end of any control section is reached, the user may choose to stop, continue in the same control routine or return to the main menu. Hence, the main program provides a means for both

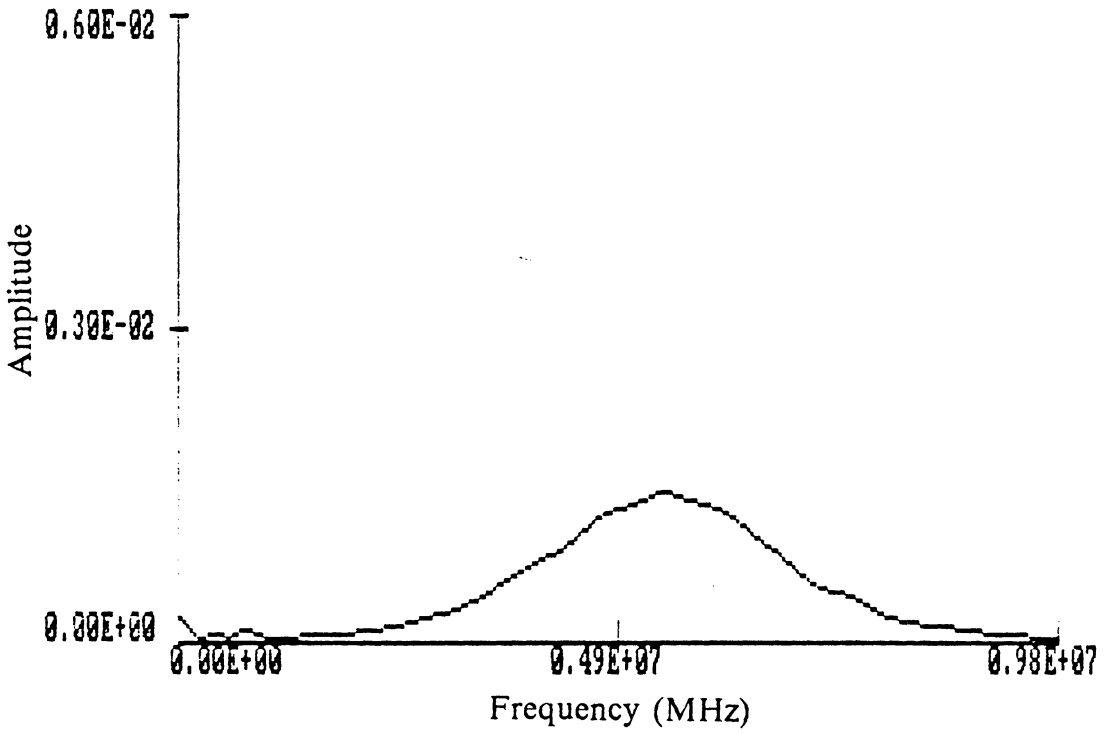

Figure 14. Input spectrum for low damping

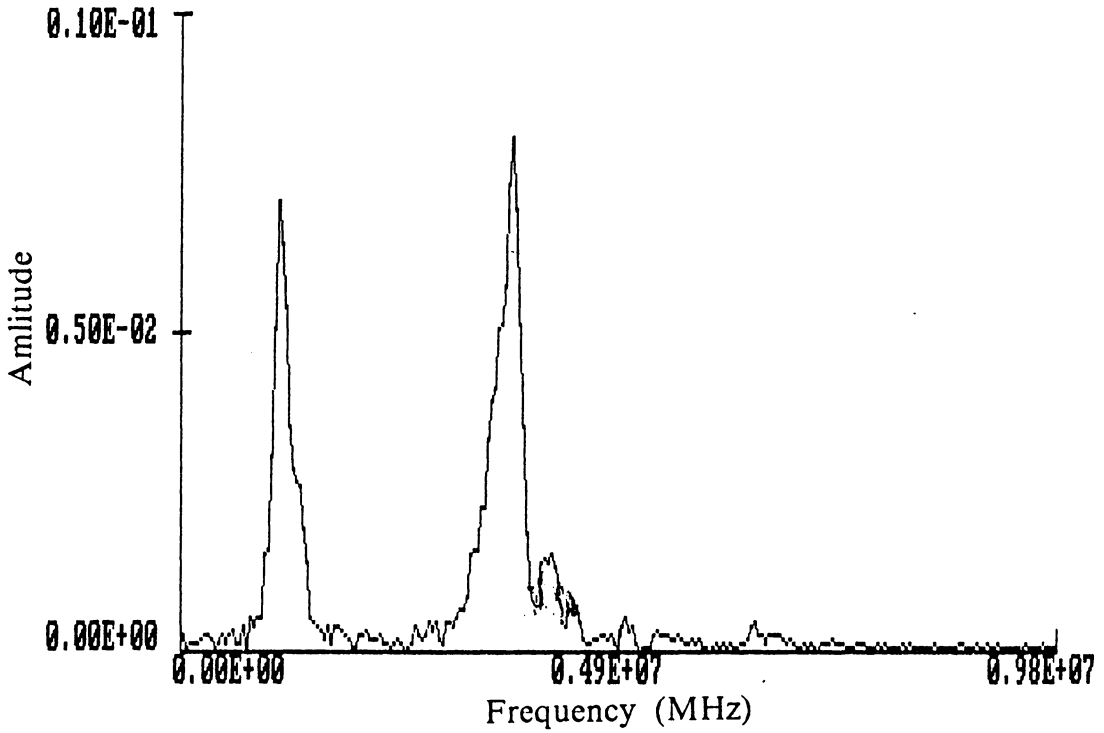

Figure 15. Output spectrum for low damping

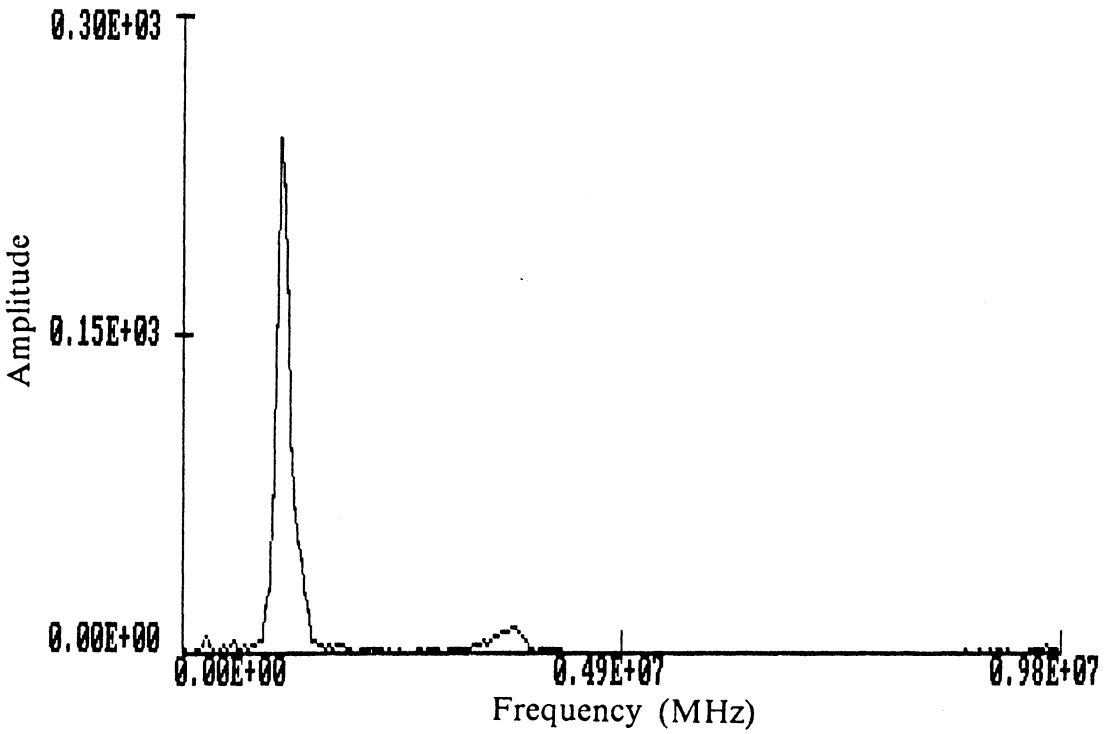

Figure 16. Transfer function for low damping

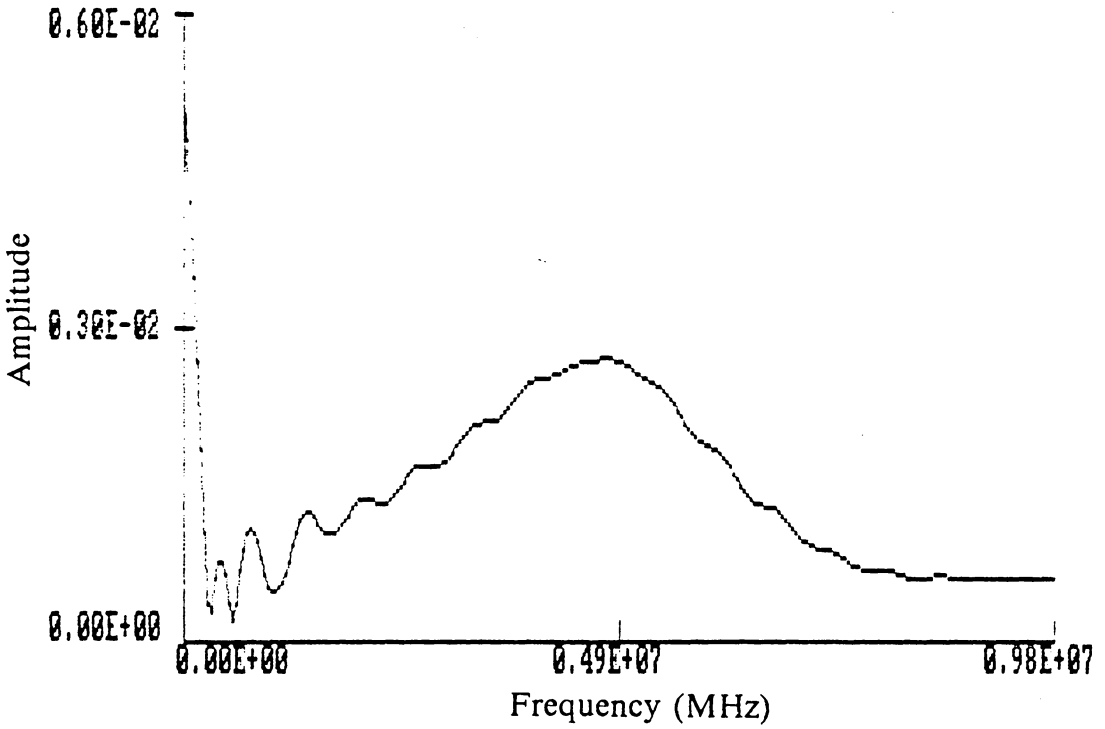

Figure 17. Input spectrum for high damping

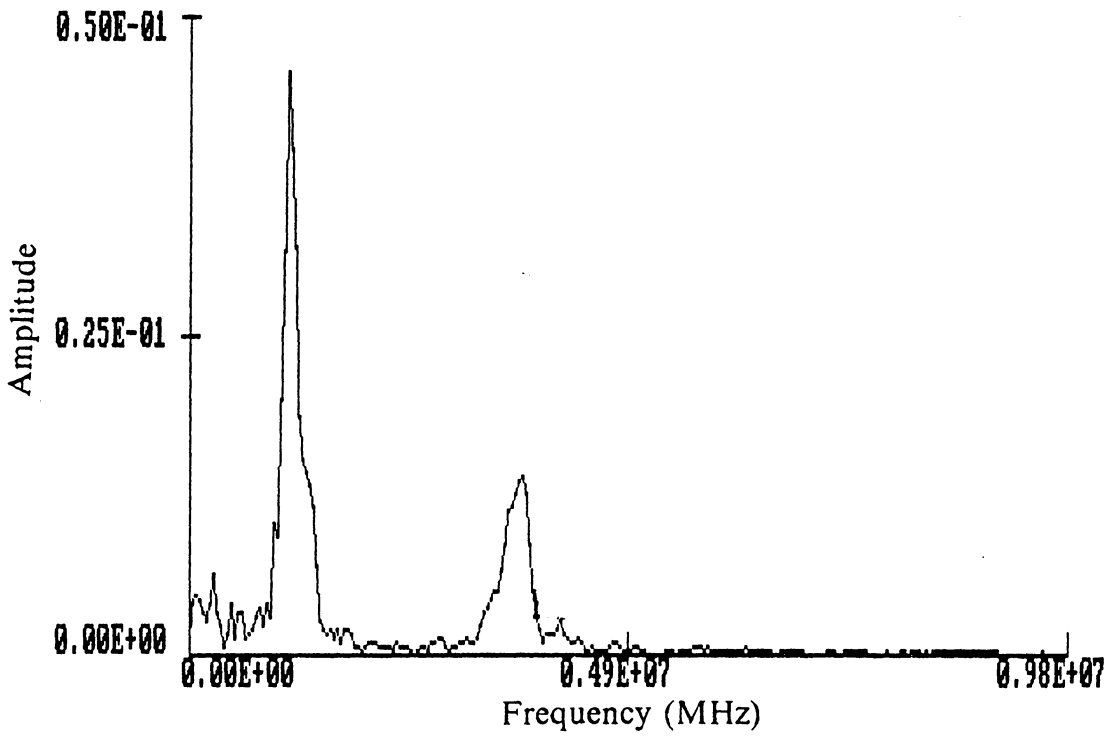

Figure 18. Output spectrum for high damping

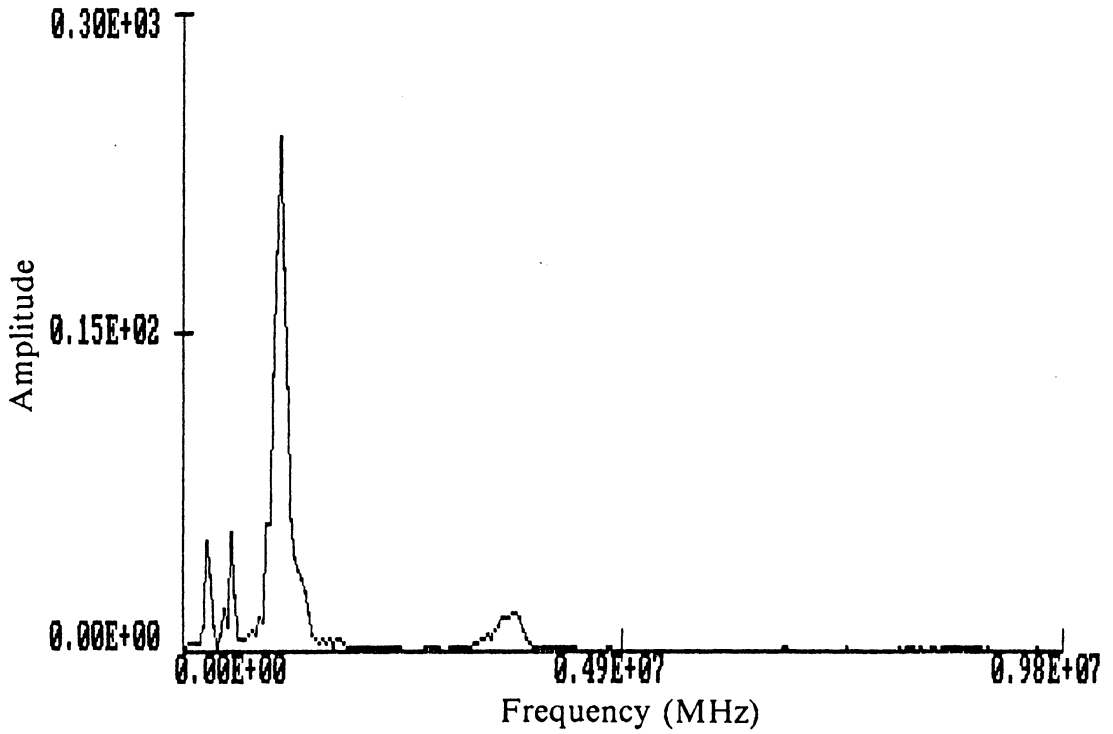

Figure 19. Transfer function for high damping

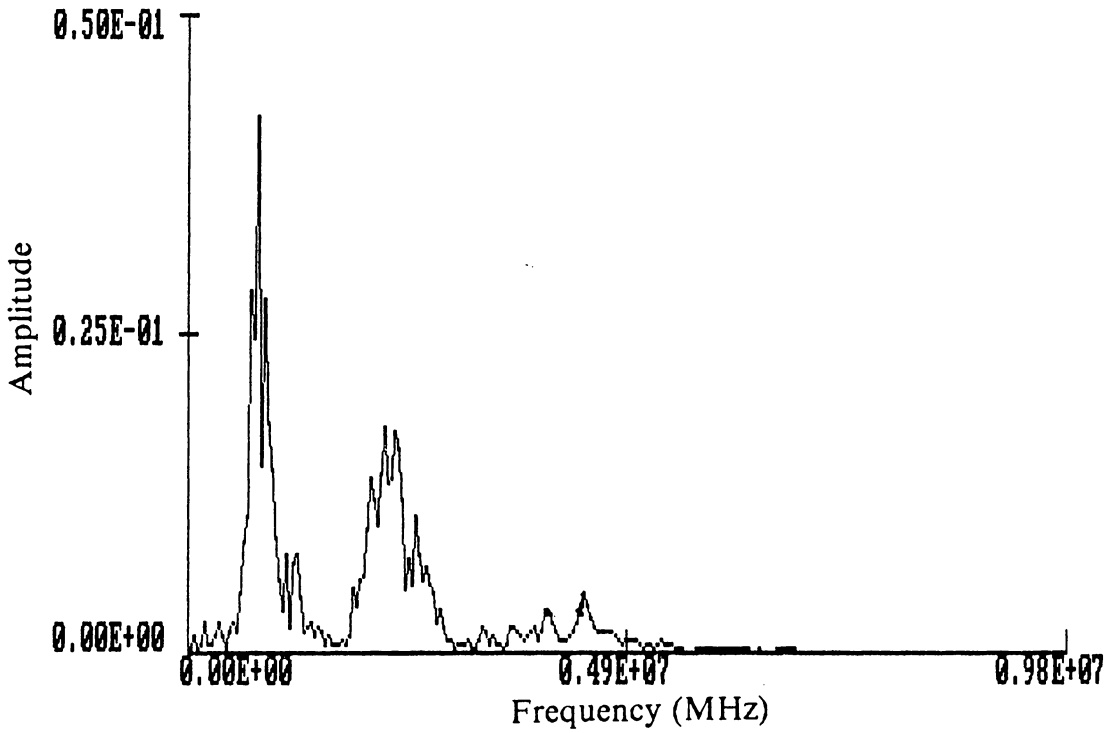

Figure 20. Power spectrum for relatively undamaged specimen

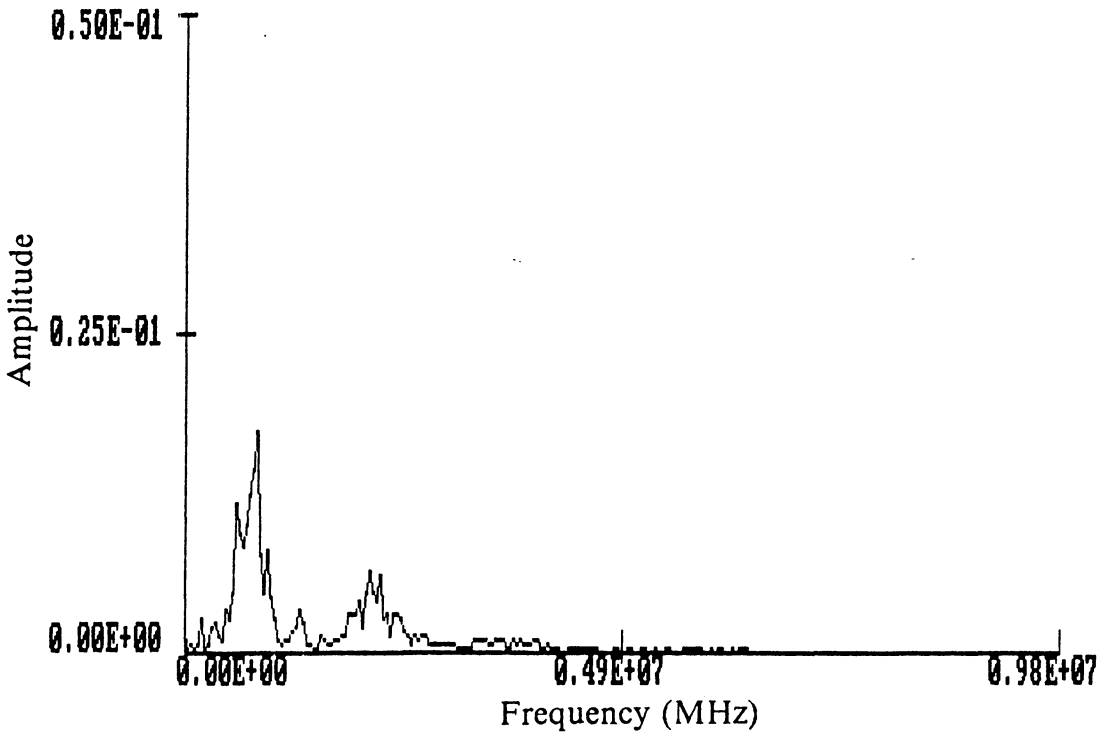

Figure 21. Power Spectrum for heavily damaged specimen

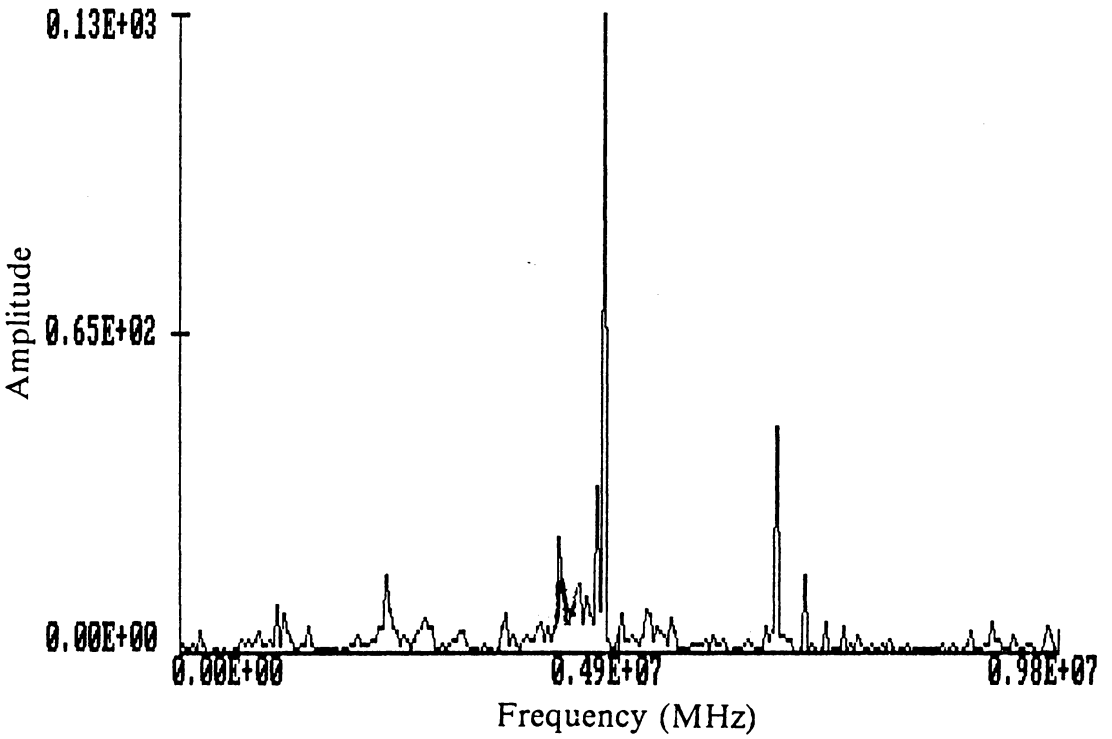

Figure 22. Coherence function for undamaged specimen spectrum over damaged specimen spectrum

viewing plots to obtain general information and making calculations to obtain quantitative parameters. In general, the main software allows the user to disect a signal to obtain a number of parameters which can be related to material state.

Lastly, an SWF Parameters Plotting Routine has been developed so that SWF parameters can be plotted as a function of any other parameter as input by the user. For example, the software was used to plot the change of SWF parameters as a function of azimuthal angle (see chapter on results). First, the user inputs the SWF parameter which is being plotted. Next, the user enters the other parameter, such as azimuthal angle, which is being plotted. Subsequently, the user inputs the number of data points (azimuthal angles). Then the user simply has to enter the value of the angle and the filename for the corresponding SWF parameter for each angle. User entered scaling information controls the bounds on the Y-axis. Using this option, comparison plots can be made between different panels. Hence, a means exists for plotting the variation of an SWF parameter as a function of any other parameter.

System Implementation

Introduction

Fundamentally, the implementation of the system begins with the coupling of the transducers to the material surface. An extended concern being where on the material and at what orientation relative to the material this is performed. This can be combined with information on material construction (ie. ply orientations) and other knowledge of material state to provide fundamentally sound results which can subsequently provide a means for assessing material state.

For work described here on a flat surface, coupling is done directly by applying a layer of ultrasonic couplant (ie. Sonotrace 20, marketed by Echo Ultrasound Inc.) to the transducer faces, placing the transducers on the material surfaces at a specific distance apart and at a particular orientation relative to the material. The present system utilizes the previously mentioned spacing fixture to keep the transducers the prescribed distance, one inch, apart and to allow for precise orientation relative to the specimen geometry. The use of the system with more complex geometries requires the implementation of coupling mechanisms in order to introduce a consistent disturbance to the material. For example, plexiglas wave guides or coupling blocks can be used to transfer the pulse disturbance

to the material surface. The coupling block can be cut to fit the contour of the specimen and also to have a flat surface on which to place the transducer. Specifically, coupling blocks were used to make preliminary tests on aluminum/graphite tubes and direct application of the transducer to the material surface was used to perform a more detailed investigation on graphite/epoxy laminated plates.

As with any nondestructive evaluation technique, the end goal of the acousto-ultrasonic method is to correlate output parameters with the mechanical properties and state of the material. Thus, basic knowledge of the properties for a material can be employed to relate system results and parameters to physical interpretations. In turn, this can be combined with theories of wave propagation and consideration of the system to glean as much information as possible from the signal concerning the material state. Furthermore, attention must be given to flaws or damage which may exist in the material and the effect this may have on overall material properties, construction, wave propagation and how this would manifest itself in the system output. Basically, an attempt is being made to unite as much information as possible to help gain maximum insight from the acousto-ultrasonic method. Hence, this chapter will advance some physical considerations for use in understanding or making relations from acousto-ultrasonic system results.

This chapter will outline the implementation of the acousto-ultrasonic system for both the preliminary investigation of aluminum/graphite tubes and the more involved study of graphite/epoxy laminates. This will include a description of the material systems and some material properties, in hopes of setting the stage for making relationships between SWF parameters and mechanical properties.

Application to Al/Gr Tubes

Description of Al/Gr Tubes

The tubes studied were approximately one inch in diameter and were constucted from Union Carbide P100 fibers imbedded in a 6061 aluminum alloy. The tubes were manufactured by MCI (Materials Concepts Incorporated) of Columbus, Ohio. Ultimately, the tubes are to be used as structural elements for space structures. So, process control and optimization of process parameters are of prime importance. In order to insure this, MCI is pursuing various nondestructive testing techniques and thus provided tubes for a preliminary study of the acousto-ultrasonic technique as applied to the tubes.

First, a liquid metal infiltration technique was utilized to manufacture precursor wire. The precursor wire was then formed into a tube and joined using a clad overlay. For the tubes which were studied all the fibers were running along the length of the tube. Additionally, all tubes studied were 2 plies thick. See Figure 23 for a picture of a representative tube.

The first aspect of the tube construction which should be considered is the exsistence of the clad overlay. Naturally, any geometric discontinuity should be expected to behave in a different manner than the bulk material. Also, a possible debonding might take place between the layers in a system constructed from rolled precursor wire and layers of aluminum cladding. Finally, attention can be shifted to the effects which the aluminum may have on the signal if it is subjected to enough load to cause permanent deformation, due to possible changes in wave speed or to the changes in the attenuation coefficient of the aluminum [ref. 15]. Also, processing variables could affect the microstructure of the aluminum and thus the frequency dependent attenuation coefficient of the material. Although the system appears to mainly sense structural vibrations, the pulse waves, which

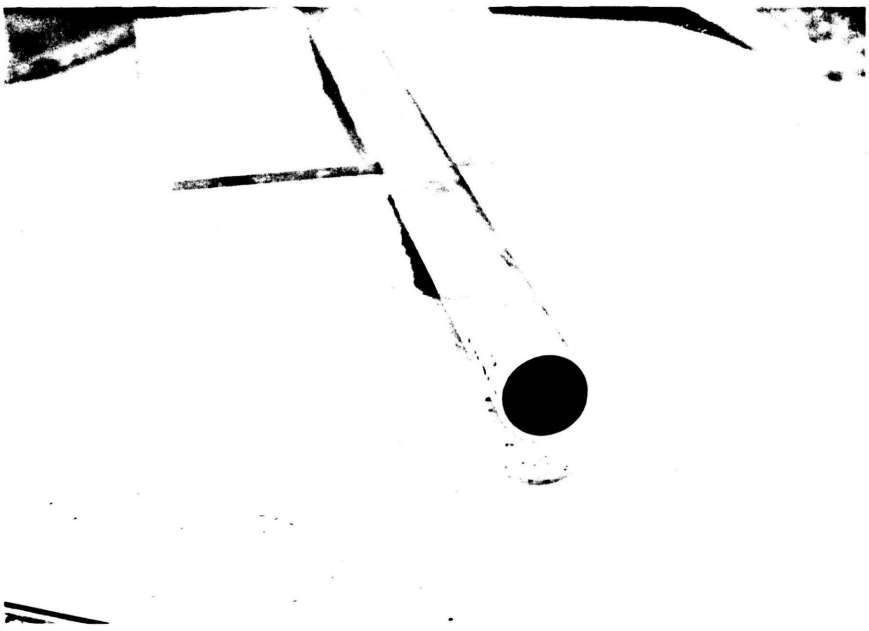

Figure 23. Picture of tube

combine to make the vibration, still travel through the material and are affected by the material's microstructure and the material's resulting frequency dependent attenuation [ref. 15].

Experimental Procedure for Al/Gr Tubes

As mentioned, the research on the aluminum/graphite tubes was preliminary and as a consequence was more qualitative rather than quantitative. Of first concern was the ability to couple the transducers to the specimen surface. This required providing a flat surface for the transducer face and a semi-circular curve surface to allow for coupling with the tube. In order to more fully investigate the acousto-ultrasonic method as applied to the tubes, capabilities were developed to look both at the acousto-ultrasonic signal for a disturbance directed along the tube length and around the circumference of the tube. Hence, a number of tests were performed using both methods, in order to compare sensitivity.

The first tests were performed on the tubes by sending stress waves along the length of the tube using the configuration pictured in Figure 24.
Tests were performed at various locations along the length and on the circumference in order to note the general variation of the detected output. Additionally, the method was used to note differences between the system output for both a mechanically loaded and a virgin tube. Specifically, tests were performed at various locations along the circumference on both of these specimens to determine the circumferential variation.

Next, work was done to develop the capability to perform the acousto-ultrasonic method around the circumference of the tube. A coupling block had to be designed to couple both transducers to the tubes (Figure 25). It was decided to cut a triangle out of 3/4 inch thick plexiglas and to cut an arc out of the apex of the triangle to fit the contour of the tube. Then thin cuts were made from the center of the drilled hole and the center of the side which was opposite the tip where the hole

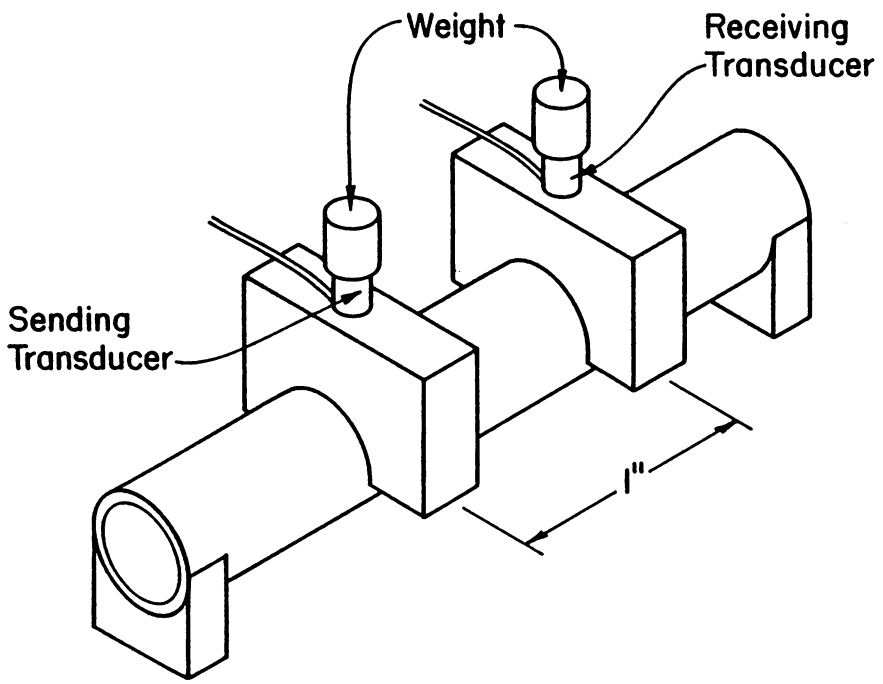

Figure 24. Fixture for length wise acousto-ultrasonic application

was cut. Thus, the slits were cut co-linear and to a length so that approximately a quarter inch of material was holding the two half triangles together. Hence, the side with the slit cut in the middle provided a surface with two sides, one for the sending transducer and one for the receiving transducer. The arc provided a means to couple the block to the tube surface. However, ensuing tests showed that a disproportionate amount of the energy was flowing through the plexiglas that was left between the two cuts. As a result, the slots were widened and finally joined, thus forming two symmetric half pieces. These were then bonded to a piece of corrugated cardboard which acted as an ultrasonic insulator, so that all energy reaching the receiver entered from the tube.
The disturbance is transferred along the circumference of the tube and received at the arc on the opposite side of the cardboard, where it is sent to the receiving transducer. Ultimately, this design proved to be adequate for relatively sensitive signal reception.

Next, a variety of alterations had to be made to the testing procedure in order to attain the reproducibility which was sought. Basically, these involved increased attention to block alignment, transducer placement on the coupling block and the effect of the coaxial cables pulling on the transducers. Specifically, it was found that to obtain a reproducible signal, the cables had to be elevated slightly, before the connection to the transducer. With these modifications the system provided consistent results.

Having established reproducible results, tests were performed to note how the circumferential acousto-ultrasonic signal compared to the lengthwise signal and how the circumferential signal varied with position.

The preliminary testing of graphite/aluminum tubes established the feasibility of studying processing variations using acousto-ultrasonics.

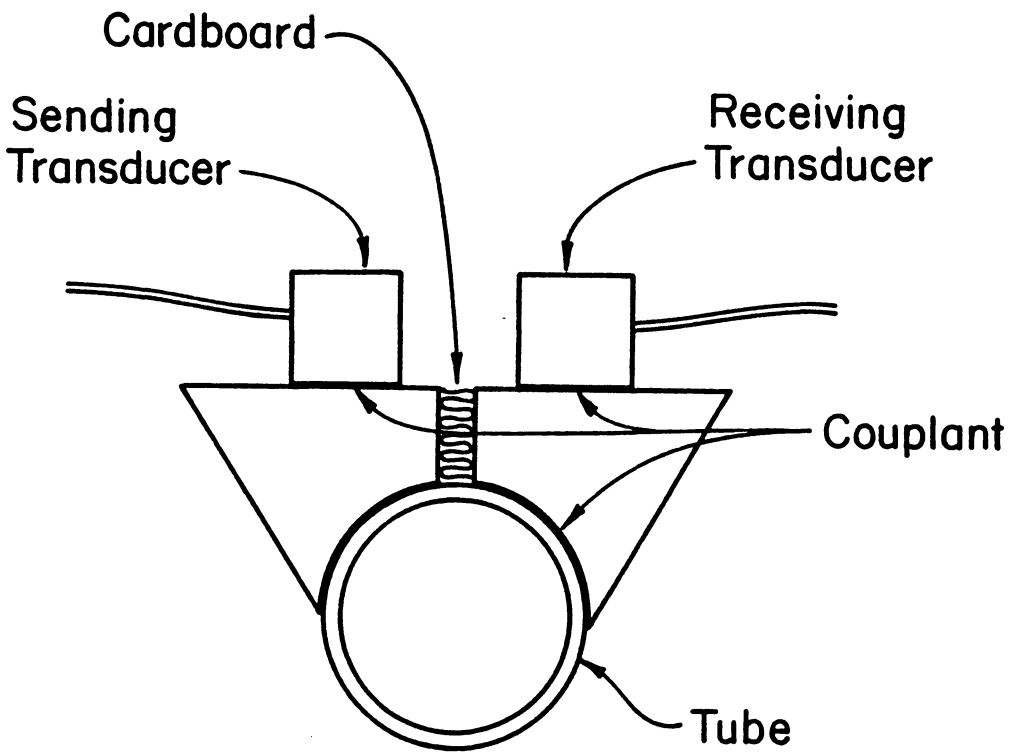

Figure 25. Fixture for Circumferential acousto-ultrasonic application

Application for Graphite/Epoxy Plates

Experimental Procedure for Graphite/Epoxy Plates

With considerable evidence having previously established that the acousto-ultrasonic method is sensitive to variations in the condition of graphite/epoxy materials, a systematic basic study was undertaken. The graphite/epoxy plates used in this research were constructed from Hercules AS4 3501 prepreg.. In order to gain a general understanding of the acousto-ultrasonic method as applied to laminated graphite/epoxy plates, a number of lay-ups were utilized in the testing procedure. Included are three 4-ply layups all with two 0 degree inner plies (fundamental element), an 8-ply all zero degree layup and a 4-ply zero degree layup with a prefabricated delamination at the midply interface. Experiments can be grouped into three phases:

- Phase one- Acousto-ultrasonic behavior of unidirectional graphite/epoxy
- Phase two- Acousto-ultrasonic behavior of the fundamental element as affected by ply constraint
- Phase three- Acousto-ultrasonic behavior of fundamental element as affected by delamination.

Phase One Experiments

First, an 18 inch by 12 inch [0,0,0,0] laminate was constructed. Since this configuration is relatively simple to understand, it was used to conduct basic tests to be compared to material properties. Ensuing figures illustrate the variation of several material properties as a function of azimuthal angle to fiber orientation (Figure 26).

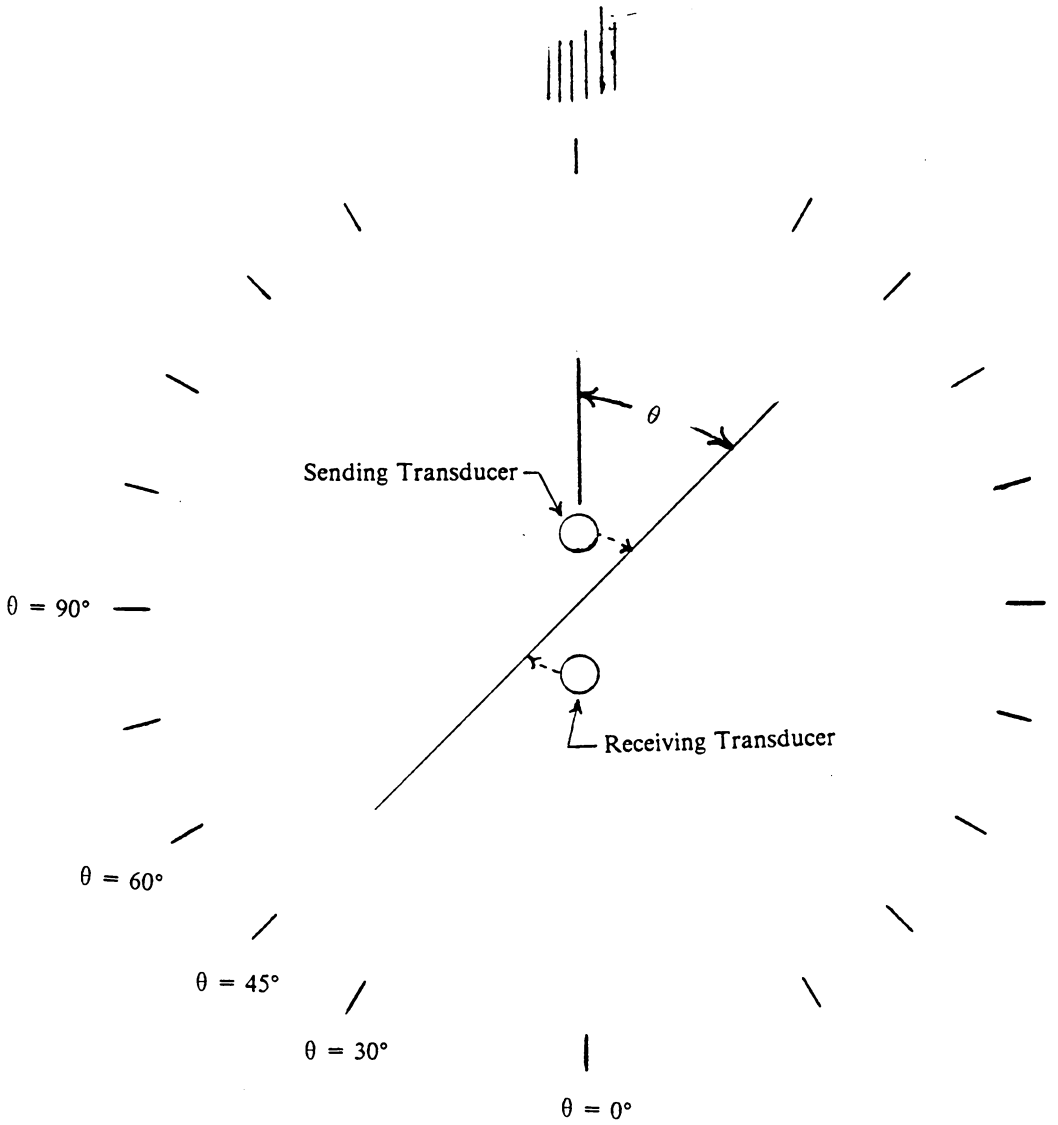

Figure 26. Definition of azimuthal angle on gr/ep plates

Since the material properties are what determines the character of the wave propagation, a relationship should exist between property variation with angle and stress wave variation with angle. In these plots, the following material properties were used :

$$E_1 = 20.8 \times 10^6 psi$$

$$E_2 = 1.43 \times 10^6 psi$$

$$\nu_{12} = .28$$

$$G_{12} = .86 \times 10^6 psi$$

Observe the variation of E_x as a function of fiber orientation in Figure 27.

Note, that E_x is an indication of the stiffness in a particular direction for a state of uniaxial stress. In other words, it is the stiffness for a piece of material which is loaded, so that Poisson's ratio effects from end constraints do not add extra stiffness. Note in Figure 27 how the curve drops quickly at low angles from its peak value at 0 degrees. Next, observe the variation of $\overline{Q}_{11}$ as function of angle in Figure 28, where $\overline{Q}_{11}$ is the first term in the transformed reduced stiffness matrix.

Notice how the value of $\overline{Q}_{11}$ drops slowly. Additionally, note the way the curve bows outward. Thus the effect of material constraint is predominant at the low angles. Both E_x and $\overline{Q}_{11}$ reach asymptotic values, but E_x at a much faster rate. Additionally, plots are given of the variation of Poisson's ratio, the coefficient of mutual influence and the shear modulus as they vary with orientation to fiber direction (Figures 29-31).

Since these basic type of mechanical properties are what dictates global material behavior in any linear elastic model, they are related to the basic nature of any linear elastic model of wave transfer. Thus, a relationship should exist between the way in which the basic material properties vary with angle and the way stress wave propagation varies with angle. Hence, figures have been included so that comparisons can be made to set the stage for later interpretations.

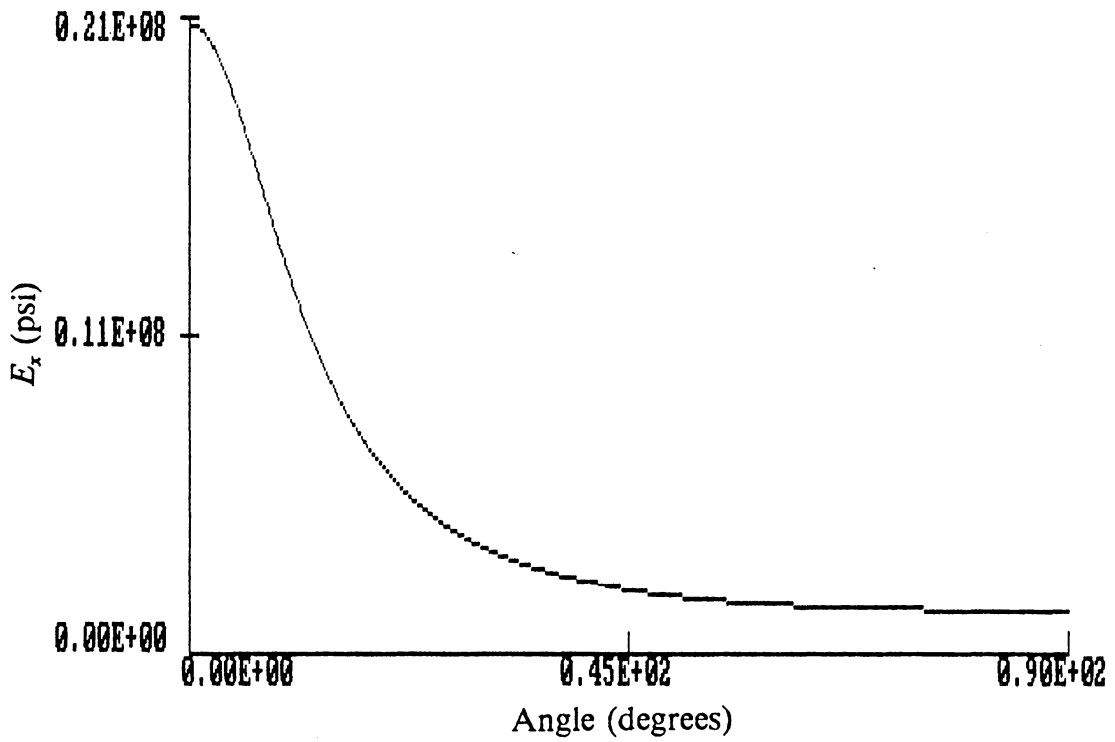

Figure 27. Plot of E_x as a function of azimuthal angle

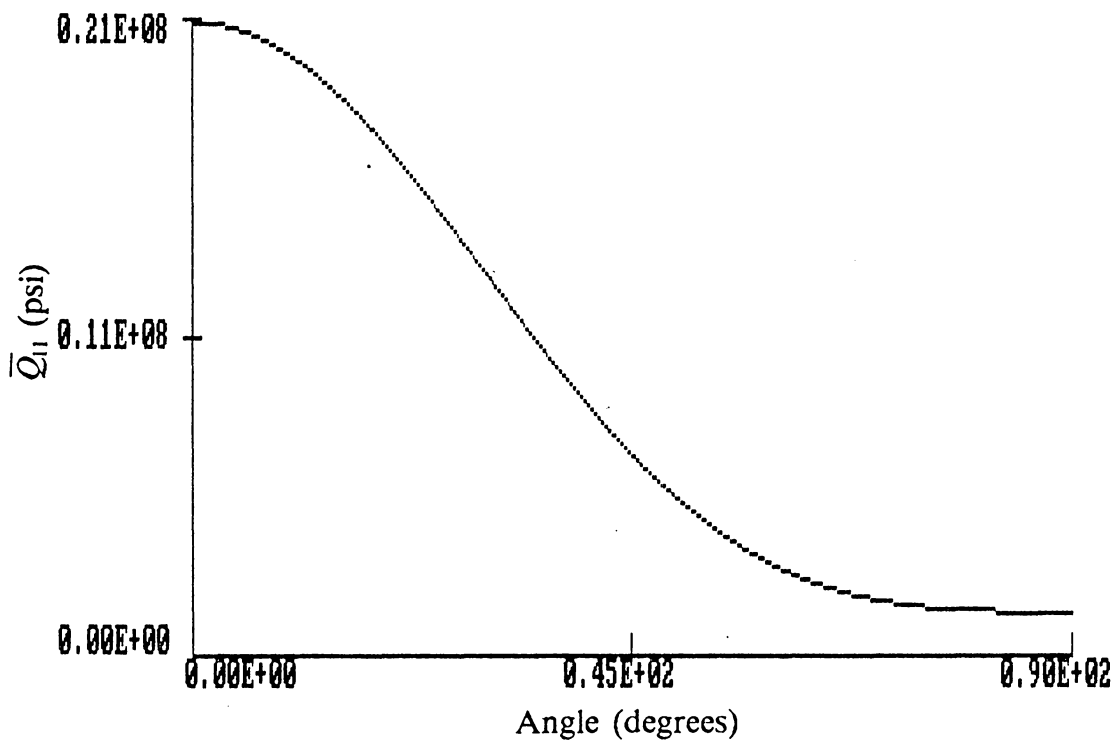

Figure 28. Plot of $\overline{Q}_{11}$ as a function of azimuthal angle

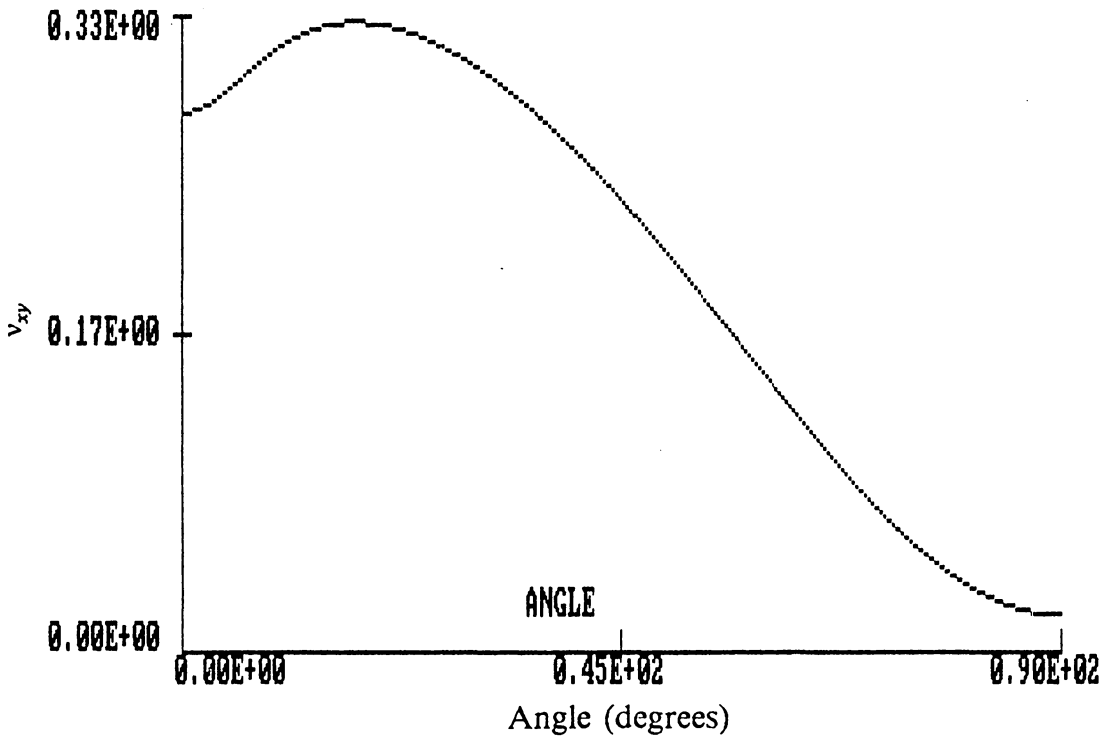

Figure 29. Plot of ν_{xy} as a function of azimuthal angle

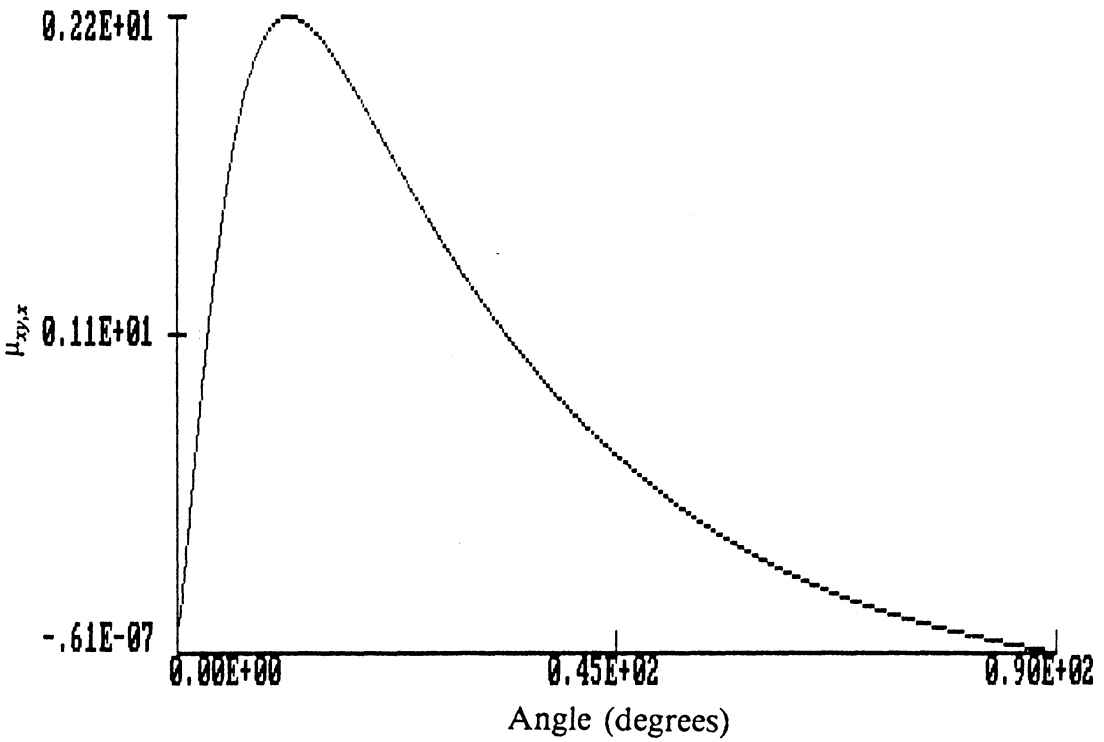

Figure 30. Plot of $\mu_{xy,x}$ as a function of azimuthal angle

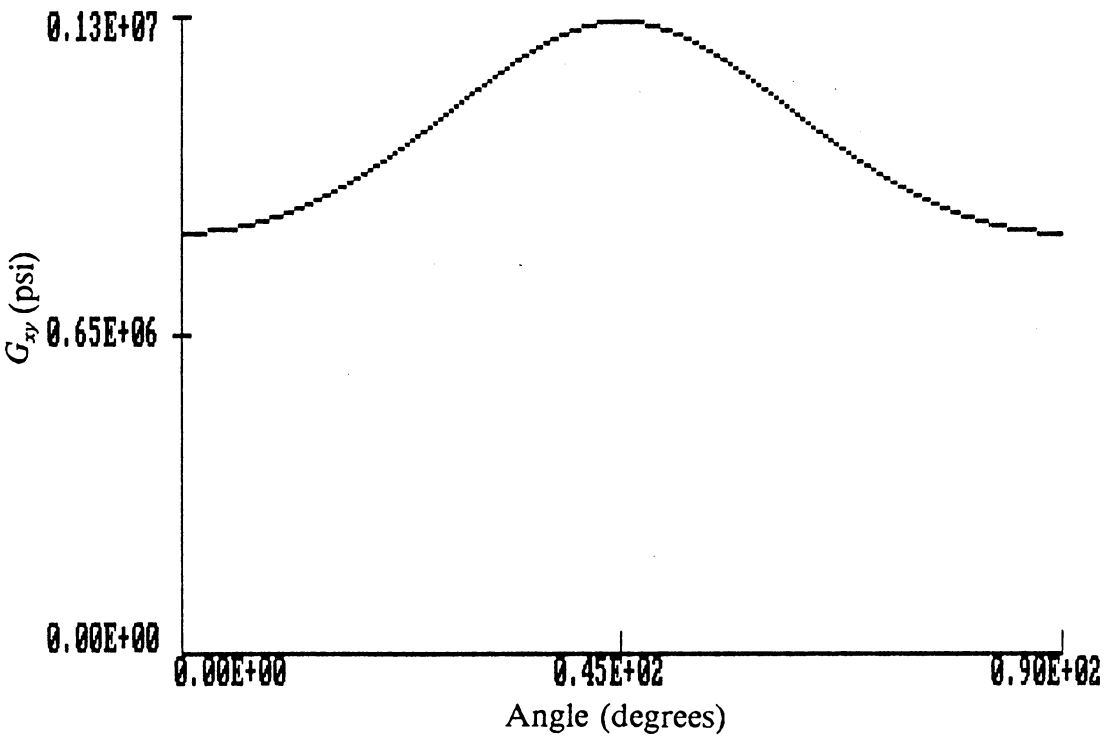

Figure 31. Plot of G_{xy} as a function of azimuthal angle

The first test performed in the beginning phase examined how the signal varied as a function of azimuthal angle for a 4-ply zero degree laminate. It was decided that the variation was best characterized by considering the SWF as a function of azimuthal angle. Voltage/time plots were used in conjunction with amplitude/frequency plots to determine time domain gates and frequency filters for calculation of SWF parameters.

An 8-ply unidirectional graphite/epoxy plate was examined parallel and transverse to the fiber direction to gain insight into the influence of plate thickness on the acousto-ultrasonic technique.

A few tests were performed to see how the signal changed if the receiving transducer was placed on the opposite side of the plate as the sending transducer. The distance between the transducers was kept at one inch and a weight was put on the material above the receiving transducer to simulate as close as possible the conventional SWF configuration.

Two additional tests were conducted, one being to ascertain the effect of changing the 5 MHz sending transducer to a 10 MHz sending transducer on system output and the other being to note the effect of applying pressure on the plate between the transducers.

The results of these tests will be discussed in a following chapter, as it is the purpose of this chapter to introduce the tests which were conducted.

A certain amount of information on the composite material system is essential to making statements on an acousto-ultrasonic signal. Basically, the level to which one can model a problem is directly related to the amount of basic information concerning the system. One must understand what exists originally to understand how it could degrade and how this might affect its general behavior. Hence, this chapter provides only slight information on the tubes, since only basic tests were performed. But, a more detailed body of information is provided for the epoxy/graphite laminates, in order to provide a more detailed analysis of results and a resulting more refined NDT technique.

Phase Two Experiments

The purpose of these tests was quite simply to determine the effect of ply configuration on the acousto-ultrasonic technique. This involved conducting tests analogous to those performed on the 4-ply zero degree plate on both a [90,0,0,90] and a [45,0,0,45] laminated plate. Notice that both laminates contain the fundamental element (two zero degree inner plies). Results can be used to determine the effect of outer ply constraint on SWF parameters as a function of azimuthal angle. The damage development in constrained plies is governed by the state of stress in those plies, which is dictated by constraining plies [ref. 16]. Hence, an understanding of the mechanical effects of ply constraint is essential to understanding the damage process. Since the ultimate goal of any NDE technique is to assess material state and predict future material behavior, evaluating the effects of ply constraint could have obvious application to developing an NDE method rooted to the basic mechanics which govern damage development in the critical element. More specifically, test results will show the difference between the SWF parameters as a function of angle for these laminates, indicating the effect of the outer plies on energy flow characteristics. Additionally, this information can be used to note the way in which the signal differs in the 0 degree direction and the 90 degree direction for the [90,0,0,90] laminate to ascertain the sensitivity of the method to both inner and outer plies.

Phase Three Experiments

Finally, tests similar to those conducted on the other laminates were performed on a 4-ply zero degree laminate with a prefabricated delamination. The delamination was introduced by placing a quarter inch by quarter inch piece of folded acetate between the mid-plies during lay-up, this being the beginning of a series of tests to determine the way in which damage alters system output. Since the purpose of the system is ultimately to assess the damage state in composite materials, this series

of tests has obvious application. However, with an understanding of the basic physics associated with the method, an indication might be obtained as to the basic mechanical effects of damage. This information is important to understanding the way damage alters material state and how this relates to the damage process, which is precisely the reason a need for NDT techniques exists. Hence, this series of tests is designed with the thought of providing a complementary body of knowledge to be utilized for a more advance NDT technique, which actually considers the exact mechanical effects of damage.

Results

The results obtained during the course of carrying out the experimental procedure are presented here.

Al/Gr Tube Results

The preliminary tests on the tubes demonstrated the ability of the method to be applied to different geometries.

A result of applying the method to a virgin tube can be seen in Figure 32.
In comparison, notice the results obtained by applying the test to a tube which has been mechanically loaded, Figure 33.
Notice the signal for the loaded tube has additional frequency content and has in general a more attenuated voltage level (See Appendix A). Also, both the signals obtained from the clad overlay seam contained different peak frequencies than did signals obtained from other positions around the circumference. Moreover, reloading of the originally loaded tube showed that the tube failed at the

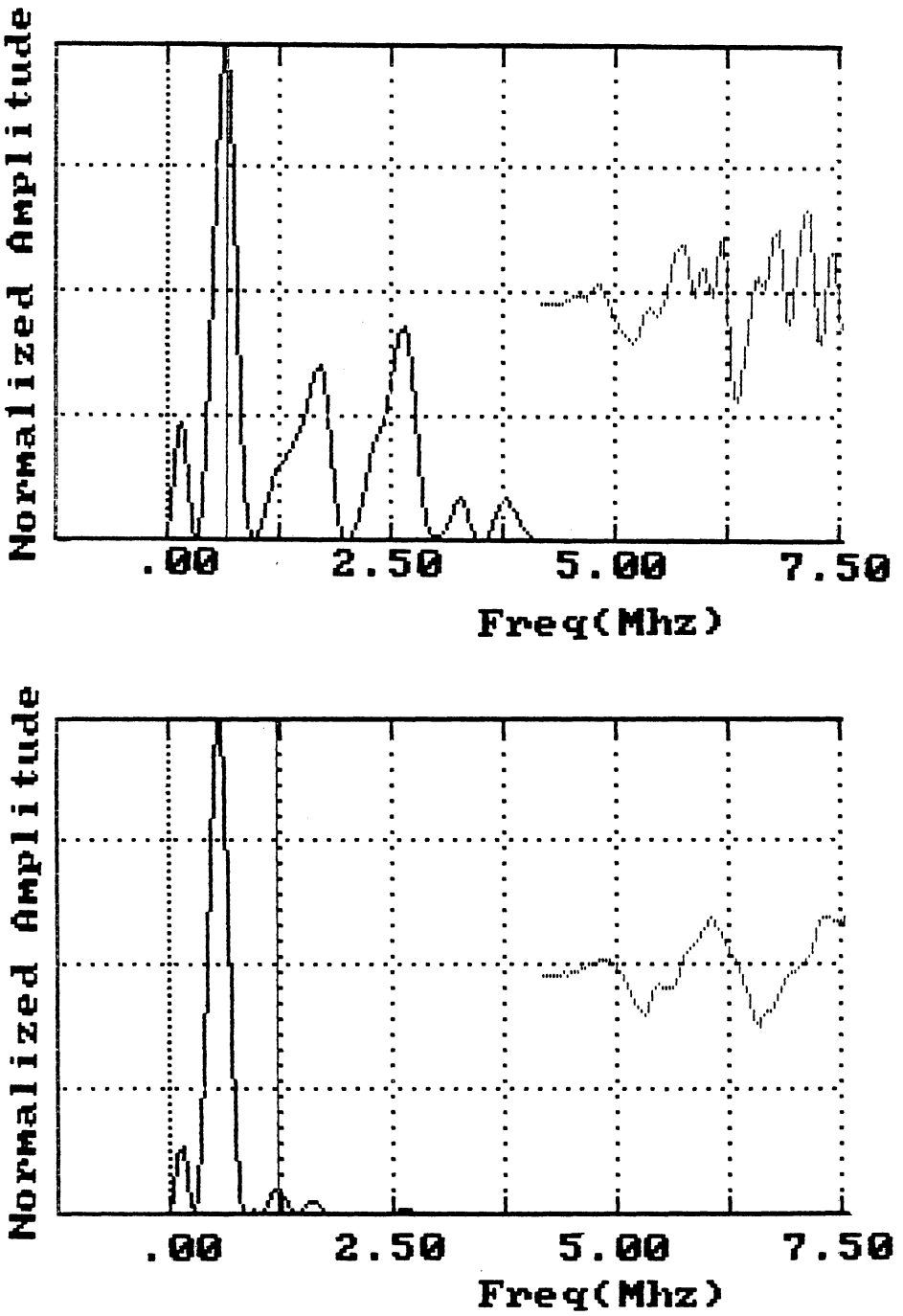

Figure 32. Virgin tube a)Region with clad overlay b)Region without clad overlay

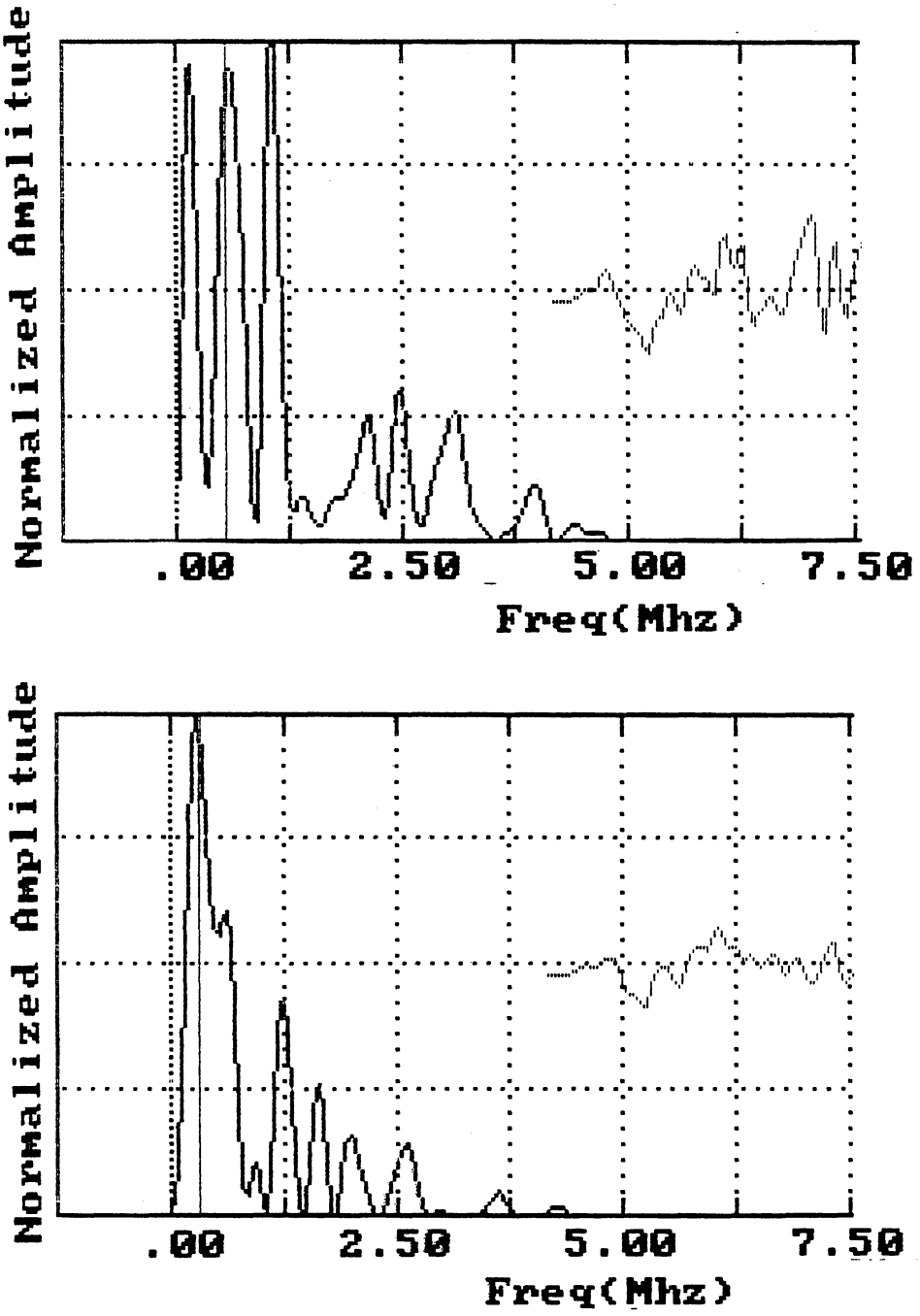

Figure 33. Loaded tube a)Region with clad overlay b)Region without clad overlay

position of the detected seam. Hence, it appears that the acousto-ultrasonic technique is sensitive to material variability in the Gr/Al tubes which could lead to failure. Figure 34 shows the variation of lengthwise SWF1 as a function of circumference, for the loaded tube. Note, the area around the circumference where 3 regions of low SWF1 exist and are bordered by high energy points (Positions 2, 3 and 4 on the circumference). Region 1 on the circumference, a high signal energy region, corresponds to the circumferential region of failure. The unloaded tube showed much less variation in SWF1 around the circumference, all values being between those at position 0 and position 1 in loaded tube (see appendix A).

In Figure 35 and Figure 36, a comparison can be seen between the variation of the lengthwise and circumferential SWF2 for an unloaded tube. The lengthwise SWF2 drops in the same region where the circumferential SWF2 peaks. This could possibly be due to a clad overlay region.

Finally, Figure 37 shows how the lengthwise SWF1 varies with length at a given circumference. The linear relationship with position only occurred in one portion along the length. However, the variation seemed to exist for various regions around the circumference in that portion of length. In fact, all SWF1 values for the high position on the graph were higher than those for the low position, regardless of circumferential region.

In general, results showed that signals varied from place to place on one tube, varied from tube to tube, varied as a result of a clad overlay and varied as a result of mechanical loading. Both the circumferential and the lengthwise application of the method seem to sense a signal variation in the same region, which altered SWF2 but did not result in changes in SWF1. Hence, in certain instances SWF2 may indicate material variation which SWF1 does not sense.

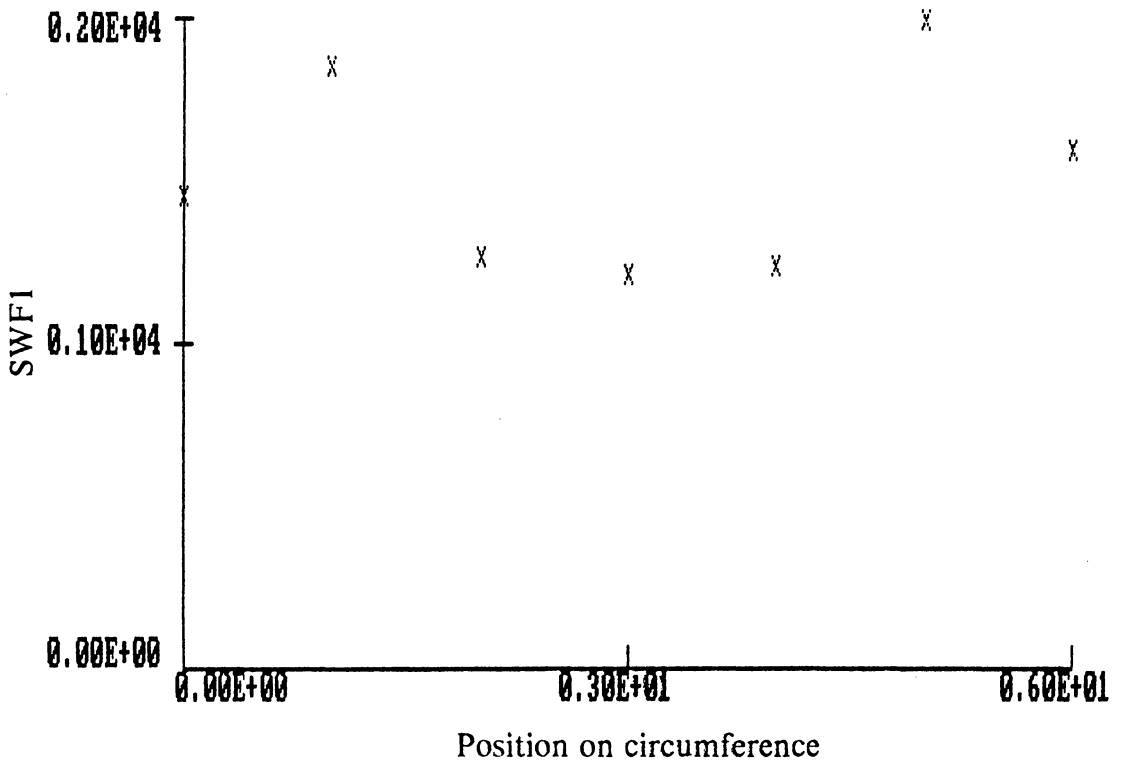

Figure 34. SWF1 versus circumferential region for lengthwise SWF of loaded tube

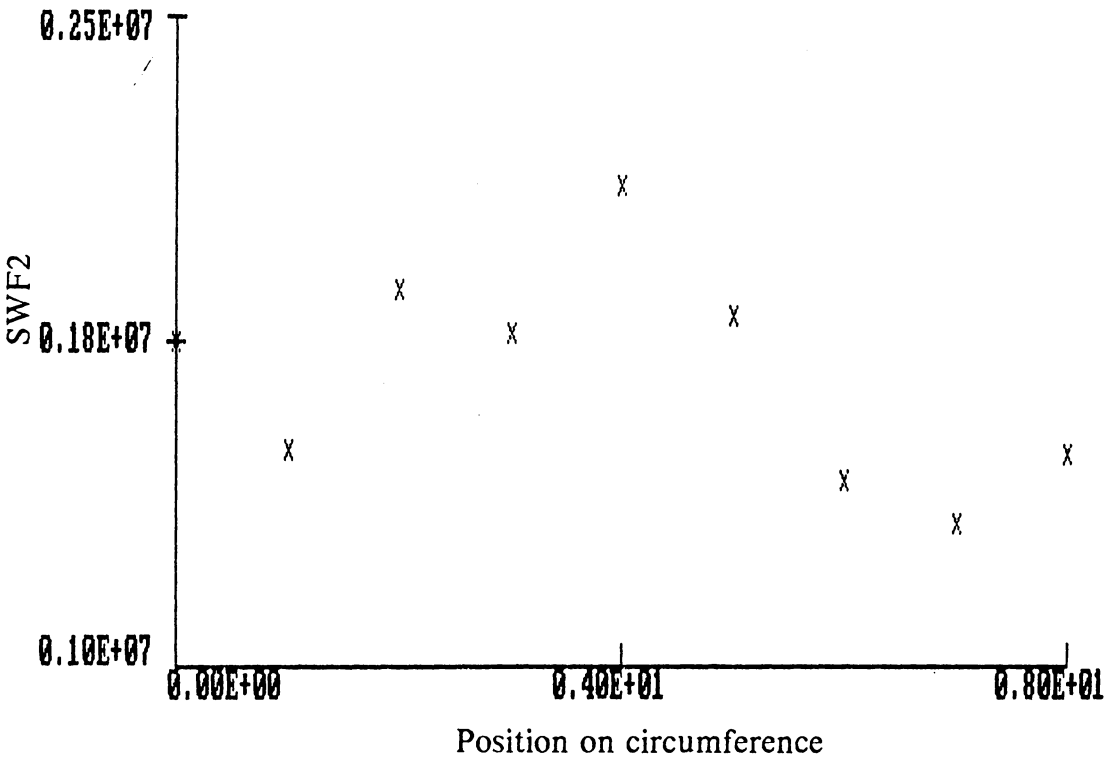

Figure 35. SWF2 versus circumferential region for lengthwise SWF of unloaded tube

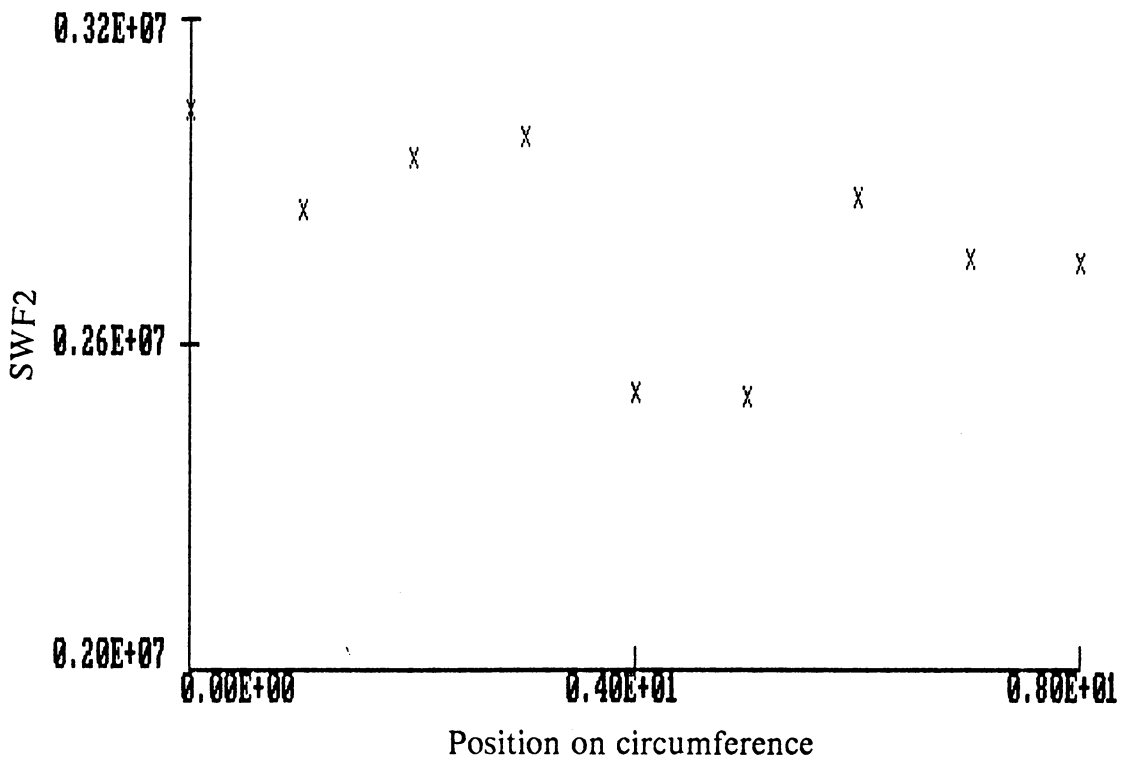

Figure 36. SWF2 versus circumferential region for circumferential SWF of unloaded tube

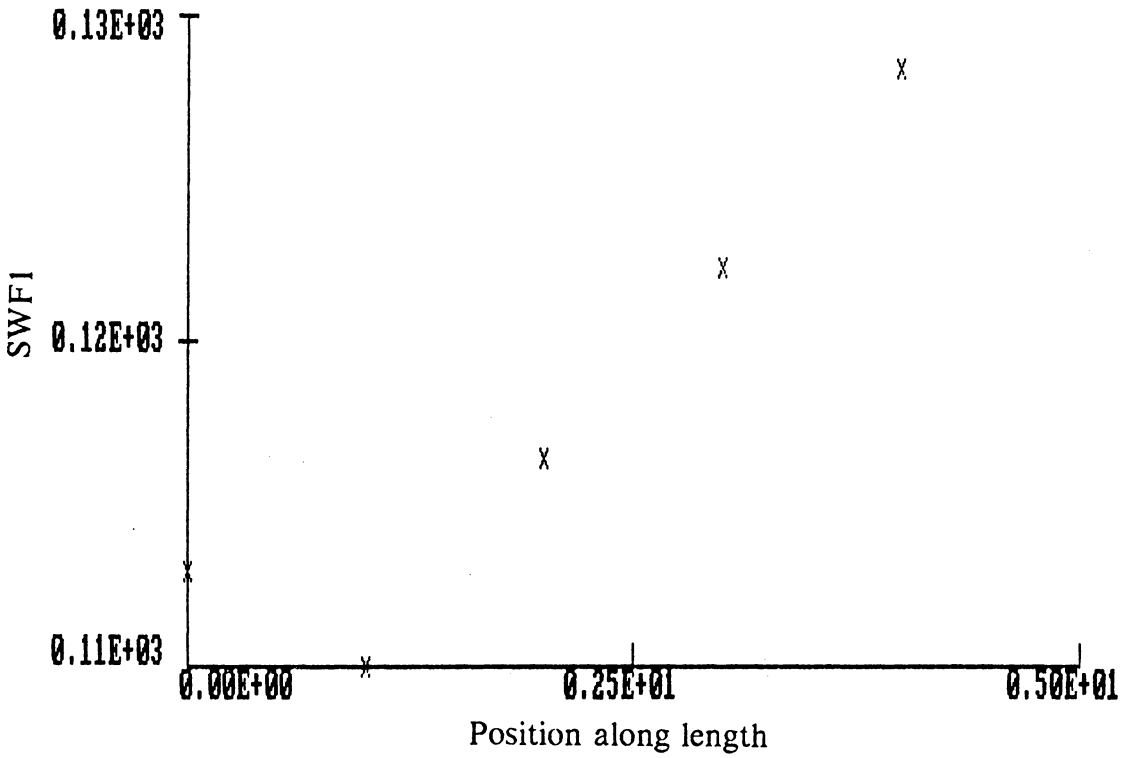

Figure 37. SWF1 versus length region for lengthwise SWF of unloaded tube

Graphite/Epoxy Plate Results

Description of Graphite/Epoxy Results

The results of the tests conducted on the graphite/epoxy plates will be presented in three sub-sections. The first being ancilliary tests conducted simply to obtain information on general wave propagation characteristics. Second, will be the results of the tests conducted to note the general variation of the SWF parameters as a function of azimuthal angle for the 4-ply layups. Lastly, will be a presentation of the results for a delaminated specimen.

Results of Phase One

The first tests were conducted to note the change in the frequency spectrum for a change in plate thickness. A representive spectrum for the 4-ply specimen is seen in Figure 38
and for an 8-ply specimen, in Figure 39.
Note that the 8-ply laminate contains a 1.7 MHz peak in the spectrum instead of the 3.4 MHz peak in the spectrum of the 4-ply specimen. Also, the 8-ply (Figure 40) contains a 600 KHz resonance in place of the 1.0-1.2 MHz peak in the 4-ply specimen.

Tests conducted to interrogate the effect of placing the receiving transducer on the bottom instead of the top revealed essentially the same spectrum, except the high frequency peak was lowered form 3.4 MHz to 3.0 MHz (See Figure 41).

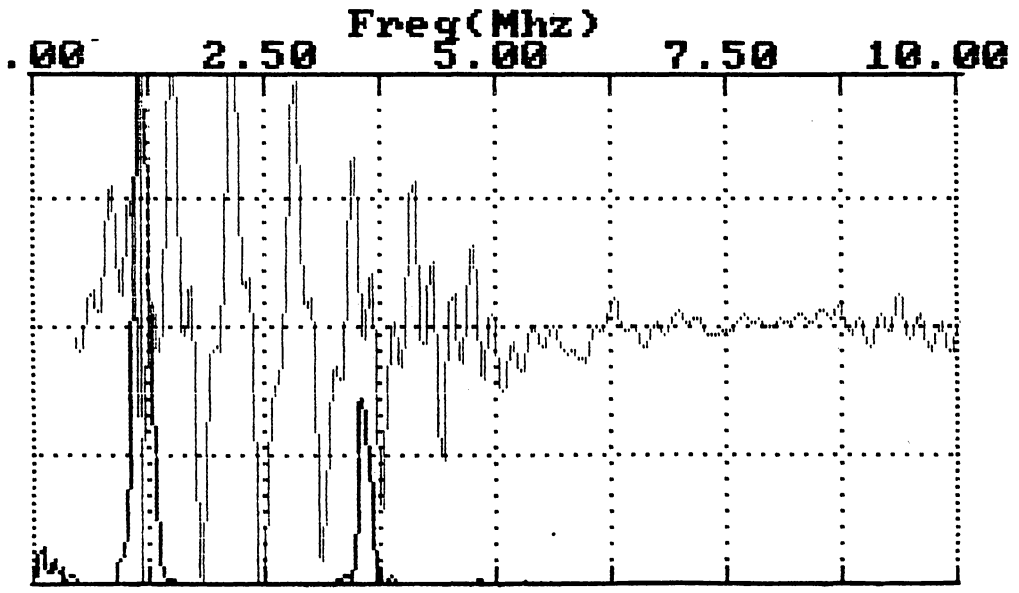

Figure 38. Spectrum for 4-ply zero degree laminate

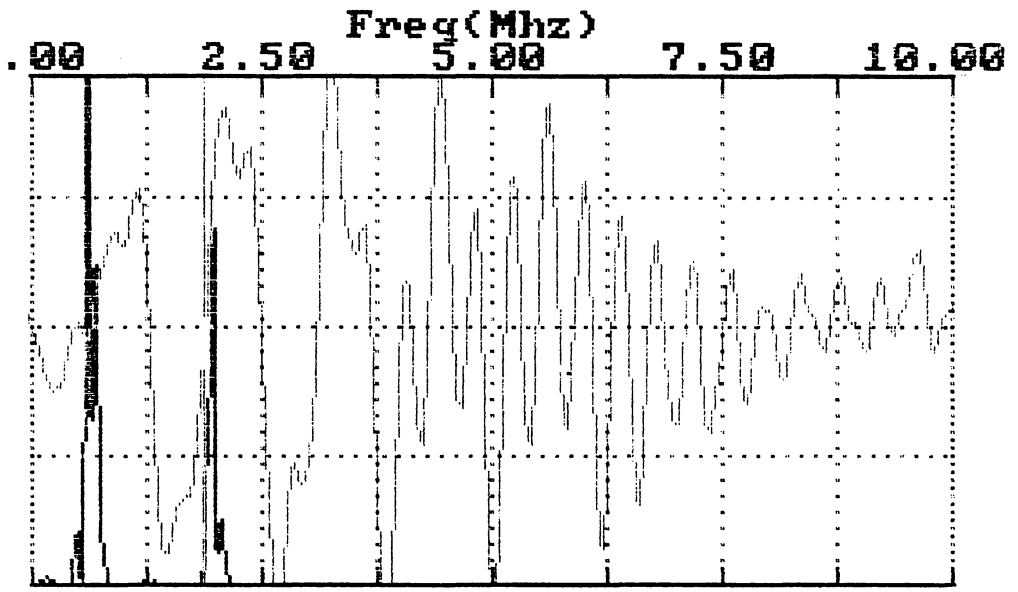

Figure 39. Spectrum for 8-ply zero degree laminate

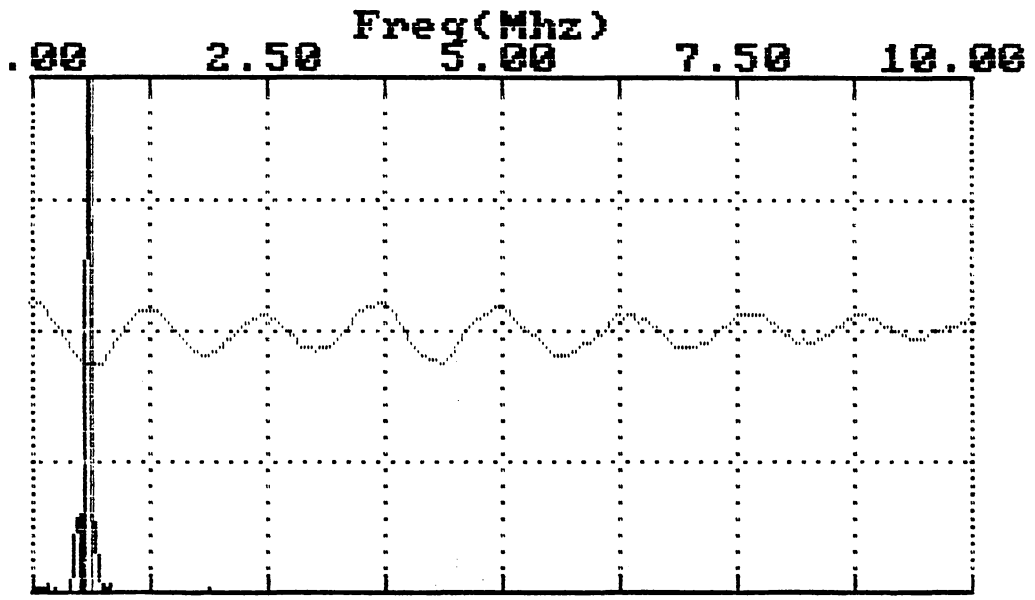

Figure 40. Spectrum for back part of wave from 8-ply zero degree laminate

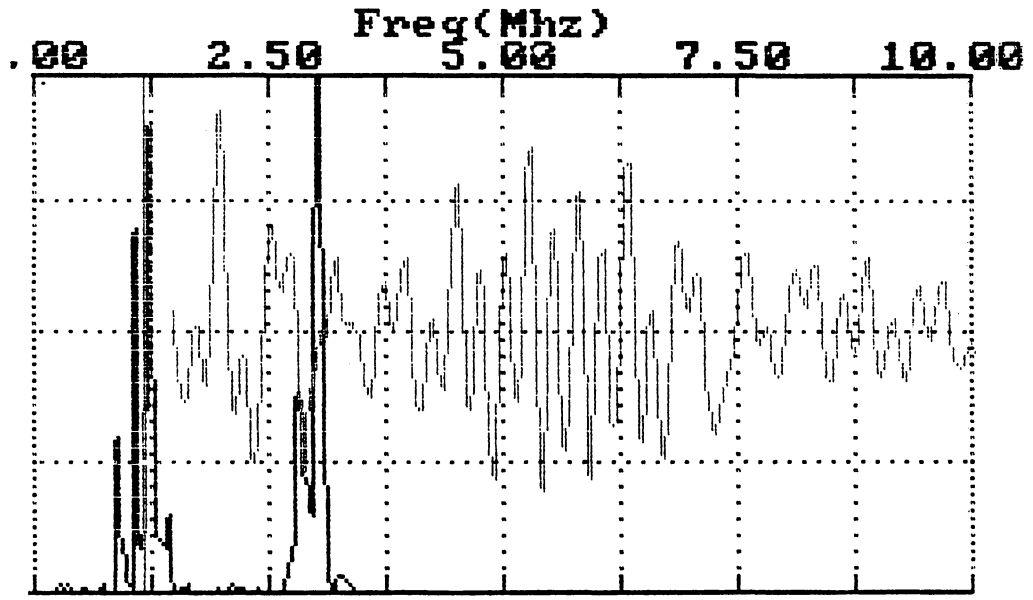

Figure 41. Spectrum as seen with receiving transducer on bottom of laminate

A test conducted to note the effect of changing the input transducer revealed no real change in the spectrum as a result of changing transducers. In particular, notice the spectrum of a 10 MHz sending transducer, Figure 42, compared to that of the regular 5 MHz transducer, Figure 43.

Figures 43 and 44 show the results of the test conducted to determine the effect on the output spectrum of placing pressure on the specimen between transducers.
Notice that both the low frequency and high frequency peak decreased in energy content.

SWFs Versus Azimuthal Angle Results for Phase One and Two

Tests were conducted on the [0,0,0,0], the [90,0,0,90] and the [45,0,0,45] laminates to note variations of the SWF parameters with azimuthal angle.

Results of work on the 4-ply zero degree laminate displayed a couple of interesting features. First, the signal contained a high amplitude 1-1.2 MHz component at the beginning of the signal (approximately 2.5 microseconds after the trigger) for the zero degree direction. Following this was a lower amplitude high frequency component, Figure 45.
Next, notice in the spectrum of the signal for the zero direction that the low frequency content shows up as a high amplitude peak at 1-1.2 MHz while the high frequency content shows up as a lower amplitude peak at about 3.4 MHz, Figure 46.
In Figures 47-50, corresponding plots are given for the 20 degree and 90 degree directions, respectively.
Comparing these, notice the relatively large high frequency content in the twenty degree direction and the relatively small amount of high frequency content in the ninety degree direction. In fact, the relatively little high frequency content in the ninety degree direction causes the time signal to appear as a pure sine wave signal.

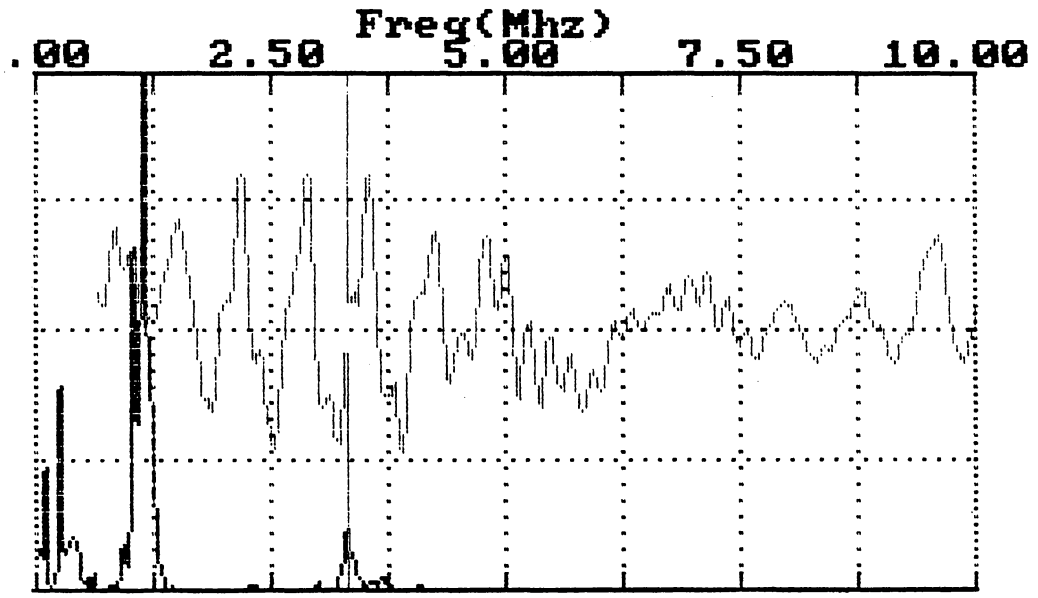

Figure 42. Output spectrum for ten MHz sending transducer

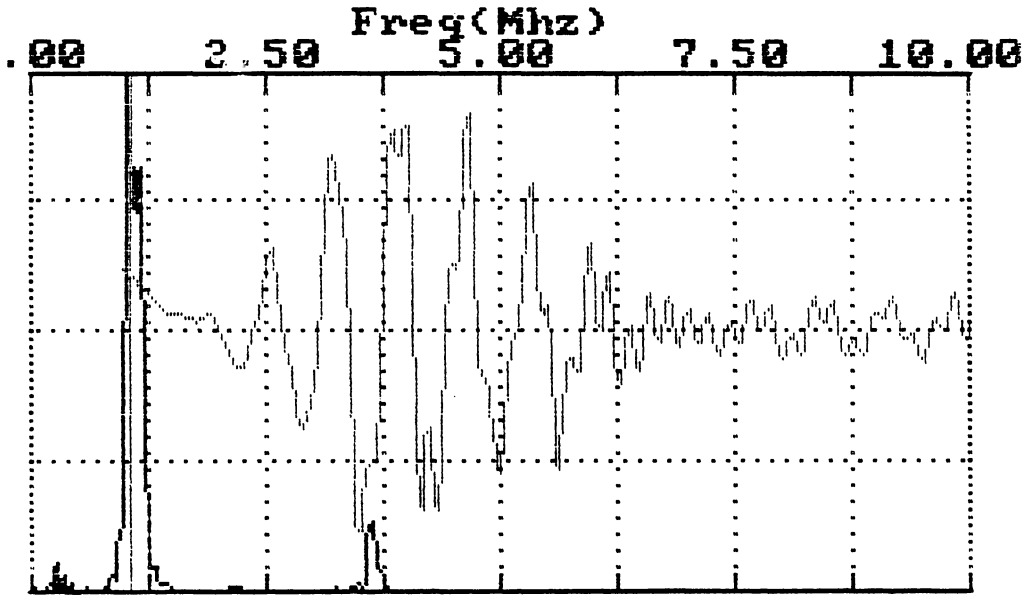

Figure 43. Output spectrum with no pressure applied in area between transducers

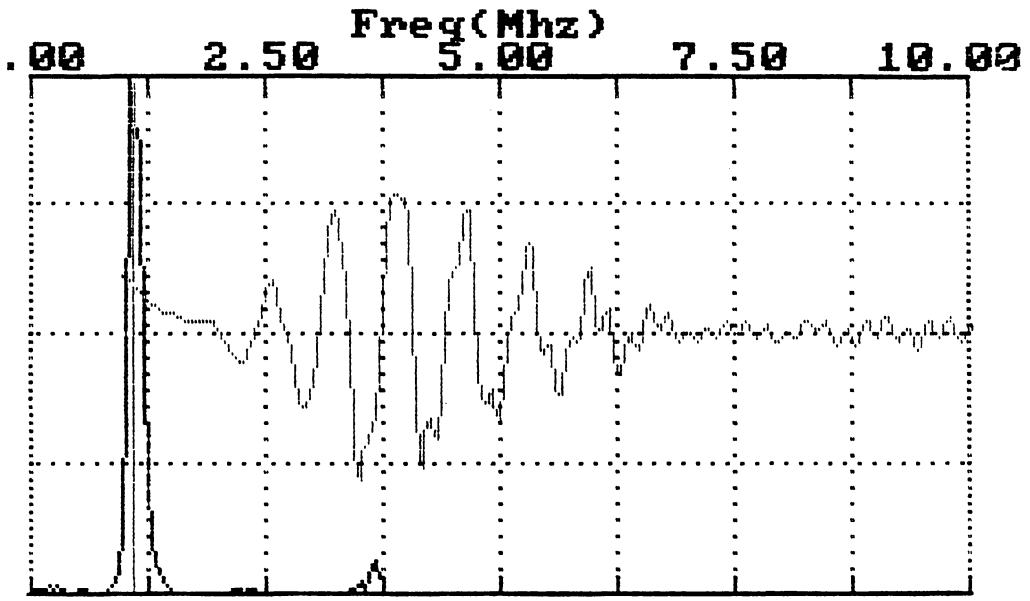

Figure 44. Output spectrum with pressure applied in area between transducers

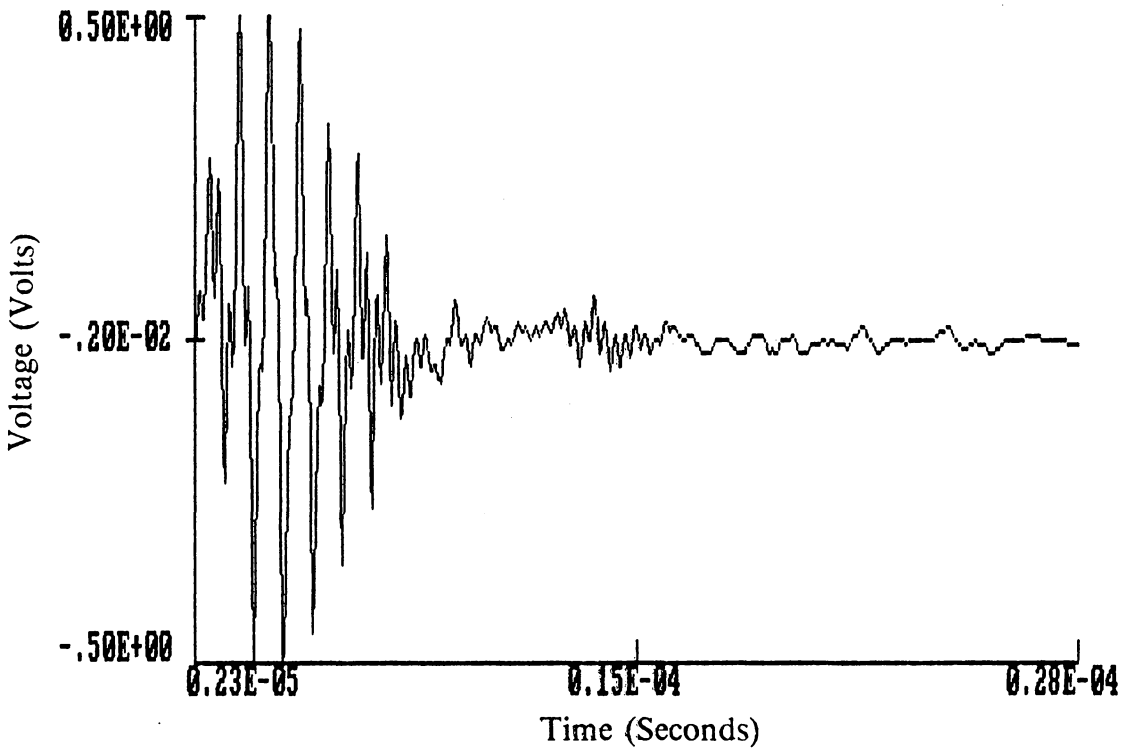

Figure 45. [0,0,0,0] time/voltage plot 0 degree direction

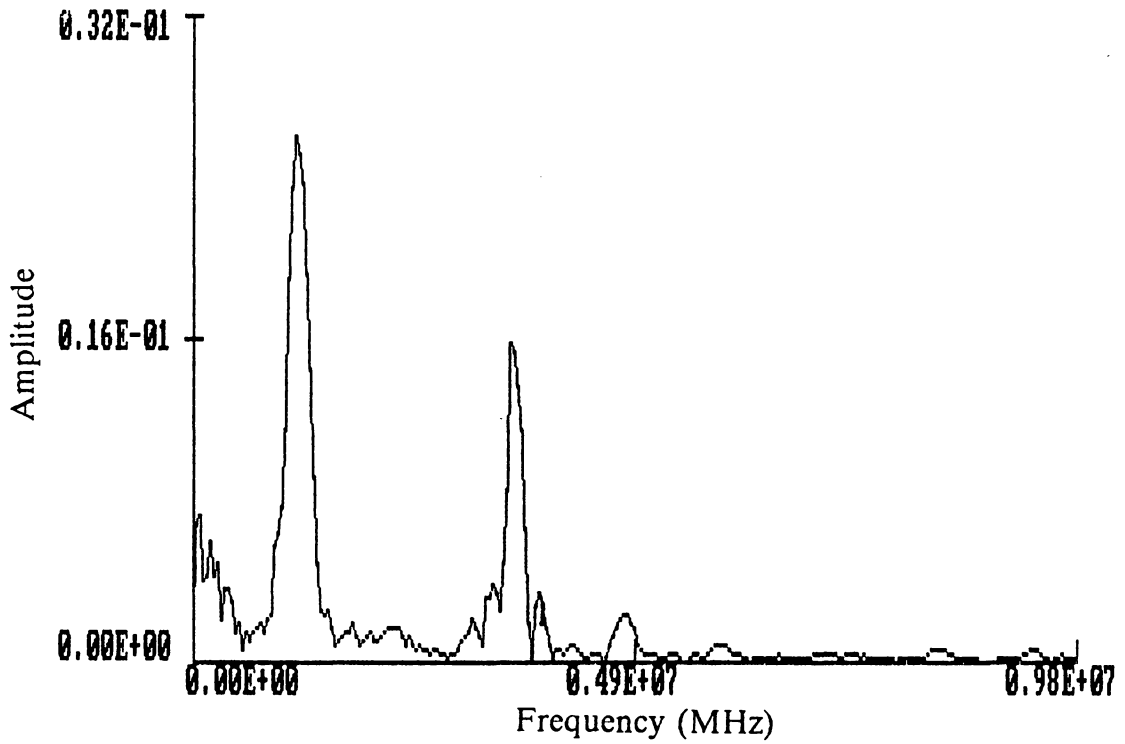

Figure 46. [0,0,0,0] spectrum for zero degree direction

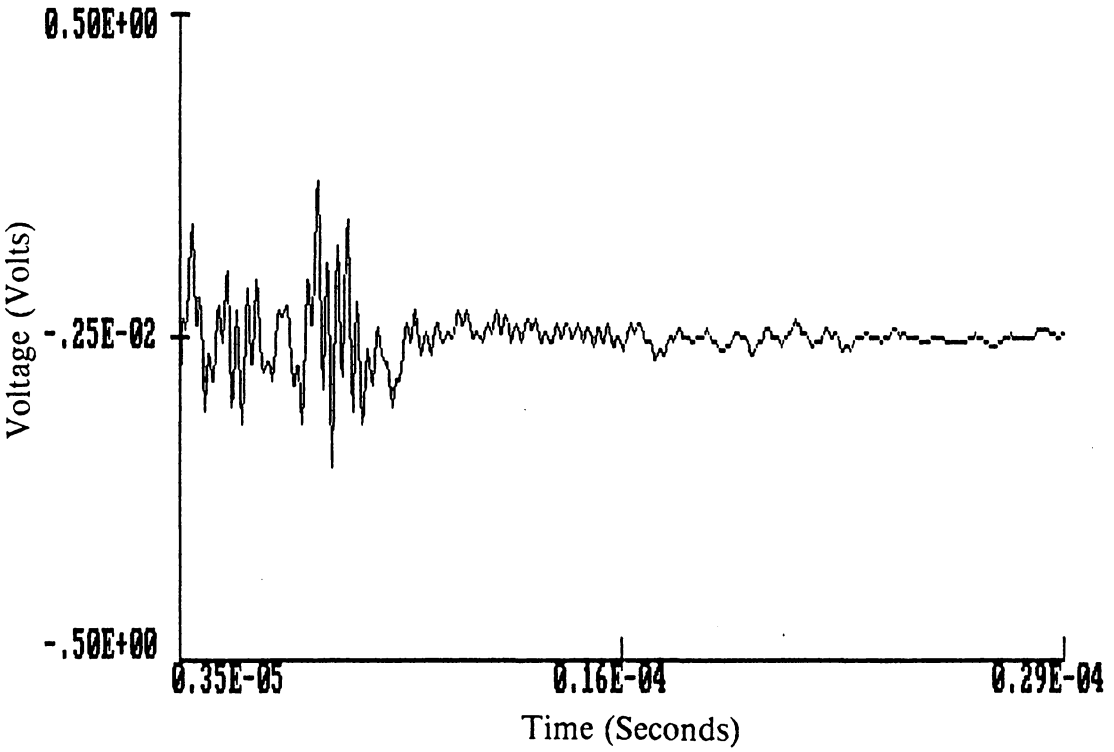

Figure 47. [0,0,0,0] time/voltage for twenty degree direction

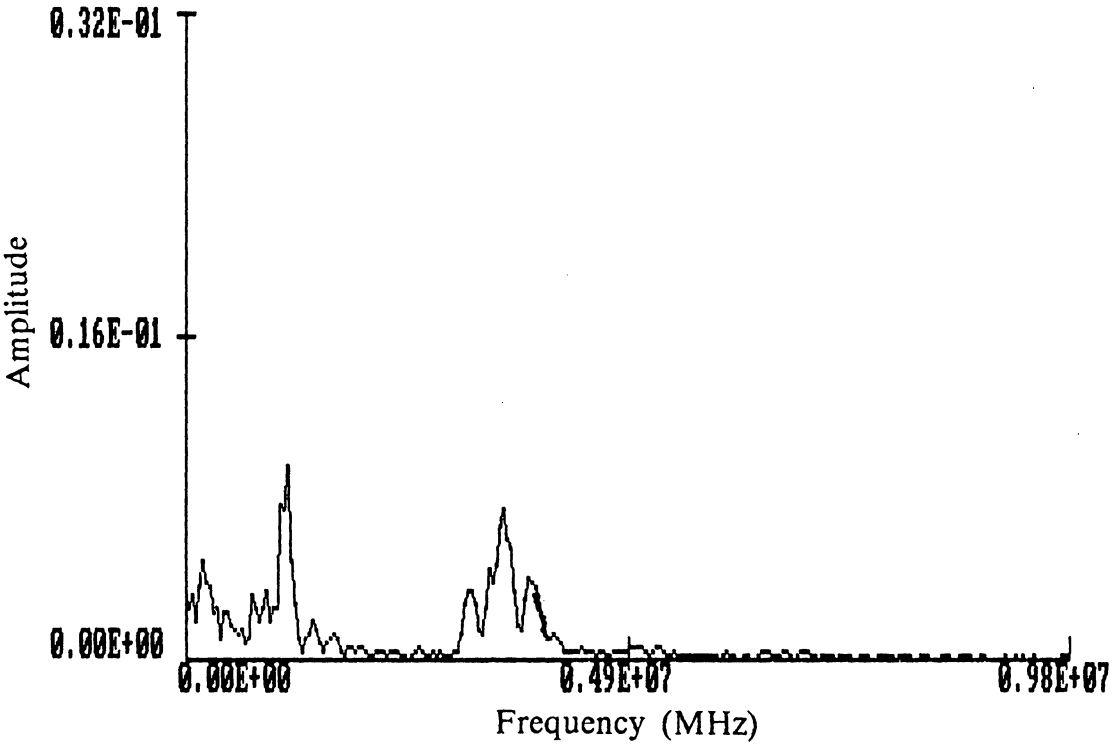

Figure 48. [0,0,0,0] spectrum for twenty degree direction

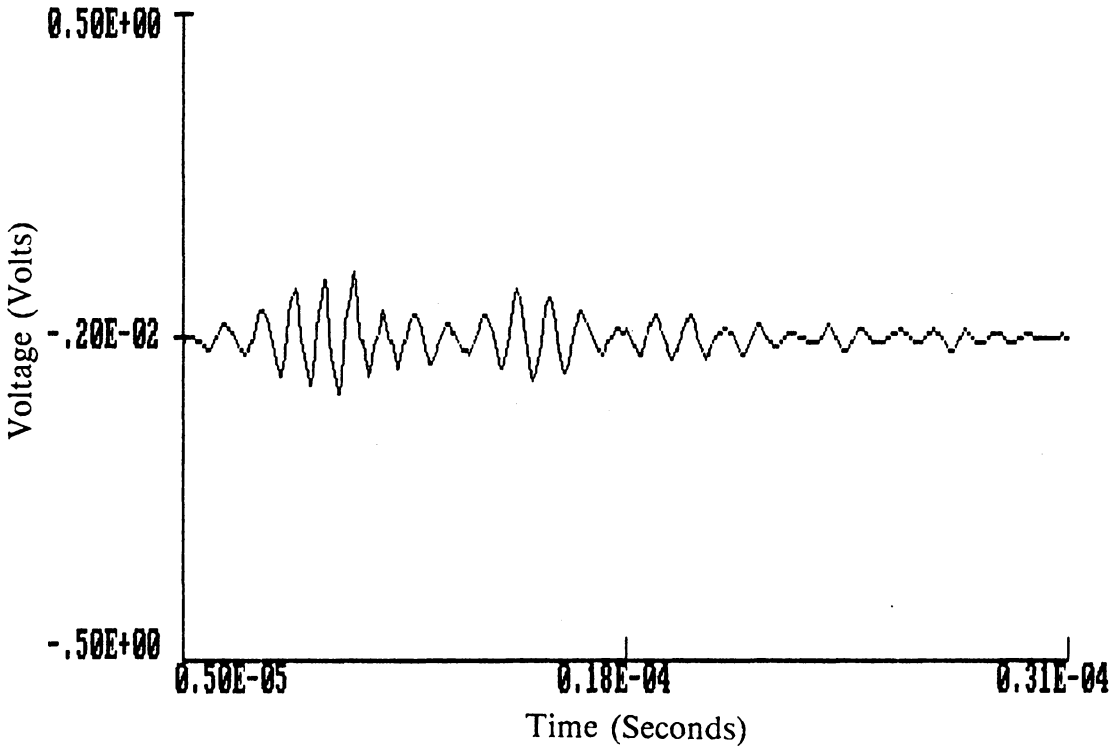

Figure 49. [0,0,0,0] time/voltage for ninety degree direction

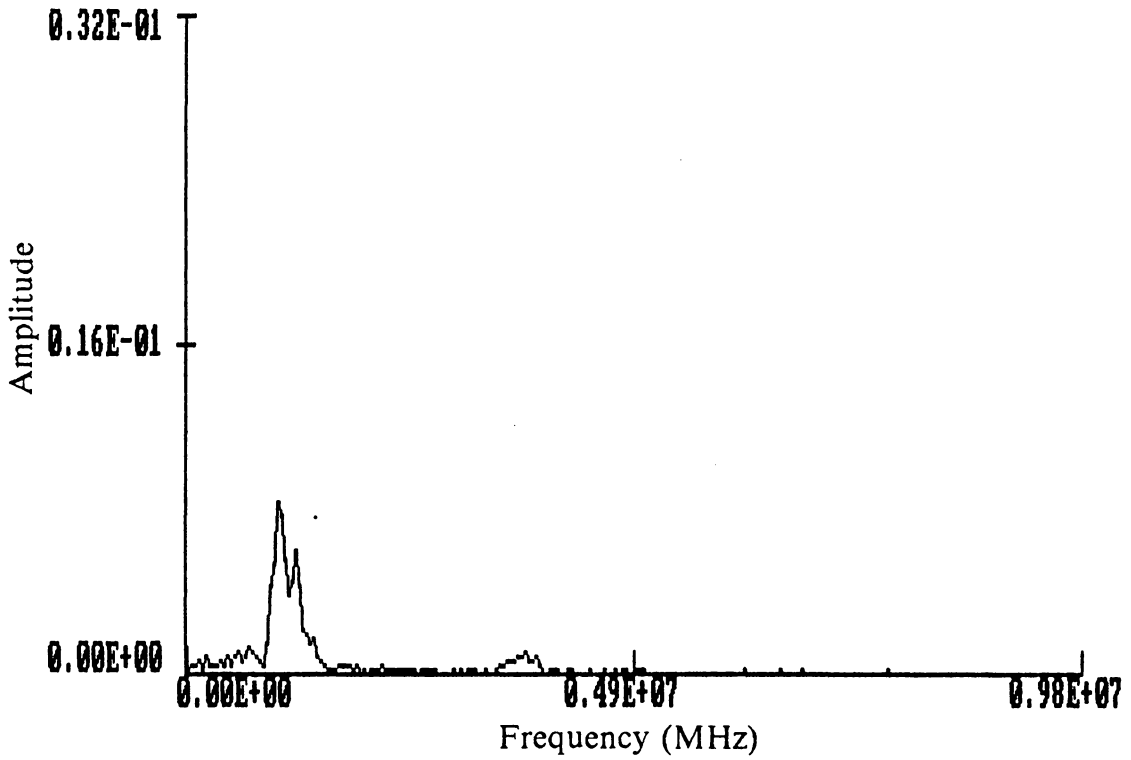

Figure 50. [0,0,0,0] spectrum for ninety degree direction

Figures 51-55 show the variation of different SWF parameters as a function of azimuthal angle for the 4-ply zero degree plate. First is the variation of the SWF1 parameter. Second, is the variation of SWF1 filtered to include only the energy in the one MHz peak. Next, is a plot of the SWF1 filtered to include only the high frequency peak. Finally, there is a plot of SWF2 and SWF3/SWF4. The major points to be made with these plots are that the SWF1 filtered for the high frequency peak varies slowly at early angles while the low frequency peak descends quickly. Also, a significant point is the relative peak of the SWF2 and SWF3/SWF4 parameters at approximately 15-20 degrees.

Plots similar to those produced for the 4-ply zero degree laminate were generated for the [90,0,0,90] laminate. First, are the time/voltage and spectrum plots for the 0, 15, 75 and 90 degree directions (Figures 56-63).

The major point to be made with these plots is the relative similarity between the zero degree plot and the 15 degree plot for the 4-ply zero degree laminate and the 75 and 90 degree for the [90,0,0,90]. They all show a large energy content for the 3.4 MHz peak relative to the one MHz peak. Specifically, the ratio of the 3.4 MHz peak to the 1.0 MHz peak seems to peak at between 15 to 20 degrees relative to the outer ply fiber direction.

Similarly, SWF plots exist for the [90,0,0,90] laminates. In order these include SWF1 unfiltered, SWF1 filtered to include only energy in the 3.4 megahertz peak, SWF2 and SWF3/SWF4 (Figures 64-67).

These plots indicate that the SWF1 parameters peak at both the zero and ninety degree orientations, but that they drop much faster in the zero degree direction. Also, the SWF2 plot shows a strong peak at 75 degrees and a slightly smaller one at 15 degrees. An additional peak occurred at 30 degrees, this may be associated with some other related phenomenon or be a result of some local material variation associated with the material where the sending or receiving transducers are situated.

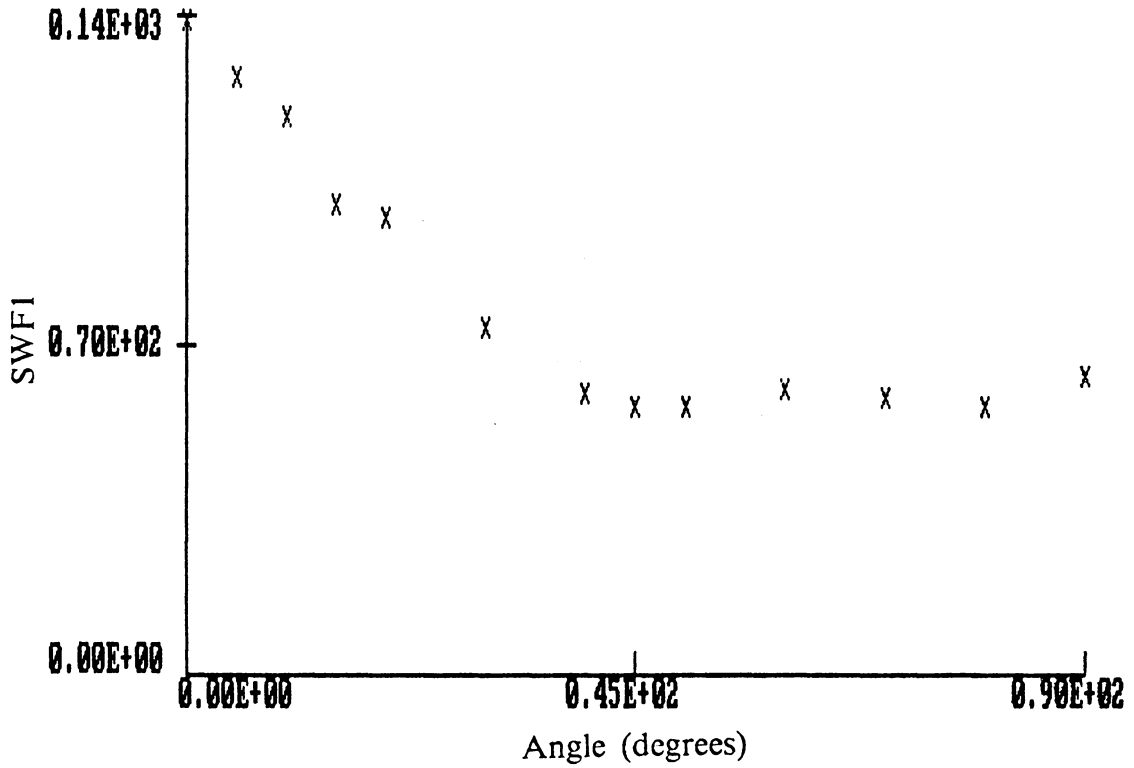

Figure 51. [0,0,0,0] SWF1 unfiltered as a function of azimuthal angle

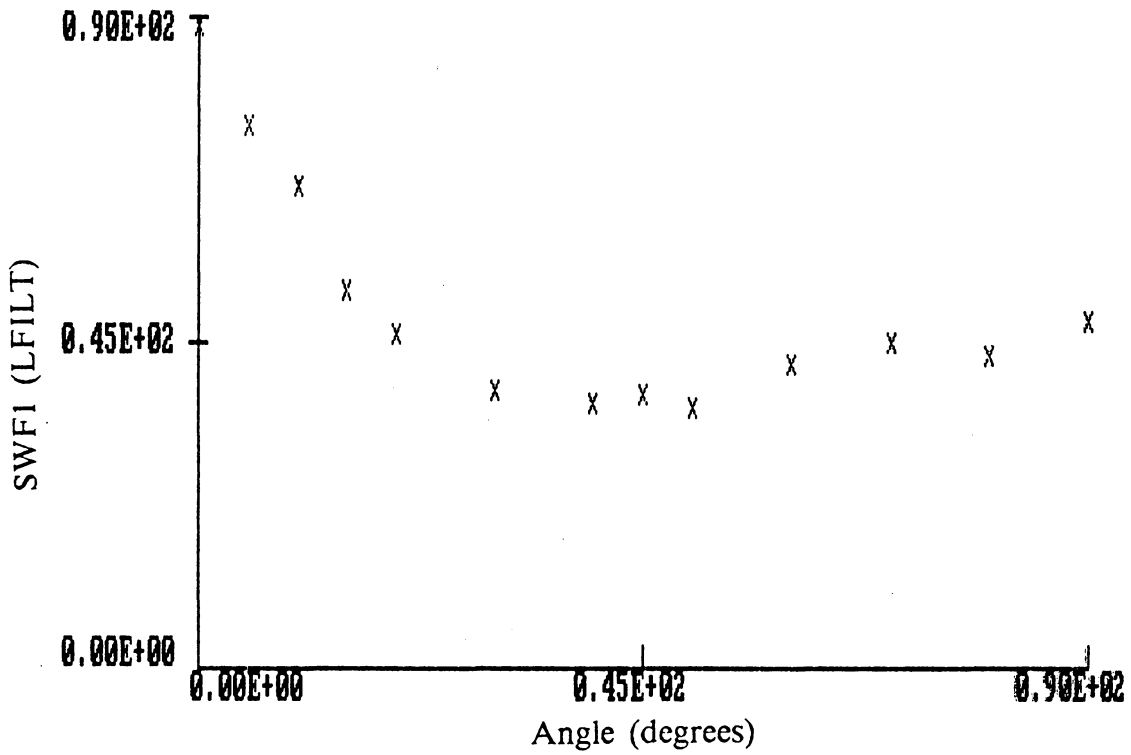

Figure 52. [0,0,0,0] SWF1 filtered as a function of azimuthal angle: Filtered to include only the energy in the one megahertz peak

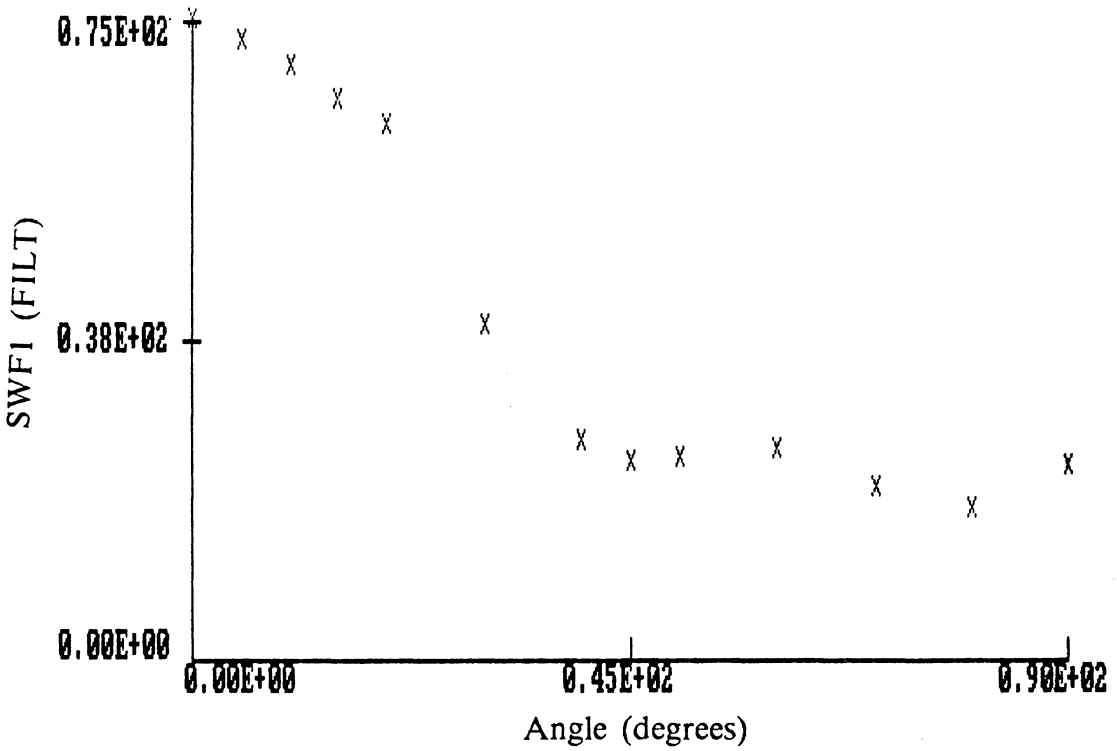

Figure 53. [0,0,0,0] SWF1 filtered as a function of azimuthal angle: Filtered to include only the energy in the 3.4 megahertz peak

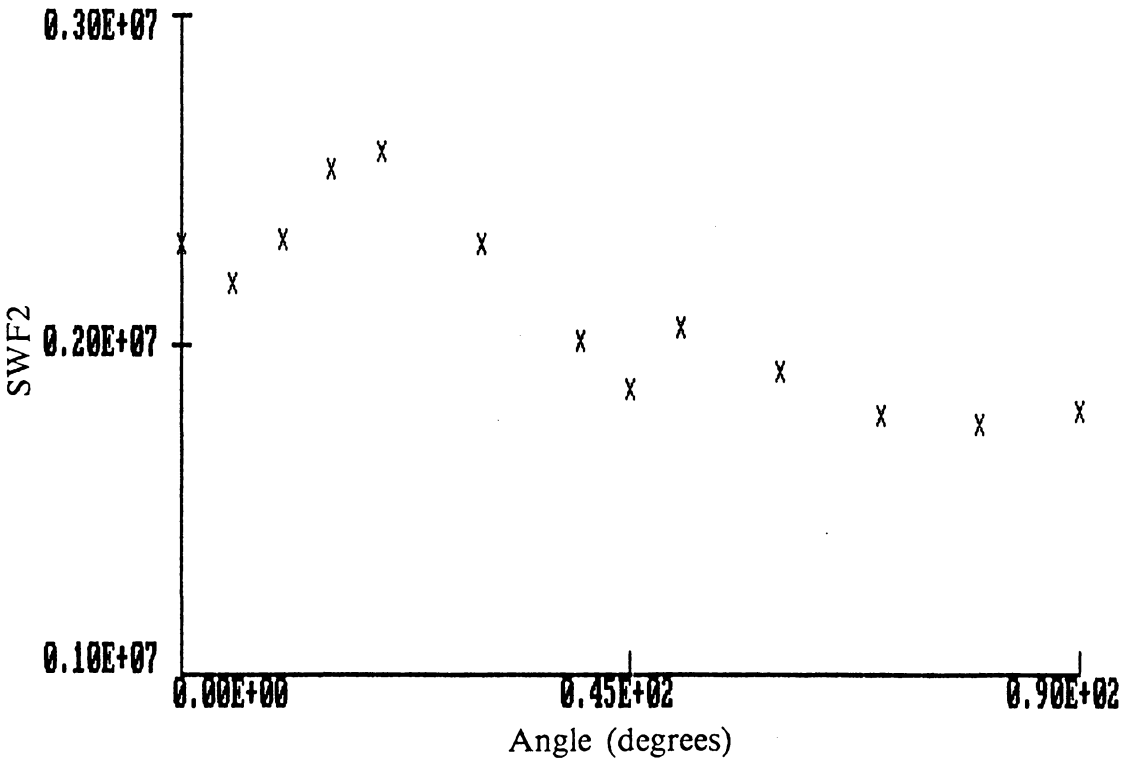

Figure 54. [0,0,0,0] SWF2 unfiltered as a function of azimuthal angle

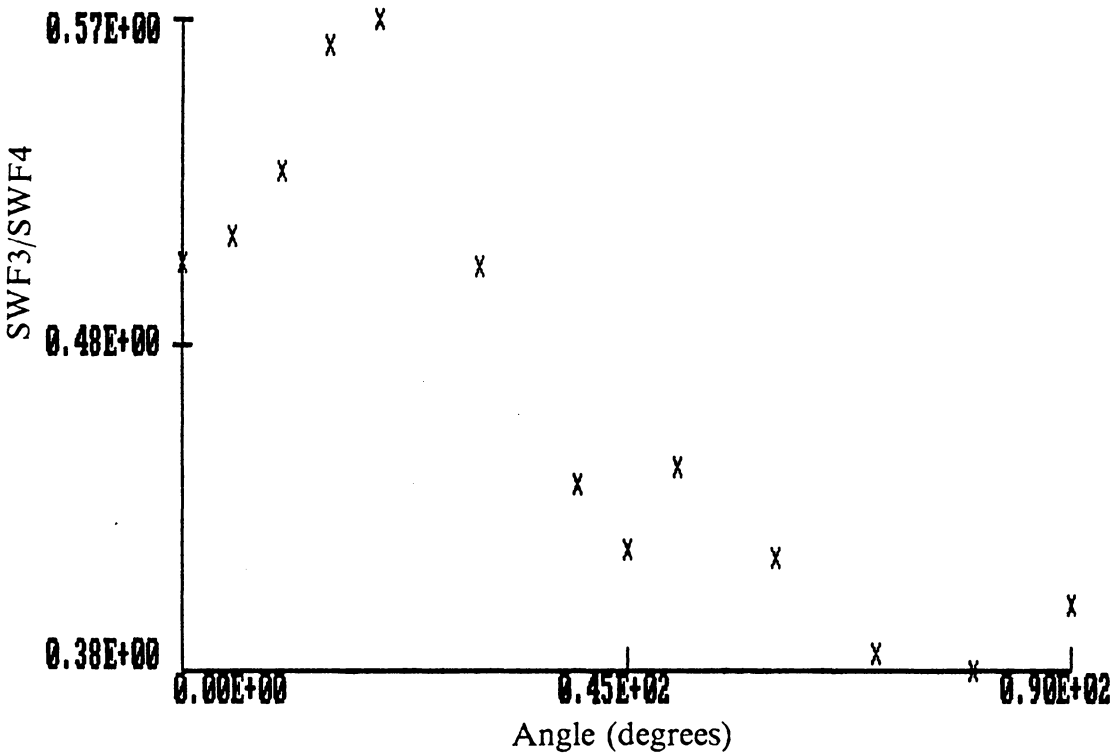

Figure 55. [0,0,0,0] SWF3/SWF4 unfiltered as a function of azimuthal angle

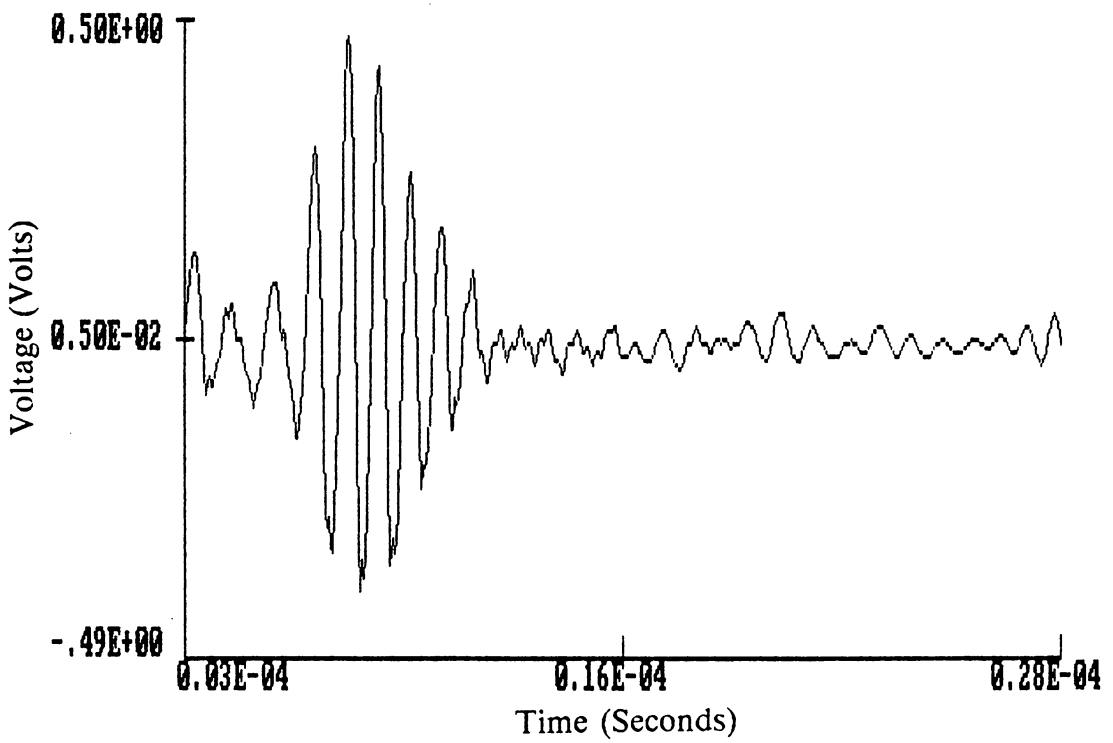

Figure 56. [90,0,0,90] time/voltage for zero degree direction

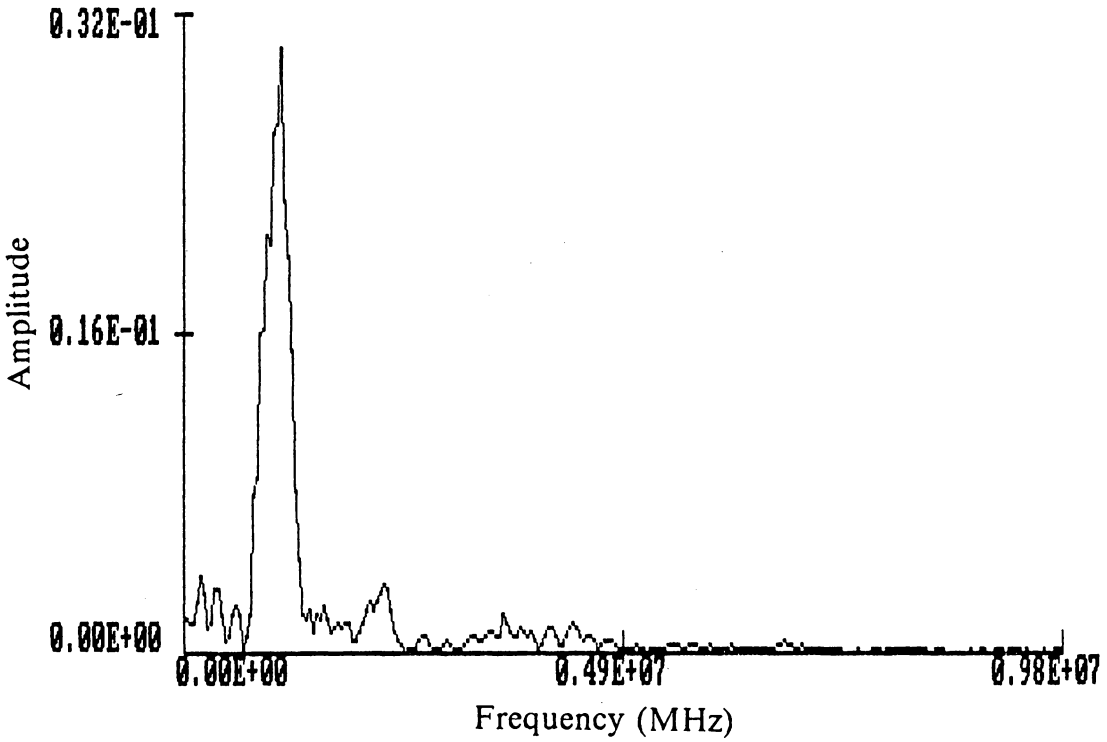

Figure 57. [90,0,0,90] spectrum for zero degree direction

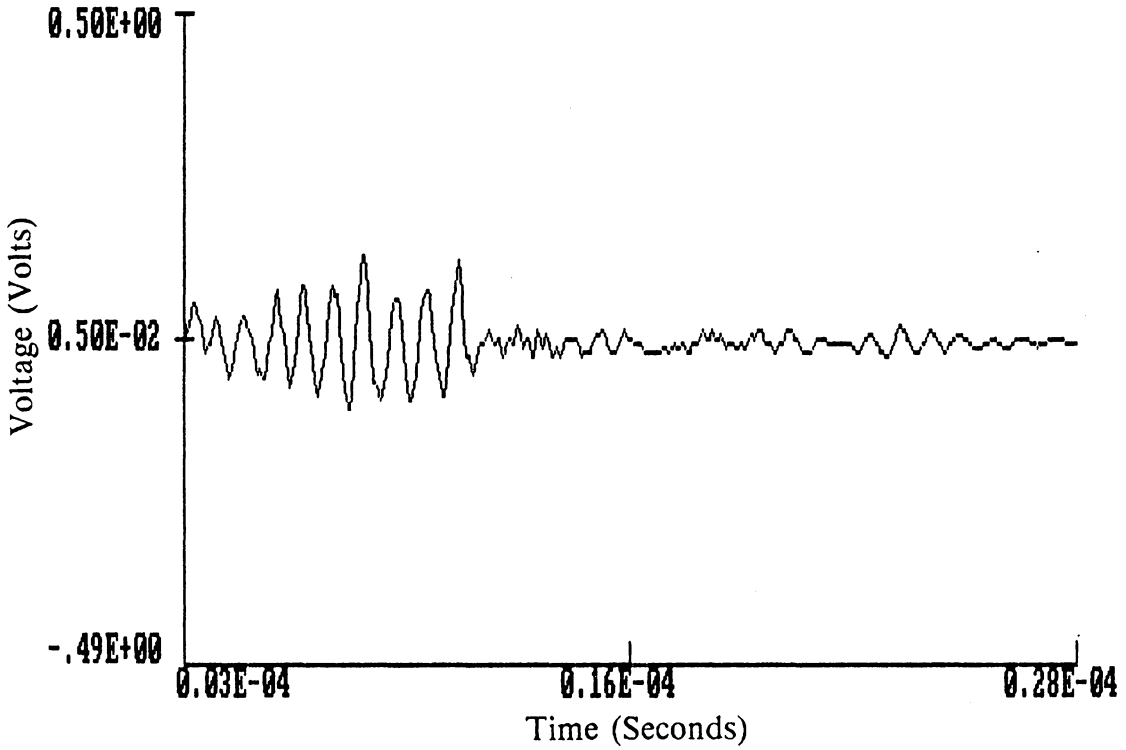

Figure 58. [90,0,0,90] time/voltage for fifteen degree direction

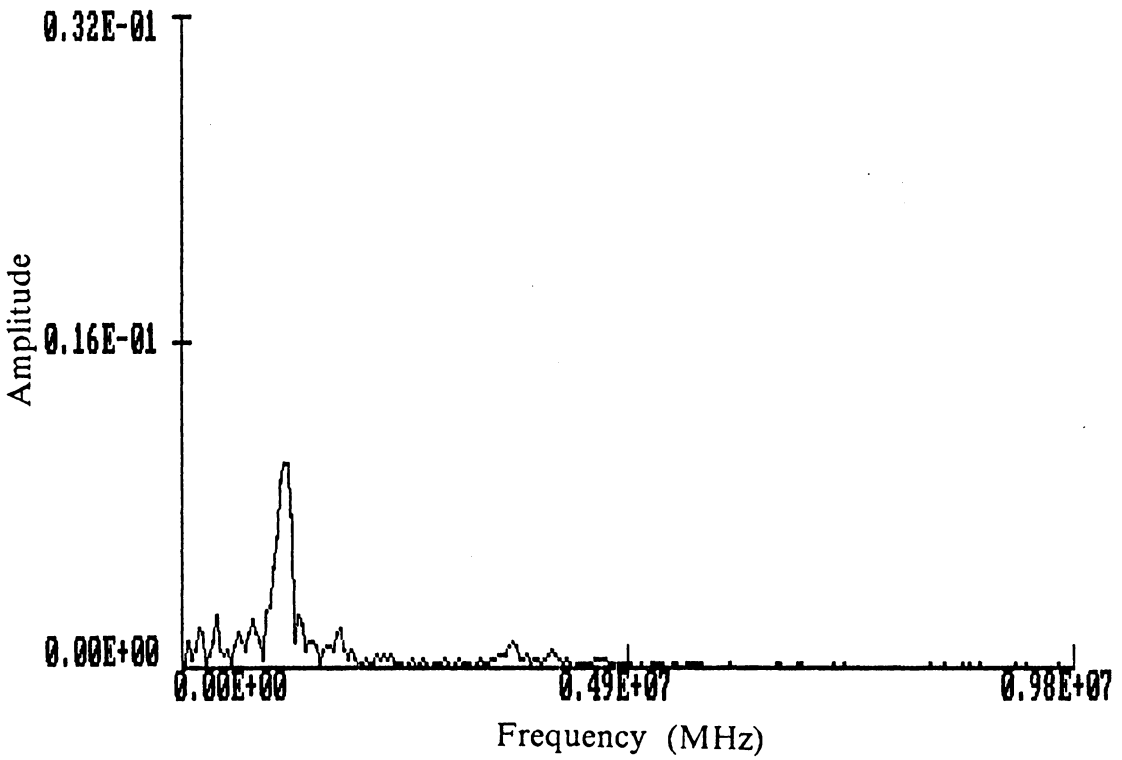

Figure 59. [90,0,0,90] spectrum for fifteen degree direction

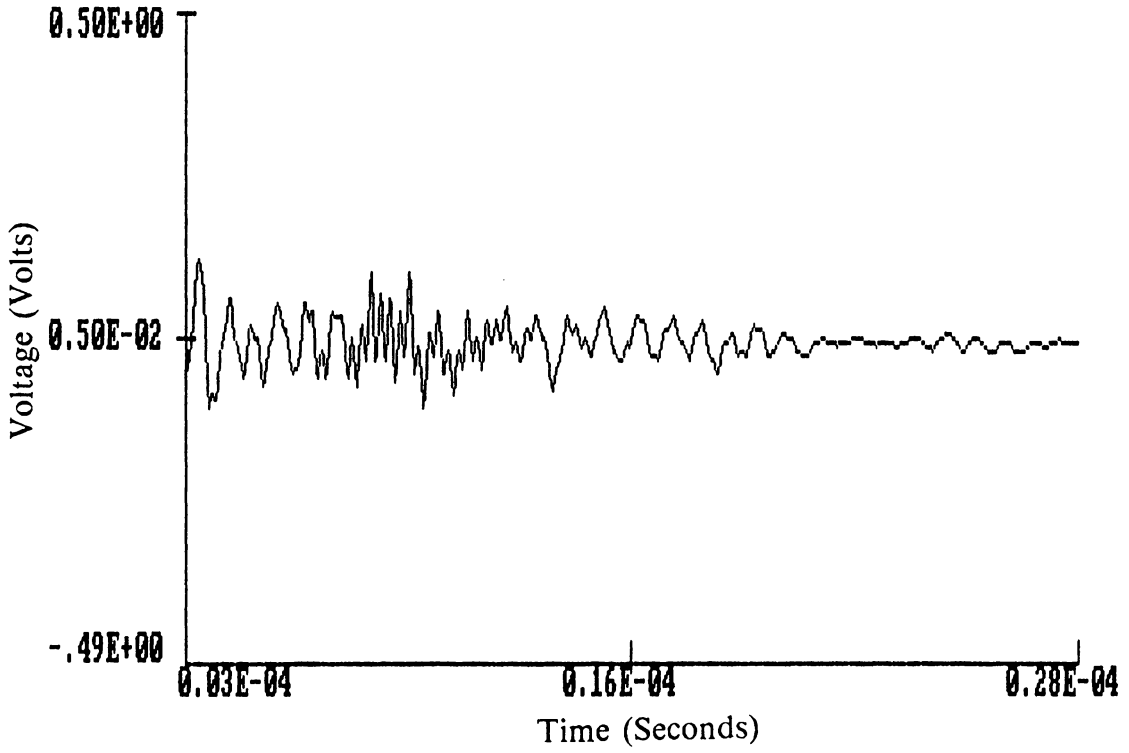

Figure 60. [90,0,0,90] time/voltage for 75 degree direction

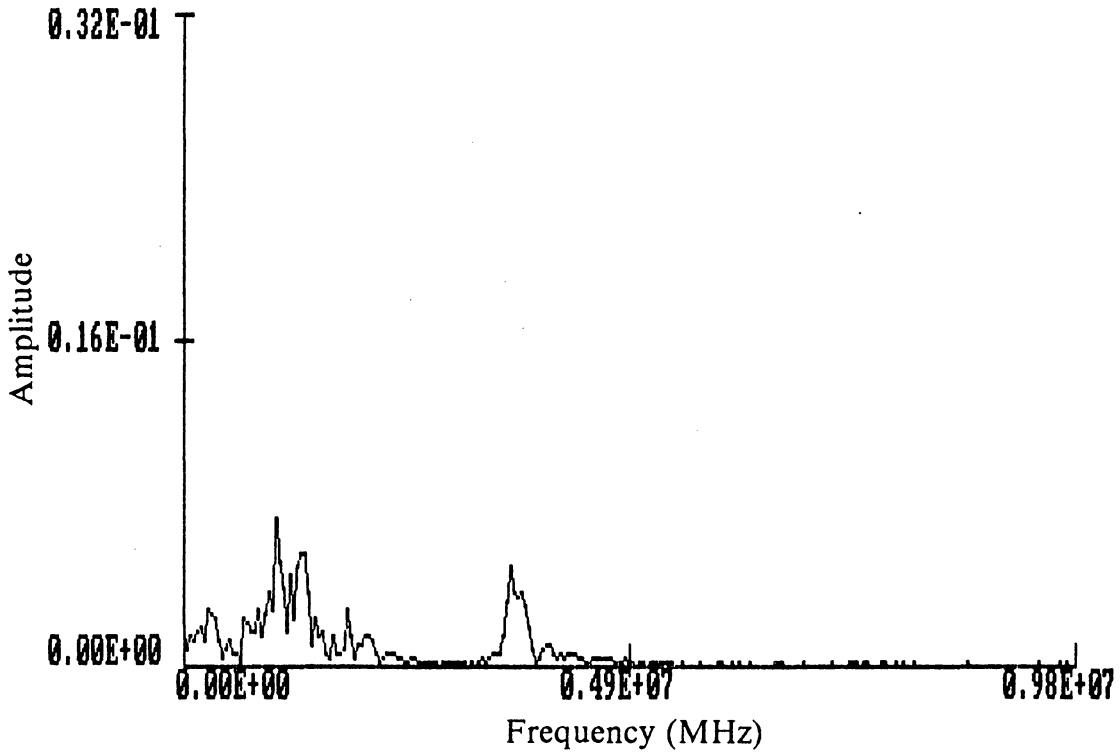

Figure 61. [90,0,0,90] spectrum for 75 degree direction

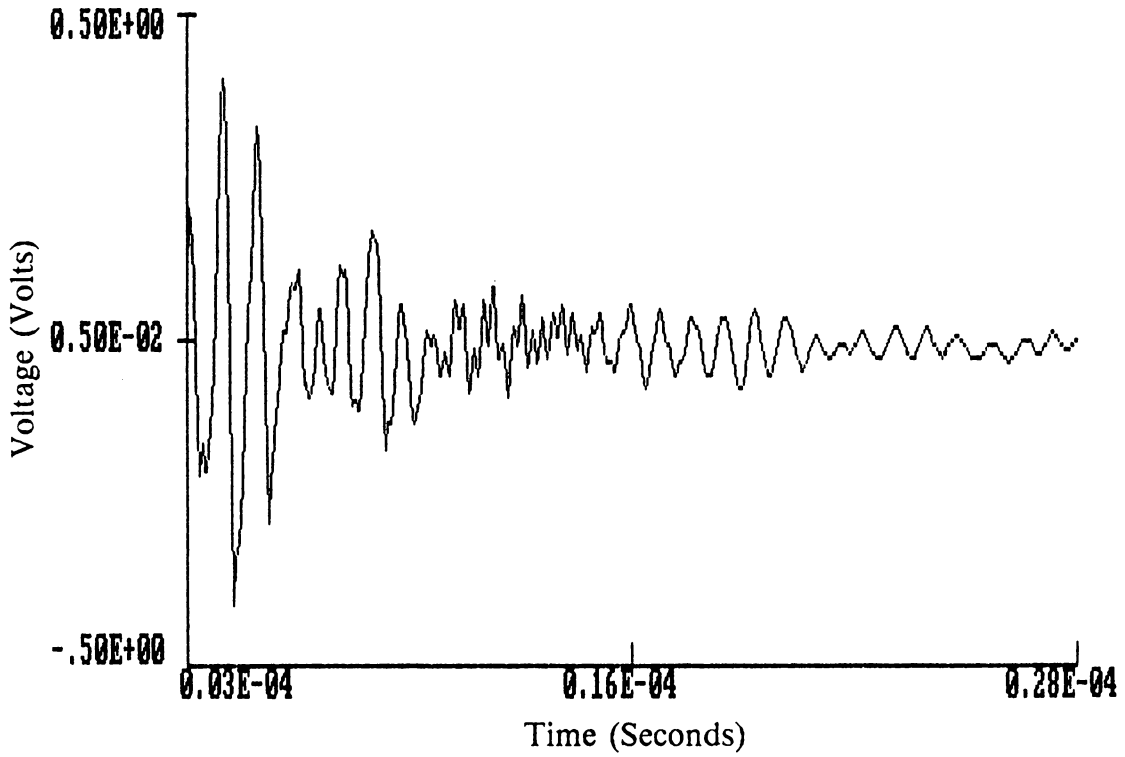

Figure 62. [90,0,0,90] time/voltage for ninety degree direction

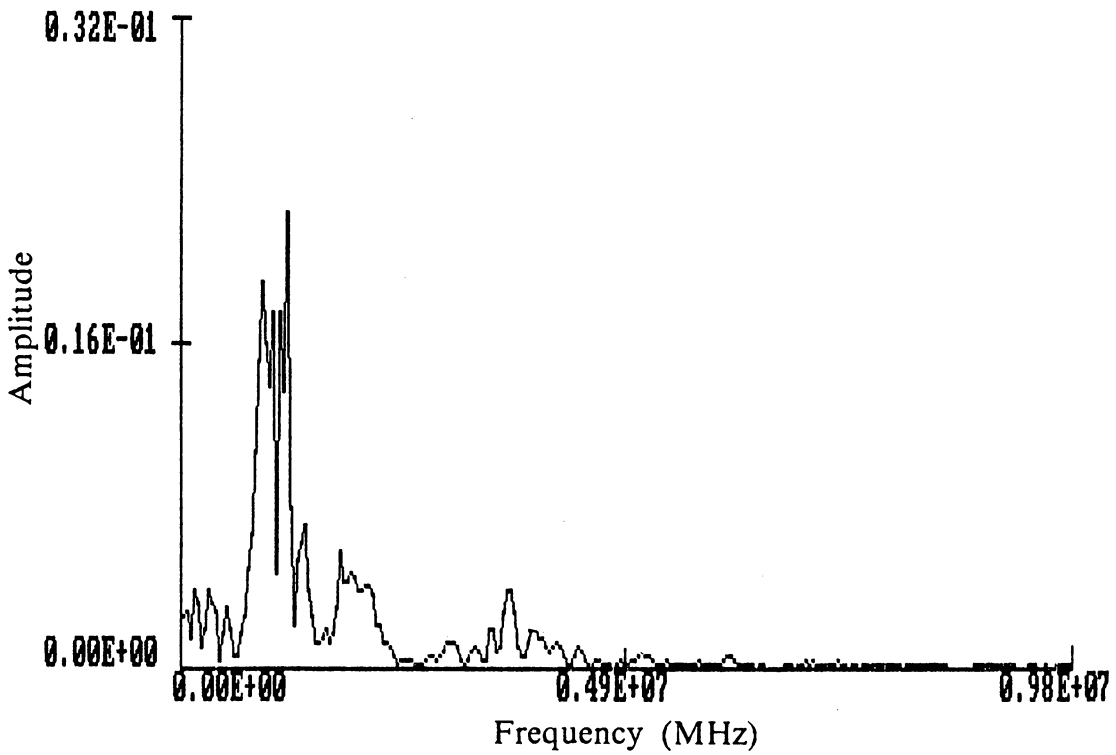

Figure 63. [90,0,0,90] spectrum for ninety degree direction

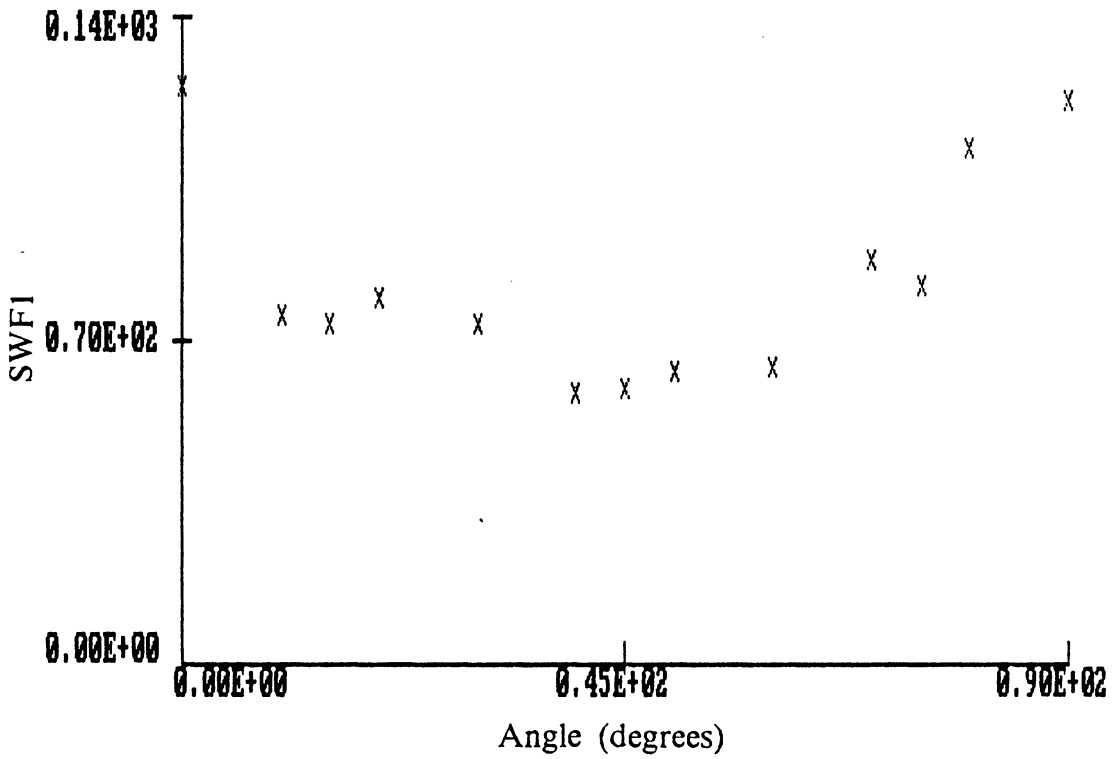

Figure 64. [90,0,0,90] SWF1 unfiltered as a function of azimuthal angle

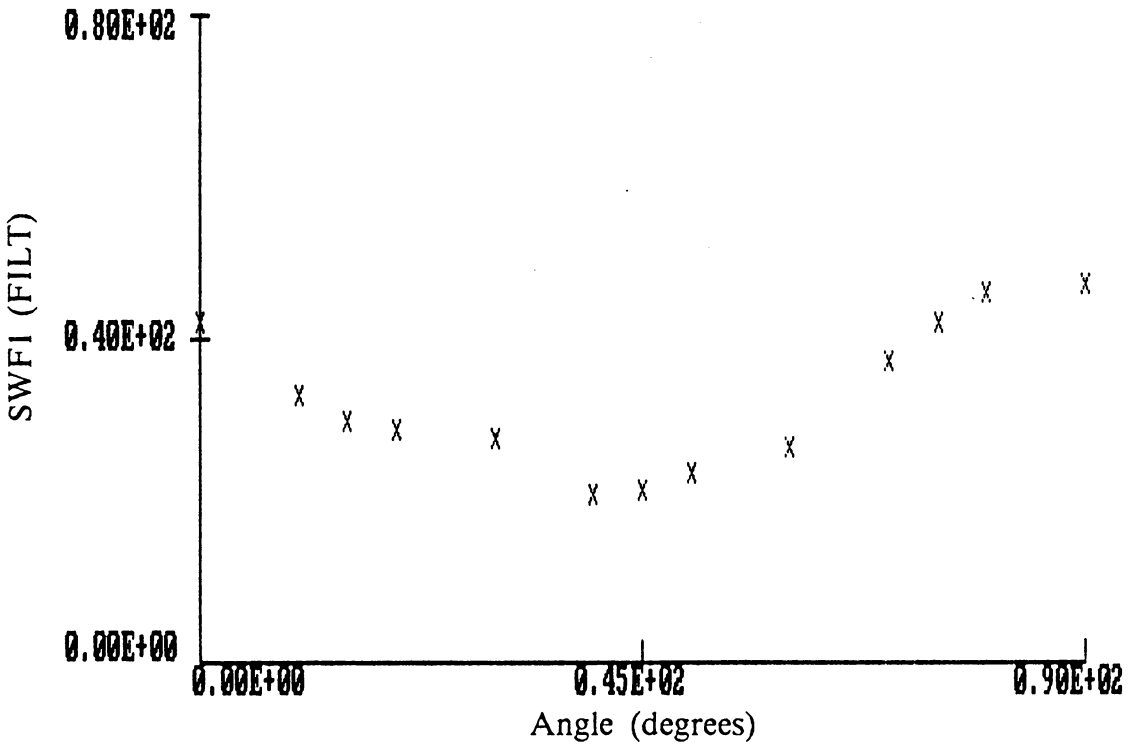

Figure 65. [90,0,0,90] SWF1 filtered as a function of azimuthal angle: Filtered to include only the energy in the 3.4 megahertz peak

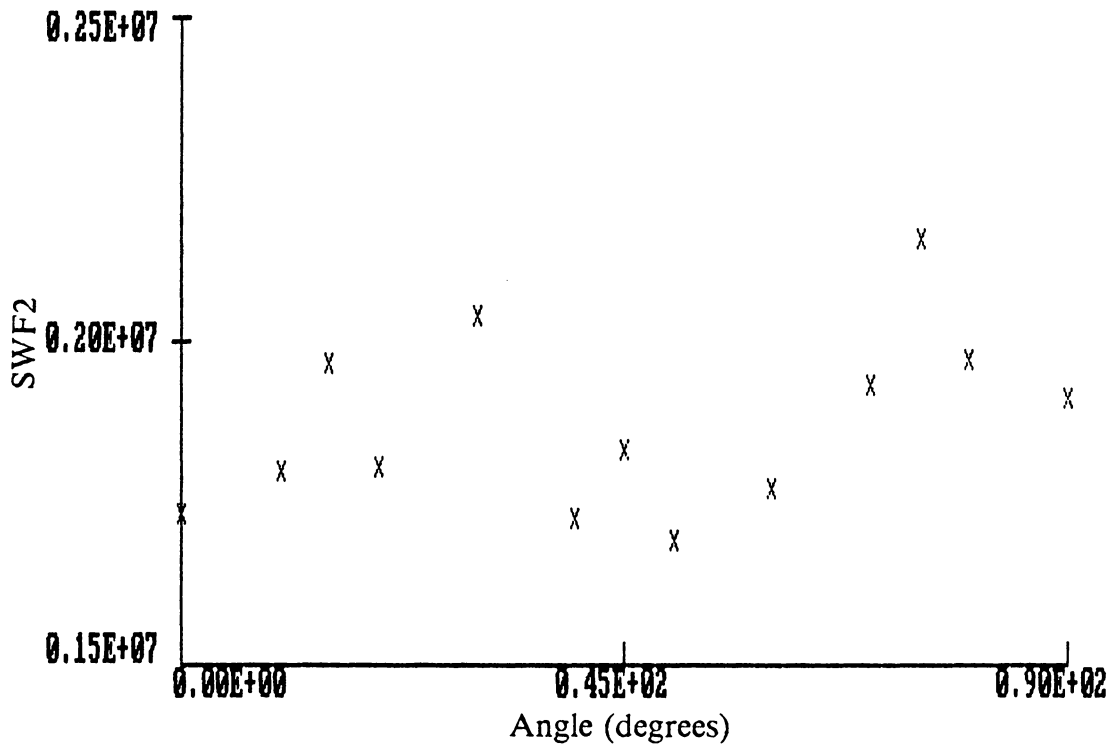

Figure 66. [90,0,0,90] SWF2 unfiltered as a function of azimuthal angle

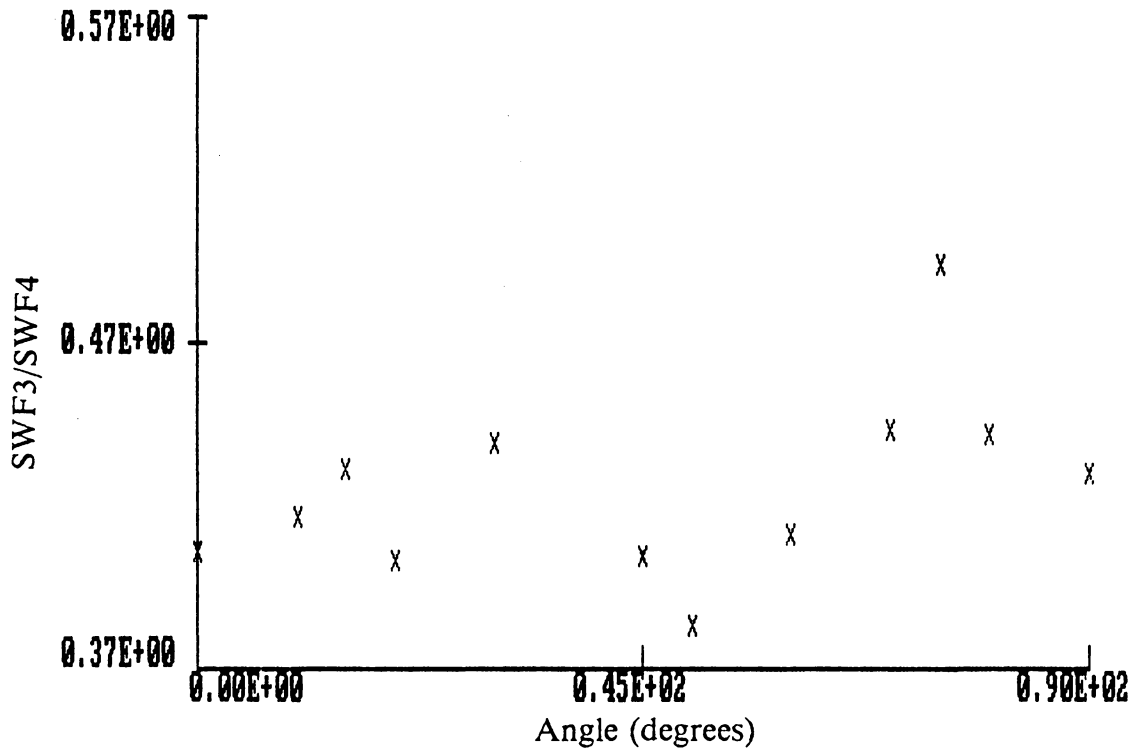

Figure 67. [90,0,0,90] SWF3/SWF4 unfiltered as a function of azimuthal angle

In addition, the SWF parameters are given for the [45,0,0,45] laminate. These include the SWF1 unfiltered, the SWF1 filtered to include just the energy in the 3.4 megahertz peak and SWF2 (Figures 68-70).

These results once again show a peak at 15 degrees off from the fiber direction for the surface ply.

Results For Phase Three

Finally, results were obtained for the panel with the prefabricated delamination. In order, plots are given for SWF1 unfiltered, SWF1 filtered to only include energy in the 3.4 megahertz peak, SWF2 and SWF3/SWF4 (Figures 71-74).

These plots vary greatly from those obtained on the 4-ply zero degree laminate without a delamination. For instance, the plot of the SWF1 parameters has none of its usual behavior and is somewhat attenuated in comparison to that for the unflawed specimen. Finally, inspection indicates that the SWF2 and SWF3/SWF4 parameters do not show any prominent peaks for azimuthal angles between 15 and 20 degrees as do the undamaged plates.

Summary

Results are given for a number of different tests that were performed to learn more about the acousto-ultrasonic technique. These ranged from the simple preliminary tests for the tubes to the more involved tests at various azimuthal angles for the plates.

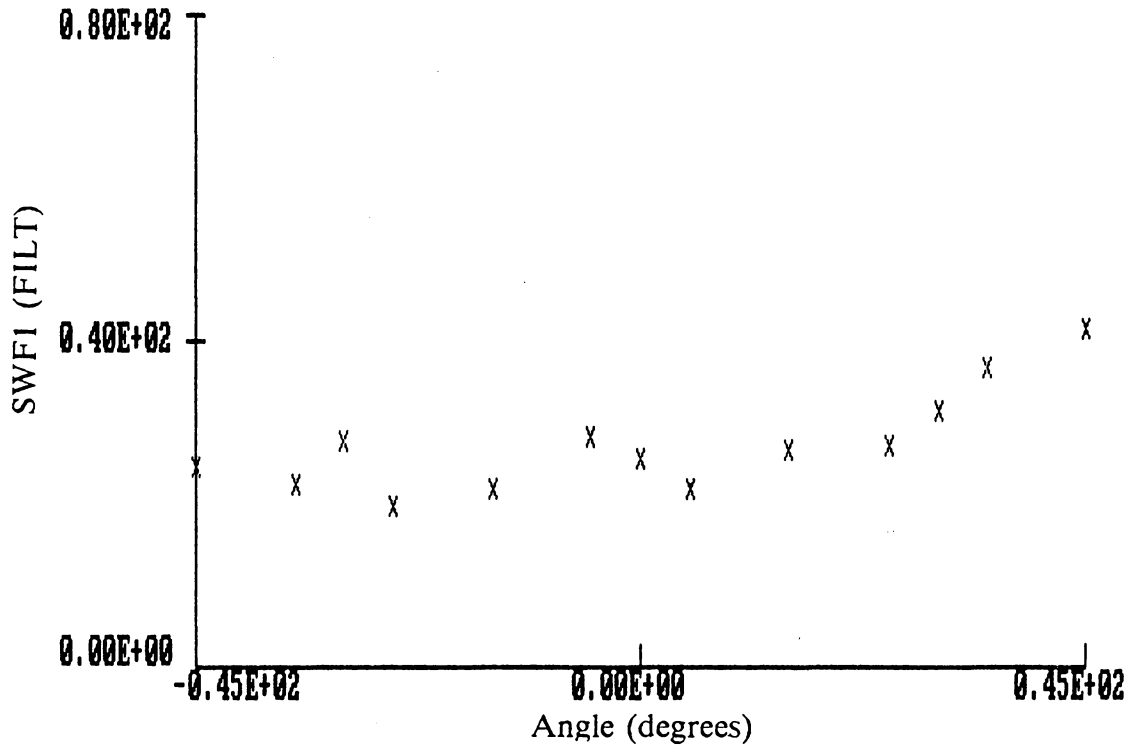

Figure 68. [45,0,0,45] SWF1 unfiltered as a function of azimuthal angle

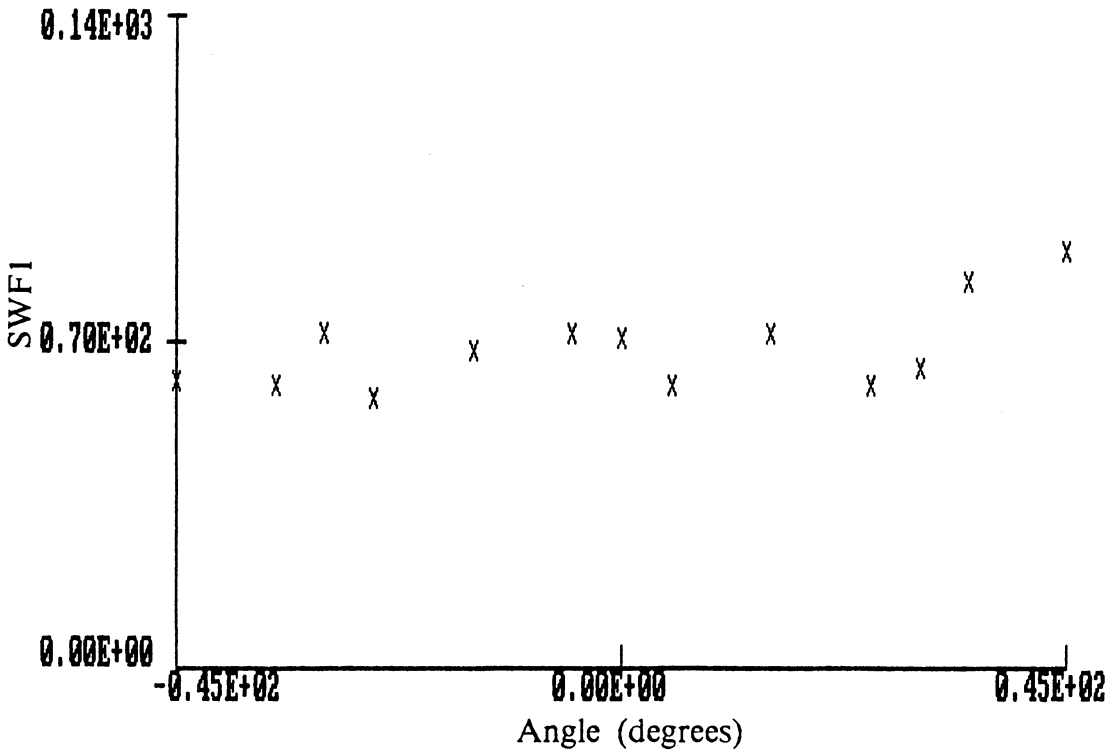

Figure 69. [45,0,0,45] SWF1 filtered as a function of azimuthal angle: Filtered to include only the energy in the 3.4 megahertz peak

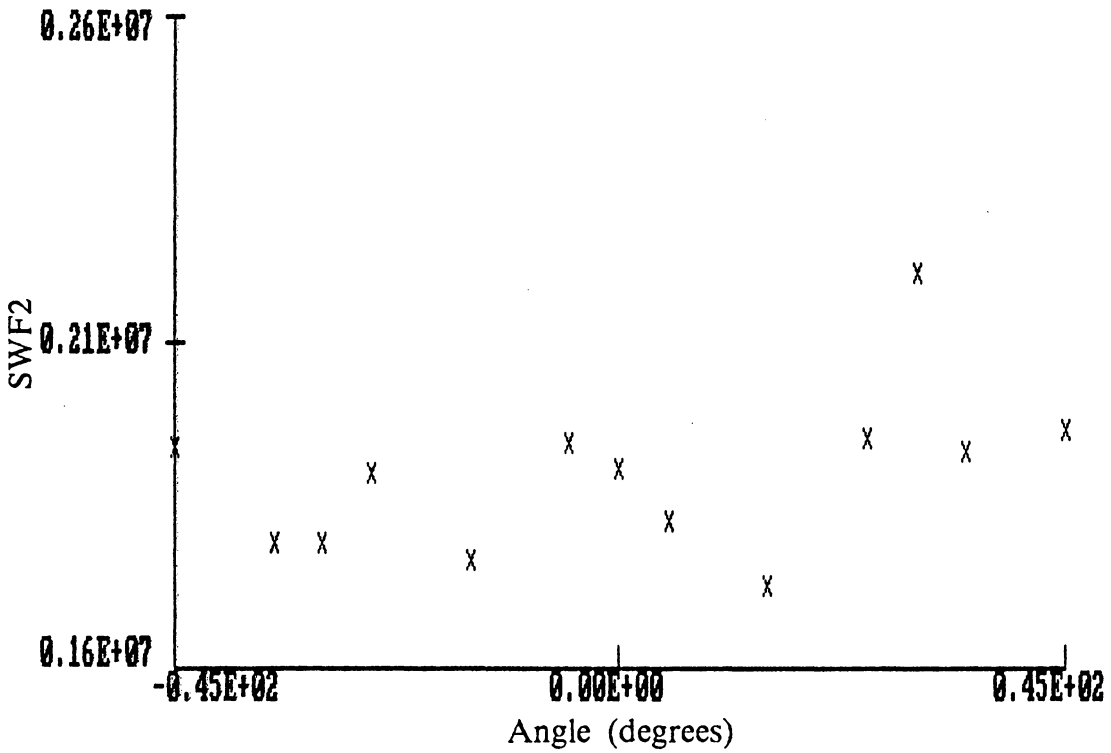

Figure 70. [45,0,0,45] SWF2 unfiltered as a function of azimuthal angle

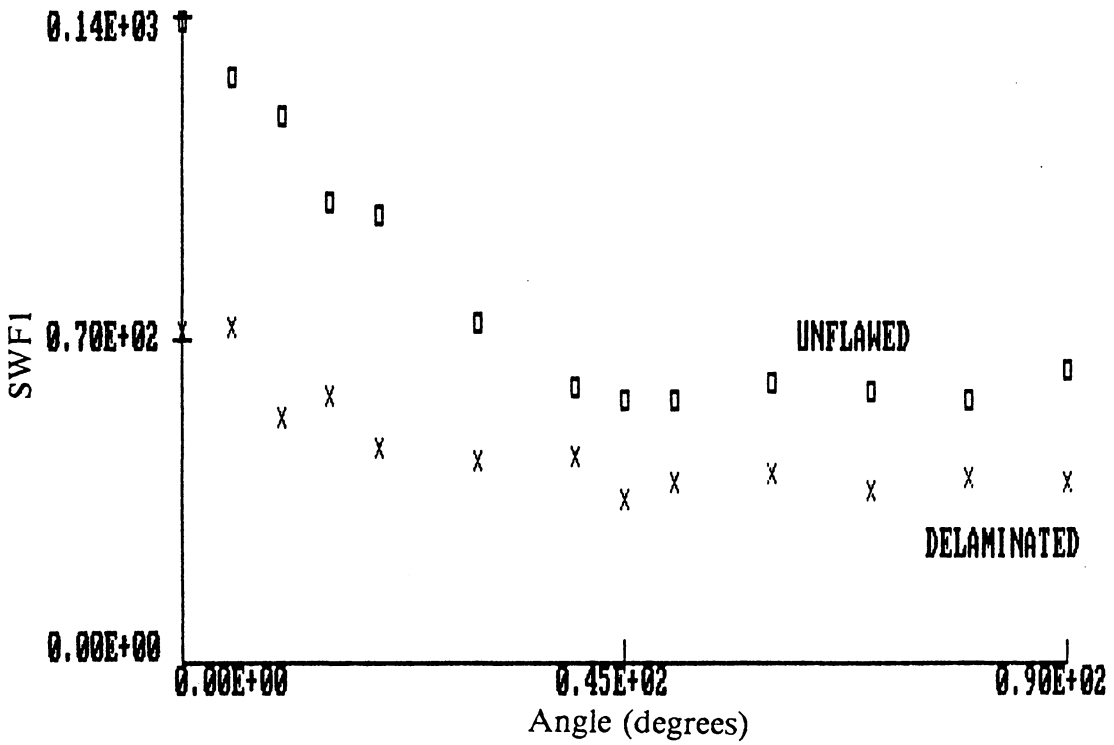

Figure 71. Delaminated SWF1 unfiltered as a function of azimuthal angle

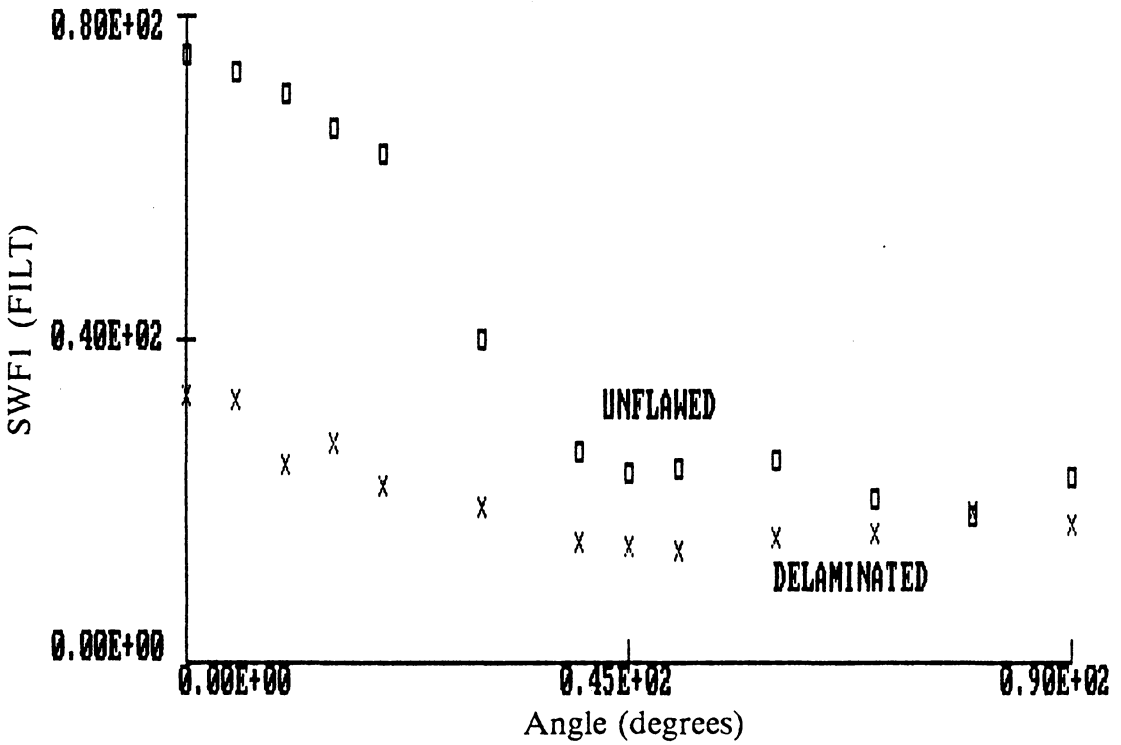

Figure 72. **Delaminated SWF1 filtered as a function of azimuthal angle:** Filtered to include only the energy in the 3.4 megahertz peak

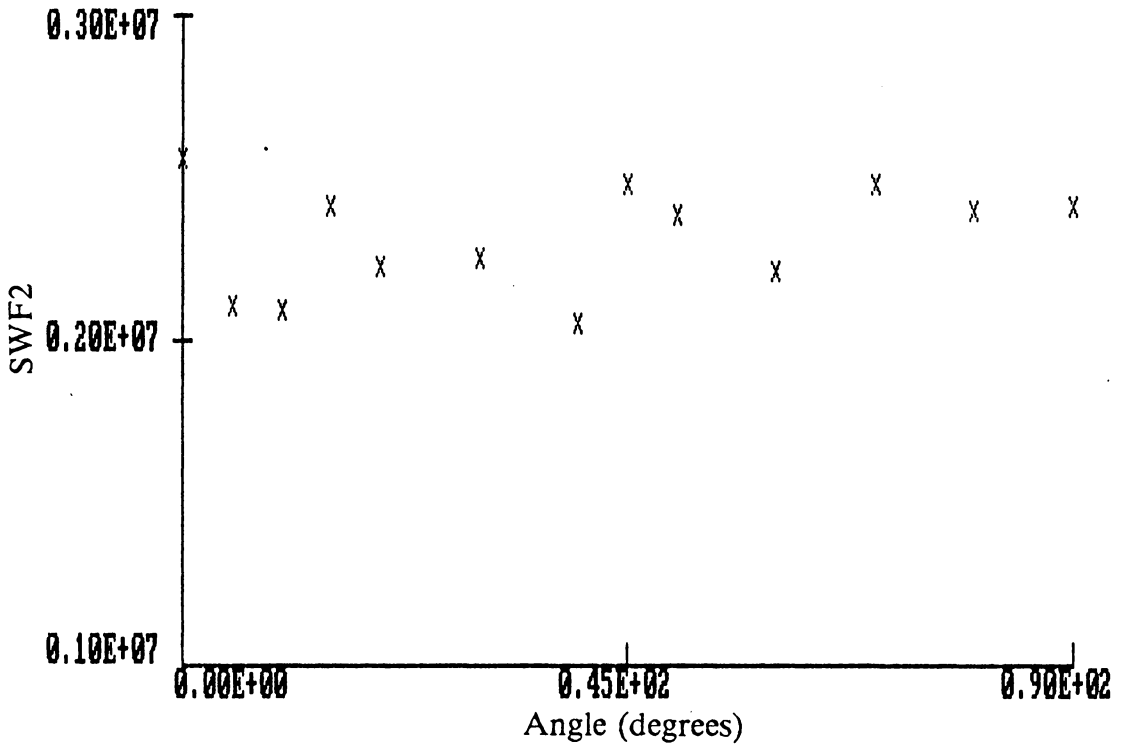

Figure 73. Delaminated SWF2 unfiltered as a function of azimuthal angle

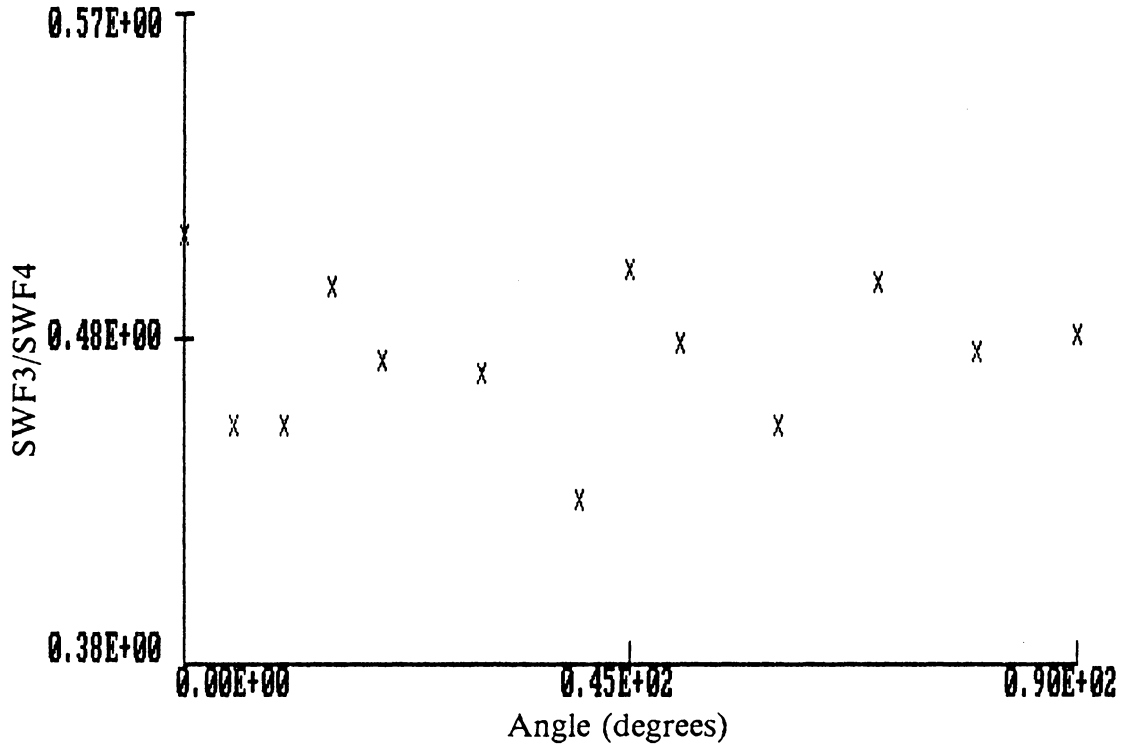

Figure 74. Delaminated SWF3/SWF4 unfiltered as a function of azimuthal angle

Discussion of Results

Introduction

As a result of work that has been done in developing and implementing the acousto-ultrasonic system a variety of both specific and general observations have be made. First, a couple of brief comments will be given based on the preliminary investigation of the implementation of the acousto-ultrasonic system on the aluminum/graphite tubes. Next, some generalizations will be made on the results from the epoxy/graphite laminates. Starting with general observations and ending with some speculative comments in the hope of promulgating further research efforts on the implementation of the acousto-ultrasonic system to obtaining fundamental physical information on the laminates. Finally, a general statement will be made regarding the present acousto-ultrasonic system and the method in general.

Aluminum/Graphite Tube Conclusions

Although results obtained on the aluminum/graphite tubes were preliminary, a couple of general statements can be made on the application of the acousto-ultrasonic system to the tubes. In general, the results seemed to indicate that the method, upon modification of experimental technique, was fairly reproducible for a given spot on a tube. The ability to perform the method on the tube length was somewhat more reproducible than the ability to perform the technique about the circumference. Also, results seemed to indicate that the technique was sensitive to damage caused by mechanical loading. Although, note that the results show that not all SWF1 values were lower on the loaded specimen than on the virgin specimen. Specifically, in Figure 34, notice the low values of SWF1 in regions 2, 3 and 4 compared to relatively higher values for regions 1 and 5. Also, notice that region 1, a high SWF1 region, corresponds to the clad overlay seam which failed upon further loading. SWF1 values for the virgin tube showed relatively uniform values of SWF1, being slightly lower than the SWF1 value for region 1 in the mechanically loaded specimen. Finally, an attractive feature of the method as applied to the tubes is the capability to detect the clad overlay seams. A major point is that SWF1 may not be sensitive to certain flaws, which are discernable in the frequency spectrum or for which SWF2 is sensitive. Moreover, with continued work, a means may be developed for assessing the quality of the clad overlay seam by noting variations in the signal for different seams and subsequently observing the quality of the seam by other means.

In summary, a variety of observations were made that seem to indicate the potential of the method as an NDE technique for assessing the quality of the aluminum/graphite tubes. Further work should include comparison of results with other NDE techniques and the identification of wave models to help understand the mechanical basis for the results.

Graphite/Epoxy

Phase One

The research that has been conducted on the graphite/epoxy laminates indicates a combination of interesting results. As established previously, the acousto-ultrasonic technique is sensitive to both initial variations in graphite/epoxy materials and damage induced by fatigue. Moreover, the results seem to show an information packed frequency specrtrum which changes with damage. With these established results, work was geared toward conducting basic tests to obtain a fundamental understanding of the method. Toward this end, the previously described tests were conducted.

The results of a few ancilliary experiments revealed some interesting phenomena to be used in understanding the basic character of the wave propagation which is responsible for system results. Some revealing information more immediately applicable to drawing conclusions than others.

First, a comparison frequency spectrum of for the frequency spectrum of the 8-ply specimen to that of the 4-ply specimen revealed that the 4-ply specimen had peak frequencies twice that of the 8-ply specimen for both the low frequency peak and the high frequency peak (Figures 39 and 40). Although not enough tests have been performed to make any definite conclusions, results show the high frequency peak and the low frequency peak to possibly be inversely dependent on plate thickness. However,the spectrum for the 8-ply panel had more peak frequencies and also showed a greater variation in the relative magnitude of peaks from spot to spot on the specimen. The 1.7 MHz peak, in the 8-ply specimen's spectrum seemed to vary in a similar manner, with respect to azimuthal angle, as did the 3.4 MHz, in the 4-ply specimen's spectrum. This would indicate an approximately linear inverse dependence of frequency on plate thickness for this mode. If the 600 KHz peak corresponds to the 1.0-1.2 MHz peak, then it would seem that frequency is inversely dependent on plate thickness. Although both peaks are in the early portion of the time signal, the

600 KHz content is mainly present in the back part of the wave train. An inverse dependence on thickness for peak frequency would correlate with a cutoff frequency analysis for Lamb waves [ref. 7]. However, the 1.7 MHz mode, for the 8-ply plate, seems to show characteristics of the 1 MHz mode, for the 4-ply plate (ie. wave speed measurement). Thus, the 8-ply showed more frequency peaks that showed up at all angles and were of sizeable magnitude. Also, it showed a variation from spot to spot in the relative magnitudes of peaks. Tests performed on other composite materials seemed to show similar behavior. However, extra frequency peaks also appeared and the relative magnitude of the energy content, of the various frequency peaks varied with thickness and material type. Also, certain plates showed greater variation from spot to spot then others. Generally, the 1 MHz and 3.4 MHz frequency peaks did exist for the 4-ply panels and showed similar characteristics. The complications involved with making exact statements indicates the difficulties which arise when trying to use the present system to extract physical information from an acoustic signal, highlighting problems which are created by not yet being able to completely model the problem as well as experimental variations and other effects which can cloud issues.

Another interesting result was the change in the spectrum for the 4-ply specimen when the receiving transducer was placed on the bottom of the specimen instead of the top (Figure 41). The fixed value of the low frequency peak could be interpreted as evidence of its being a plate mode. The reduction in frequency of the high frequency peak is rather hard to interpret. Perhaps this could be used to relate the high frequency peak to a surface wave or some other wave besides a pure plate wave. However, this is simply conjecture and presently this result can only be kept in mind for later use in forming a total understanding of the method as applied to graphite/epoxy laminates.

The fact that the frequency spectrum remained relatively unchanged when the conventionally used five MHz sending transducer was replaced by the ten MHz transducer does indicate that results are rooted to the mechanical properties of the plate as opposed to being a total manifestation of the input (see Figure 42). In other words, the output spectrum is not simply a result of the frequency at which the transducer is resonating. However, further tests need to be conducted with other

transducers to determine the effect of changing transducer size and other transducer characteristics on the system output.

Finally, a simple test was performed to note the general effect of applying pressure between transducers on the output spectrum. As results indicate both the peaks decreased slightly, the high frequency peak decreasing a very slight bit more (Figures 43 and 44). This should simply serve as a basis for conducting more tests on the general effects of changing boundary conditions on the system output.

Variation of Output with Azimuthal Angle for Phase One and Two

The variety of results obtained from varying the orientation of the transducers relative to the plate revealed some interesting results, which could have some practical ramifications as far as non-destructive testing. However, at this point the results can only be used as guidance for where further research should be oriented.

First, considering the arrival of the trigger to be the excitation and the first voltage rise in the time/voltage signal to be the time of arrival for the wave and calculated phase velocity, one would calculate a phase velocity of 370,000 inches per second for the low frequency wave. The theoretical phase speed for a pure extensional wave is 400,000 inches per second. Moreover, other phase velocities seem to correlate with theoretical calculations (Appendix B). Hence, the 1.0 MHz mode seems to perhaps be a pure extensional wave. However, further tests are being conducted to corroborate this opinion and to clarify uncertainties.

Secondly, inspection of the time domain revealed that the high frequency signal content arrived at a slightly later time than that of the low frequency content. This can be seen in Figure 45. If this wave was in the form of a surface wave or Rayleigh wave it should have a phase velocity that is slower than that of the flexural wave or extensional wave. Although the phase speed of the high

frequency peak was difficult to determine exactly, it seemed to vary in a different manner with respect to azimuthal angle. More rigorous tests are being conducted to try to determine how the wave velocities of both modes vary as a function of azimuthal angle.

In general, the frequency spectra at all angles on the 4-ply plates revealed the existence of the 1.0 MHz peak and the 3.4 MHz peak. However, some other peaks did occasionally occur, but not with the regularity of the 1.0 and 3.4 MHz peaks. Thus, the calculated parameters and the resulting plots are mainly influenced by these peaks. Also, the fact that both modes were present in different quantity in different parts of the wave train made the calculation of wave speeds difficult, especially for the 3.4 MHz mode.

In the [0,0,0,0] plate, the plots of SWF parameters versus angle exhibited several interesting trends. First, the unfiltered SWF1 showed a fairly smooth descent from a maximum at 0 degrees to a minumum at 90 degrees (Figure 51). However, the unfiltered SWF1 can be considered the combined effect of the energy in the high frequency peak and in the low frequency peak. Hence, inspection of the filtered SWF1 can reveal the variation of energy transfer for each of these modes as a function of angle. The high frequency peak, SWF1(FILT) (Figure 51), trailed off slowly and the low frequency peak, SWF1(LFILT) (see Figure 52), dropped off very quickly reaching asymptotic behavior well inside of 45 degrees. Although no specific relations can be made, it is interesting to note that the SWF1(FILT) plot beared a resemblence to the Q_{11}, while the E_1 showed some of the same characteristics of the SWF1(LFILT) plot. Hence, the variation of energy transfer for the low frequency wave varied as the plane stress modulus, while the high frequency energy transfer varied as the plane strain modulus. The SWF2 parameter, which is an indication of the relative amount of energy transfer at high frequencies to that at low frequencies, showed a definite tendency toward peaking at between 15 and 20 degrees. Hence, the SWF2 parameter plots (Figure 54) showed that the high frequency mode had a relatively high energy content compared to the low frequency at an angle between 15 and 20 degrees. The SWF3/SWF4 parameter (Figure 55) showed the same general tendency as the SWF2, however, it is hard to make any spe-

cific comments on the reason for this, beyond the fact that both give an indication of high frequency to low frequency content.

Although no specific conclusions can be made, one explanation for results obtained on the 4-ply zero degree laminate could be that the low frequency peak is a pure extensional wave and hence has an energy flux which is controlled by a plane stress wave, while the high frequency peak may correspond to a surface wave, which is a plane strain wave (ie. end constraints dominate). As mentioned, this may not be the exact explanation for results, but one can not ignore the relationship between material property variations and the variation of SWF parameters, specifically, the fact that both tend to decrease rapidly at low angles and that SWF2 peaks around 15 degrees, which roughly corresponds to variations in material properties such as the peak in the coefficient of mutual influence. Thus, a more detailed understanding of these relations could lead to a method of actually measuring the direct mechanical effects of damage (as important as knowing that the damage is present) as a means of damage detection.

The results for the [90,0,0,90] showed the same frequency peaks to be present as were in the 4-ply zero laminate (Figure 60 and Figure 61). An important feature of the results is that the SWF1 parameters were approximately the same for both the 0 degree and the 90 degree orientation (Figure 64 and Figure 65). But, at the 0 degree orientation (ie. transverse to the surface ply) the SWF1(FILT) dropped off quickly as opposed to the more gradual type drop off for the 90 degree orientation where fibers on the surface ply were in the direction of wave propagation. Also, the SWF2 parameter (Figure 66) showed a peak at both 15 and 75 degrees, but the one at 75 degrees or at 15 degrees to the surface ply fibers showed a stronger peak. Thus, it seems that results are somewhat dependent on exact layup configuration and specifically on the orientation of the surface ply. But, the inner plies also do have an effect on the SWF parameters. In general, it may be surmised that results are caused by a complex interaction of surface and inner plies, related to the same complex interaction which controls the general mechanical behavior of the material and ensuing damage.

Results for the [45,0,0,45] plate show that again the SWF2 peaked when it was at 15 degrees to the fibers for the outer ply (Figure 70). Also, that the SWF1(FILT) dropped off in the same gradual manner as it did in the other plots in reference to the surface ply fiber direction (Figure 69). This again showed, as did the [90,0,0,90] specimen, that the method is sensitive to surface plies in a consistent manner for undamaged material.

Thus, results on the 4-ply laminates showed a definite trend for the SWF2 to peak when oriented at 15 degrees to fibers, especially the surface ply fibers. However, results showed that both inner and outer plies contributed to the signal. Also, it can be seen that SWF1 is a combination of SWF1(FILT) and SWF1(LFILT). Moreover, it seems that both the peaks in the general spectrum, which are represented by these various parameters, vary in a different manner with azimuthal angle and perhaps are dictated by different material properties. Additionally, stray jumps for SWF parameters as a function of azimuthal angle exist (see the relatively high SWF2 value at 30 degrees for the [90,0,0,90] laminate in Figure 66) and should be noted as limitations on the method, possibly resulting from a dependence of the signal on the material directly under the sending transducer. In summary, results appear to depend on a variety of factors which is good from a standpoint of gaining information on a number of material factors, but raises difficulties with respect to making direct interpretations.

Effect of Delamination on Results

The 4-ply zero degree laminate with the prefabricated delamination showed several interesting results. First, the signal was much more attenuated than the plate without delamination. Also, the SWF1 and SWF1(FILT) plots did not show the same low angle behavior that they did on the unflawed plate. In addition, the SWF2 and SWF3/SWF4 plots did not show the peak at 15 degrees to the fiber direction. Hence, results indicate that the SWF parameters are sensitive to damage.

Furthermore, with an increased understanding of the method this may eventually be able to be related to the effect which the delamination has on the mechanical state of the composite material.

Conclusions

Conclusions on the Specific System and its Applications

As mentioned, the nature of composite materials and their technological applications are such that nondestructive evaluation techniques are needed. Moreover, the complex damage development associated with composite materials can significantly alter mechanical properties and thus techniques which can be related to these properties are of significant importance. In this vein, an acousto-ultrasonic system has been developed to yield as much information as possible for assessing material state. This involves trying to get results which are independent of the system and obtaining information which can be used to understand the physical basis of the signal. Additionally, the acousto-ultrasonic system has been implemented on two particular material systems to develope a better understanding of the technique, its limitations and the physical basis of results. Hence, this chapter will overview the system and basic conclusions drawn from its implementation.

An acousto-ultrasonic system has been developed which can provide the following output:

1. Voltage/time plot

2. Calculate phase velocity

3. Gated signal

4. Calculate power spectrum from acousto-ultrasonic signal

5. Power spectrum amplitude/frequency plots

6. Power spectrum phase/frequency plots

7. Calculated SWF parameters (filtered and unfiltered)

8. SWF parameters saved on disk

9. Plots of SWF parameters as function of any other variable

10. Calculated transfer function

11. Calculated coherence function

12. Plots of amplitude/frequency from either transfer or coherence function

13. Plots of phase/frequency from either transfer or coherence function

14. SWF parameter (filtered or unfiltered) calculated from transfer or coherence function

Preliminary research on the Al/Gr resulted in the following observations:

1. SWF can be applied to various geometries

2. Acousto-ultrasonic signal variation for a particular region of a single tube were observed using both circumfertial and lengthwise SWF

3. Unconsolidated clad overlay seam which caused failure upon tension loading was detected

4. Signal variation between a tube which had been mechanically loaded and a virgin tube

5. SWF1 varied progressively in a given region along the length

Utilizing the analysis system, the following aspects regarding the fundamental nature of acousto-ultrasonic wave propagation in laminated graphite/epoxy were concluded:

1. Surface plies affect certain signal characteristics differently than inner plies.

2. The signal is however sensitive to inner plies.

3. More than one frequency peak may be present in the acousto-ultrasonic signal (two dominate ones, at 1.0 MHz and 3.4 Mhz, were present for the 4-ply specimens).

4. At least in some situations (ie. the present one) the same frequency peaks are present at all azimuthal angles for a given panel.

5. Different frequency peaks vary in energy content as a function of azimuthal angle in different ways.

6. The acousto-ultrasonic signal is sensitive to internal delaminations.

Several other aspects of the results were inconclusive, speculations have been developed including:

1. The low frequency (1 MHz for 4-ply panels) part of the signal corresponds to an extensional Lamb wave.

2. The low frequency (1 MHz) peak's energy content, for the [0,0,0,0] laminate, drops off from a maximum value at a zero degree azimuthal angle to an asymptotic value until 90 degrees in the same fashion as does E_x.

3. The high frequency wave (3.4 Mhz) may be a surface wave.

4. The high frequency wave reaches asymptotic behavior at 90 degrees in the same manner as does $\overline{Q}_{11}$.

It should be emphasized that the energy content for the [0,0,0,0] laminate, (ie. the filtered SWF1 values) for the 1 MHz and 3.4 MHz peak did not vary exactly as did E_x and $\overline{Q}_{11}$, but, that they approached an asymptotic value in the same manner. Hence, the only intended implication is that the same mechanical properties which cause E_x and $\overline{Q}_{11}$ to vary with azimuthal angle, may also cause the filtered SWF1 values to vary with angle (obviously affecting the unfiltered SWF values too). Moreover, more specific relations may exist and be related to similarities in the wave motion and type of load which E_x and $\overline{Q}_{11}$ represent. Future research efforts should be oriented toward explaining the way in which the energy flux vector varies, modeling the wave excitation problem, gaining more understanding to the effect of other ply orientations (how SWF parameter variation compares to material parameter variation), understanding the effects of damage and, in general, pursuing speculations.

Conclusions on System and Method

In general, results seem to confirm the potential of the method as a nondestructive technique for obtaining important information on the true mechanical state of composite materials. The basic point is that knowing the effects of damage is the most efficient means for assessing damage and

predicting the ability of the composite material to perform its intended purpose without failing. A really promising feature is the possibility of obtaining quantitative parameters which can be directly related to the mechanical state of the material. However, as mentioned this will require increased understanding of system components to obtain true parameters which are indepedent of the system. For instance, it would be quite useful to check variations of SWF2 or SWF1 as a function of azimuthal angle to find quantitative information on material properties at a point for different directions. In otherwords, the ability to measure anisotropy, a major facet of composite materials, could be extremely useful for monitoring damage and assessing the exact effect it will have on the material. Also, the method and system seem to be sensitive to different modes which most likely contain information on various material properties. Thus, the present research has encompassed creating a system which allows for the disection of the acousto-ultrasonic signal in hopes of obtaining very specific information of physical relevance. In other words research has been centered on unrooting the basic physics which govern the acousto-ultrasonic method and are responsible for its usefulness. However, as noted earlier the method can only be applied at a given point at one time and is also dependent upon micro-level variations in the material. Also, much work needs to be done on understanding the nature of the wave propagation, how exactly it is excited, the effects of other system components, such as transducers, and towards obtaining results which are only material dependent.

Appendix A. SWF Values for Mechanically Loaded and Virgin Tubes

Position on circumference of tube	Mechanically loaded tube	Virgin tube
0	1450	1697
1	1840	1960
2	1250	1452
3	1212	1746
4	1219	1964
5	2163	1900
6	1578	1890

The above chart compares the SWF1 unfiltered values for an al/gr tube which has been loaded in tension to a virgin tube. The values are simply an indication of relative power in the signal.

Appendix B. Comparison of Theoretical and Experimental Wave Velocities

	[0,0,0,0]		[90,0,0,90]		$[0,0,0,0]_s$	
	0°	90°	0°	90°	0°	90°
Experimental	370,000	100,000	260,000	260,000	370,000	110,000
Theory	410,000	110,000	290,000	290,000	410,000	110,000

The above chart compares the theoretical values of phase speed to wave speeds found using system software, where the theoretical value is for an extensional Lamb wave and the experimental value is obtained with system software. The angles are the azimuthal angles and the wave speeds are in inches per second.

Appendix C. Program Listing

```
1 REM %%%%%%%%%%%%%%% SUBROUTINE LISTING %%%%%%%%%%%%%%%%%%
2 REM $3000-WRITES DATA TO FILES $ 4000-READS DATA FROM FILES$
3 REM $5000-FFT SUBROUTINE$ 6000-MAX/MIN FINDER$ 7000-GRAPHING SUBROUTINE$
4 REM $9000-ZERO AVERAGES VOLT.$ 10000-GATING SECTION$
5 REM $11000-ADDS "0'S" TO DATA$ 13000-MAKES "N" A POWER OF 2$
6 REM $15000-SPECTRUM OUTPUT SECTION$
7 REM %%%%%%%%%%%%%%% CONTROL SECTION LISTING %%%%%%%%%%%%%%%
8 REM $(10-75)=MAIN MENU$ (75-680)=TRANSFER/COHERENCE FUNC. CONTROL$
9 REM $(680-750)=OUTPUT CONTROL$ (750-970)=TIME DOMAIN/FFT CONTROL$
10 KEY OFF
13 REM !!!!!!!CONTROL PORTION OF PROGRAM !!!!!!!!!!!!
15 MAE=0:REM {{{MAE IS USED IN GENERAL RESPONSE SECT}}}
19 REM ##########  MAIN MENU SECTION  ################
20 CLS
21 FNY=0:REM @@@@@@@@@FLAG TO SKIP FFT IF = TO 1@@@@@@@@@@@@@@
24 DIM T(4096):REM @@@@@@T(I) = ORIGINAL TIME DATA@@@@@@@@@@@@@
30 SCREEN 0,1
35 LOCATE 1,1
40 PRINT "ENTER THE NUMBER "
43 PRINT "CORRESPONDING TO "
45 PRINT "INPUT CHOICE      "
47 PRINT "1)TIME DOMAIN/FFT"
48 PRINT "ROUTINE"
50 PRINT "2)CALCULATE TRANSFER"
52 PRINT "OR COHERENCE FUNCTION"
53 PRINT "PARAMETERS FROM "
54 PRINT "STORED FFT FILES"
56 INPUT "ENTER NUMBER OF CHOICE";FTY
57 PRINT "3)POST FFT OUTPUT"
58 PRINT "FROM STORED FFT FILES"
62 IF FTY=1,THEN GOTO 750
63 IF FTY=2,THEN GOTO 73
64 PRINT "WHAT IS THE NAME OF":PRINT "THE ORIGNAL FFT DATA FILE"
65 INPUT "NAME";NAM$
66 IP=3:NAMF$="B:F"+MID$(NAM$,3)
67 GOSUB 4000:REM @@@@@@@@@@@@@@@READS FFT DATA @@@@@@@@@@@@@@@@@@
68 N=NB
69 IF FTY=3,THEN GOTO 680
70 REM ##########END OF MAIN MENU SECTION ############
73 CLS
75 REM !!!!!!!!!!!!! TRANSFER FUNCTION/COHERENCE FUNCTION CONTROL !!!!!!
76 PRINT "WHAT IS THE FILE NAME"
77 PRINT "OF THE INPUT (X) DATA"
80 PRINT "SET (IE. B:FDATA)?"
83 INPUT "NAME";NAM$
85 PRINT "WHAT IS THE FILE NAME"
87 PRINT "OF THE OUTPUT (Y) DATA"
90 PRINT "SET (IE. B:FDAT)?"
93 INPUT "NAME";NAMO$
95 REM !!!!!!!!!!!!READ IN INFOR. ON DATA FILES AND SET UP FOR CAL.!!!!!
110 REM !!!!!!!!!!!READ INPUT INFORMATION !!!!!!!!!!!!!!!!!!
112 IP=3:NAMF$="B:F"+MID$(NAM$,3)
```

```
113 PRINT NAMF$:GOSUB 4000:REM@@@@@@@@READS INPUT FILE@@@@@@@@@@@@@@@
114 DIM XR(NB),XI(NB),YI(NB),YR(NB),SXXR(NB),SXXI(NB),SXYR(NB),SXYI(NB)
115 DIM HR(NB),HI(NB),PA(NB),HA(NB)
116 FOR J=1 TO NB:XR(J)=AR(J):XI(J)=AI(J):PRINT XR(J),XI(J):NEXT J
117 ERASE AR,AI
119 REM !!!!!!!!!!! READ OUTPUT INFORMATION !!!!!!!!!!!!!!
121 IF NB<500 THEN DIM Y(505):GOTO 126
123 DIM Y(NB)
126 NAMF$="B:F"+MID$(NAMO$,3):IP=3
127 PRINT NAMF$
130 GOSUB 4000:REM@@@@@@@@@@READS OUTPUT FILE@@@@@@@@@@@@@@@@
135 FOR J=1 TO NB:YR(J)=AR(J):YI(J)=AI(J):PRINT YI(J),YR(J):NEXT J
138 ERASE AR,AI
198 REM ######### END OF DATA FILE READ SETUP SECTION ############
200 REM !!!!!!!!! CALCULATE TRANSFER FUNTION INFORMATION !!!!!!!!!!
205 FOR I=1 TO NB
207 REM !!!!!!!!!!!CALCULATE SPECTRAL DENSITIES!!!!!!!!!!!!!!!!!!!!
210 SXXR(I)=XR(I)*XR(I)+XI(I)*XI(I)
213 SXXI(I)=0
215 SXYR(I)=XR(I)*YR(I)+XI(I)*YI(I)
218 SXYI(I)=XR(I)*YI(I)-XI(I)*YR(I)
219 PRINT SXXR(I),SXXI(I),SXYR(I),SXYI(I)
220 REM SYXR(I)=SXYR(I)
223 REM SYXI(I)=XI(I)*YR(I)-XR(I)*YI(I)
225 REM SYYR(I)=YR(I)^2+YI(I)^2
227 REM SYYI(I)=0
230 HR(I)=SXYR(I)/SXXR(I)
233 HI(I)=SXYI(I)/SXXR(I)
235 HA(I)=(HR(I)^2+HI(I)^2)^.5:REM@@@@@@CALCULATE TRAN/COHER AMPLITUDE@@
238 PA(I)=ATN(-HI(I)/HR(I)):REM@@@@@CALCULATE TRAN/COHER PHASE ANGLE@@@
250 NEXT I
260 CLS:PRINT "WOULD YOU LIKE TO HAVE"
263 PRINT "OUTPUT ON THE RESPONSE"
265 PRINT "SPECTRUM"
267 INPUT "1)YES 2)NO";OS
270 IF OS=2,THEN GOTO 975
273 CLS:PRINT "WHAT IS THE FILE":PRINT "-NAME OF THE TIME"
275 PRINT "DATA (IF PROGRAM HAS":PRINT "BEEN GATED VIA SOFTWARE"
277 PRINT "ADD AN -N-)"
279 INPUT "FILENAME->(IE.B:DATAOOO)";NAMO$:REM GOTO 680
396 REM !!!!!!! CHOICE OF OUTPUT INFORMATION !!!!!!!!!!!!!!
398 CLS
400 PRINT "1)TRANSFER/COHERENCE FUNCTION PLOT"
402 PRINT "2)PHASE/FREQUENCY PLOT"
404 PRINT "3)MOM. FOR TRANSFER FUNC."
405 PRINT "4)PEAK PICK. AND BAND. INFO."
417 INPUT "# OF CHOICE";CH%
419 IF CH%=1 THEN GOTO 430
420 IF CH%=2,THEN GOTO 475
421 IF CH%=3,THEN GOTO 495
422 IF CH%=4,THEN GOTO 515
430 FOR I=1 TO NB
```

```
432 Y(I)=HA(I)
433 PRINT "y="Y(I)
434 NEXT I
435 XVAR$="FREQ":YVAR$="AMPL"
436 MNX=0:MXX=500/(TS*NB):HMX=.5*MXX
439 GOSUB 6000:REM @@@@@@@@@@@@@@@MAX/MIN OF DATA@@@@@@@@@@@@@@@@@@
443 MXY=MX:MNY=MN:HMY=(MXY+MNY)/2!
445 GOSUB 7000:REM @@@@@@@@@@ FFT @@@@@@@@@@@@@@@@@@@
447 GOTO 670:REM @@@SENDS CONTROL TO END OF SECTION @@@@@@@@@@@@@@@@@@@
475 FOR I=1 TO NB
477 AR(I)=HR(I):AI(I)=HI(I)
479 NEXT I
481 MAE=0:ROC=2:N=NB
485 GOSUB 15000:REM @@@@@@@@@@@@@GENERAL OUTPUT SUBROUTINE@@@@@@@@@@@@@@
490 GOTO 670:REM SENDS CONTROL TO END OF SECTION@@@@@@@@@@@@@@@@
495 FOR I=1 TO NB
497 AR(I)=HR(I):AI(I)=HI(I)
499 NEXT I
500 MAE=0:ROC=3:N=NB
505 GOSUB 15000:REM @@@@@@@@@@@@@@@GENERAL OUTPUT SUBROUTINE@@@@@@@@@@@@@@@
510 GOTO 670:REM @@@@@@@@@@SENDS CONTROL TO END OF SECTION@@@@@@@@@@@@
670 PRINT "WOULD YOU LIKE TO SEE MORE OUTPUT"
671 INPUT "1)YES 2)NO";MOR
672 IF MOR=2,THEN GOTO 678
673 GOTO 396:REM @@@@@@@@GOES TO OUTPUT CHOICES@@@@@@@@
678 ERASE XR,XI,YI,YR,SXXR,SXXI,SXYI,SXYR,HR,HI,PA:GOTO 970
680 REM $$$$RESPONSE OUTPUT ON Y(I)$$$$$$$$$$$$$$$
681 REM !!!SETUP PORTION !!!!!!!!!!!!
683 CLS:PRINT "WHAT OUTPUT WOULD YOU LIKE?"
685 PRINT "1)VOL/TIME GRAPH":PRINT "2)AMPL./FREQ."
687 PRINT "3)RESPONSE MOMENTS":PRINT "4)PHASE/FREQ."
689 INPUT "NO. OF CHOICE";ROC
700 GOSUB 15000:REM @@@@@@@@@GENERAL OUTPUT ROUTINE@@@@@@@@@@@@@@
705 CLS:PRINT "WOULD YOU LIKE MORE RESPONSE OUTPUT"
708 INPUT "1)YES 2)NO";MOP
710 IF MOP=1,THEN GOTO 775
720 GOTO 970:REM@@@@@CHOICE TO STOP@@@@@@@@@@@@@
735 REM $$$$$$$$$$$$$$END OF RESPONSE OUTPUT SECTION$$$$$$$$$$
750 REM !!!!!FFT CONTROL PORTION !!!!!!!!!!
751 REM !!!!!AND TIME DOMAIN CALCULATIONS !!!!!!!!!!!!!
752 CLS:LOCATE 1,1:MAE=0
755 PRINT "WHAT IS THE NAME OF"
757 PRINT "THE FILE YOU WANT"
758 PRINT "TO HAVE AN FFT OF?"
760 INPUT "TYPE-(DRIVE:FILENAME)";NAM$
761 CLS
765 IP=1:REM@@@IDENTIFIES TTYPE OF FILE SYSTEM FOR IN/OUT@@@@@@
770 GOSUB 4000:REM @@@@GOES TO DATA READ SUBROUTINE@@@@@@@@@@
771 N=GLL:REM@@@GATE LENGTH (# OF DATA POINTS)@@@@@@@@@@@@@@
775 CLS:LOCATE 1,1
777 PRINT "WOULD YOU LIKE TO"
779 PRINT "LOOK AT A VOLTAGE"
```

```
780 PRINT "VS. TIME PLOT?"
783 INPUT "1)YES 2)NO";VTP
784 GOSUB 11000:REM @@@@@ SUBROUTINE WHICH CAN ADD "0'S"@@@@@
785 IF VTP=2,THEN GOTO 788
786 TS=1/(SR*1000000!):REM@@@DEFINES TIME SAMPLE INTERVAL@@@@@@@@
787 MXX=500*TS:MNX=GST:HMX=.5*(MXX+MNX)
788 GOSUB 13000:REM@@@@@ MAKES "N" A POWER OF 2 @@@@@@@@@
789 IF NB<600,THEN DIM Y(600),A(600):GOTO 791
790 DIM Y(NB),A(NB)
791 FOR I=1 TO N:Y(I)=.5/128!*T(I):A(I)=Y(I):NEXT I
792 ERASE T:IF VTP=2,THEN GOTO 812
793 GOSUB 6000:REM @@@@@FINDS MAX/MIN OF Y(I) DATA@@@@@@
794 MXY=MX:MNY=MN:HMY=(MX+MN)/2
795 XVAR$="TIME":YVAR$="VOLTAGE"
796 PRINT "N=",N,"NB=",NB,"TS=",TS
797 INPUT "INPUT C TO CONTINUE";C$
798 CLS
800 GOSUB 7000:REM {{{GRAPH TIME OUTPUT}}}}}
812 CLS
815 PRINT "WOULD YOU LIKE TO"
817 PRINT "GATE THE SIGNAL?"
819 INPUT "1)YES 2)NO";GTS
821 IF GTS=2,THEN GOTO 840
822 CLS
823 PRINT "WOULD YOU LIKE TO"
825 PRINT "USE 1)TIME DEFINED"
827 PRINT "GATES 2)KEY CONTROLLED"
829 PRINT "GATE":INPUT "# OF CHOICE";GTY
830 IF GTY=1,THEN GOSUB 10000:REM @@@@TIME VALUE GATE INPUT@@@@@@
831 IF GTY=2,THEN GOTO 839
833 REM GOSUB 11000:REM @@@@@@@@@ADD "0'S"@@@@@@
836 REM !!!!!!!!!!!!PHASE VELOCITY SECTION!!!!!!!!!!!!!!!!!!
838 CLS
839 LOCATE 1,1
840 PRINT "WOULD YOU LIKE TO"
841 PRINT "CALCULATE THE PHASE VELOCITY"
842 INPUT "1)YES 2)NO";PVC
843 IF PVC=2, THEN GOTO 850
844 CLS:PRINT "GATE START=";GST
845 PRINT "WOULD YOU LIKE TO":PRINT "ENTER YOUR OWN TIME"
846 INPUT "1)YES 2)NO";OTP
847 IF OTP=2, THEN TT=GST:GOTO 849
848 INPUT "TIME FOR PHASE VELOCITY CALCULATION";TT
849 INPUT "DISTANCE BETWEEN X-DUCERS";DBT
850 VEL=DBT/(TT*.000001):PRINT "PHASE VEL.=",VEL:INPUT "INPUT C TO CONTINUE";CIC$
851 REM !!!!!!!!!!!!END OF PHASE VELOCITY CALCULATION!!!!!!!!!!!
852 CLS:LOCATE 1,1
853 PRINT "WOULD YOU LIKE TO HAVE":PRINT "YOUR TIME DATA AVERAGED TO 0?"
854 INPUT "1)YES 2)NO";TAR
856 IF TAR=2,THEN GOTO 867
859 REM!!!!!!!AVERAGE DATA SECTION!!!!!!!!!!!!!!!!!!!!!!
863 GOSUB 9000:REM @@@@@ "0" AVERAGE DATA@@@@@@@@@@@@@
```

```
864 PRINT "WOULD YOU LIKE TO":PRINT "PERFORM AN FFT ON":PRINT "TIME DATA"
865 INPUT "1)YES 2)NO";FNY
866 IF FNY=2,THEN GOTO 903
867 GOSUB 5000:REM!!!!FFT ON DATA !!!!!!!!
875 CLS:LOCATE 1,1
879 PRINT "WOULD YOU LIKE TO":PRINT "STORE THE FFT OUTPUT"
881 PRINT "(F+FILENAME)"
884 INPUT "1)YES 2)NO";SFT
886 IF SFT=2,THEN GOTO 900
887 IP=3:NAMF$="B:F"+MID$(NAM$,3)
889 PRINT NAMF$
893 GOSUB 3000:REM @@@@@@@STORES FFT DATA IN USING DATA WRITE SUB.@@@@@
900 CLS:LOCATE 1,1
902 REM!!!!!!!!!STORE NEW TIME DATA SECTION!!!!!!!!!!!!!!!!!!!!!!!!!
903 PRINT "WOULD YOU LIKE TO":PRINT "STORE THE NEW TIME DATA?"
906 PRINT "(IE. FILENAME+N)"
909 INPUT "1)YES 2)NO";NF
912 IF NF=2,THEN GOTO 930
913 IP=1:NAMN$="B:N"+MID$(NAM$,3)
920 GOSUB 3000:REM@@@@@@@@STORES NEW TIME DATA USING DATA WRITE SUB.@@@@
923 REM!!!!!!!!!!END OF THE STORE NEW DATA SECTION!!!!!!!!!!
925 IF FNY=2,THEN GOTO 970
930 PRINT "WOULD YOU LIKE TO"
931 PRINT "SEE SOME RESPONSE"
932 PRINT "DATA OUTPUT?"
933 INPUT "1)YES 2)NO";OP
934 IF OP=1,THEN MAE=1:GOTO 680
970 CLS:PRINT "WOULD YOU LIKE TO STOP"
972 INPUT "1)YES 2)NO";STOE
973 ERASE A:ERASE AR:ERASE AI
974 IF STOE=2,THEN GOTO 15
980 STOP
985 END
988 REM !!!!!!!!!!!!END!!!!!!!!!!!!!!!!!!!!!!!!!!!!!!!!!!!!
3000 REM @@@@@ DATA WRITE SUBROUTINE @@@@@@@@@@@@@@@@@
3001 REM!!!!INPUT NB-NO. OF POINTS,TS-SAMPLING INTERVAL!!!!!!
3002 REM!!IP=3!!!AR(J),AI(J)-FOURIER COEFFICIENTS,NAMF$-DATA FILE!!!!!
3003 REM!!IP=2!!!Y(J)-VOLTAGE READING ARRAY,NAMN$-DATA FILE!!!
3004 REM ##IP%-CHOICE OF DATA SET TYPE ########
3006 REM *** IP=1 NEW TIME DATA 0-255 RES. **********
3008 REM *** IP=2  **********
3010 REM *** IP=3 FFT DATA      **********
3011 IF IP=1 THEN GOTO 3400
3013 IF IP=3 GOTO 3300
3300 REM +++++WRITE FFT DTA +++++++
3305 OPEN NAMF$ FOR OUTPUT AS #1
3308 R=NB:I=TS
3310 WRITE#1, R, I
3315 FOR J=1 TO NB
3320 R=AR(J):I=AI(J)
3325 WRITE#1, R, I
3330 NEXT J
```

```
3335 CLOSE#1
3395 GOTO 3990
3400 REM+++++++WRITE NEW TIME DATA+++++++++++++
3405 OPEN NAMN$ FOR OUTPUT AS #1
3410 R=TS
3415 WRITE#1, R
3420 R=NB
3425 WRITE#1, R
3430 FOR J=1 TO NB
3435 R=Y(J)
3440 WRITE#1, R
3445 NEXT J
3450 CLOSE#1
3470 GOTO 3990
3990 RETURN
3995 REM************************************************************
4000 REM @@@@@ DATA READ SUBROUTINE @@@@@@@@@@@@
4001 REM!!!!!!INPUT NAM$-FILE NAME FOR ORIGINAL VOLTAGE/TIME DATA!!!!!!
4002 REM!!!!!!NAMF$-FILE NAME FOR FFT DATA!!!!!!!!
4003 REM!!!!!!NAMN$-FILE NAME FOR NEW VOLTAGE/TIME DATA!!!!
4004 REM ##IP%-CHOICE OF DATA SET TYPE #####
4006 REM **** IP=1 ORIGINAL TIME TYPE DATA ***********
4007 REM!!!!OUT=GLL,SR,GST,T(J)
4008 REM **** IP=2 NEW TIME DATA ****************
4009 REM!!!!OUT=NB,TS,AR(J),AI(J)
4010 REM **** IP=3 FFT TYPE DATA ************
4011 REM!!!!OUT=TS,NB,Y(J)
4012 IF IP=2;THEN GOTO 4400
4015 IF IP=3 THEN GOTO 4300
4050 REM  %%%%%% ORIGINAL TIME DATA  %%%%IP=1%%%%%%%%
4055 DIM B$(17):'-----B$ IS HEADING INFORMATION
4060 OPEN NAM$ FOR INPUT AS #1
4065 FOR I=1 TO 17:INPUT#1,B$(I):NEXT
4070 FOR J=1 TO 4096
4075 IF EOF(1) THEN 4090
4080 INPUT#1,T(J)
4085 NEXT
4090 GLL=J-1:' GLL IS THE NUMBER OF POINTS OR GATE LENGTH
4095 B$(3)=MID$(B$(3),19,8):SR=VAL(B$(3)):'SR ---IS THE SAMPLING RATE
4096 B$(2)=MID$(B$(2),40,8):GST=VAL(B$(2)):'GST IS GATE START
4098 CLOSE #1
4100 'RETURN
4105 ERASE B$
4120 GOTO 4995
4300 REM %%% READ FFT DAT %%%%%IP=3%%%%
4310 OPEN NAMF$ FOR INPUT AS #1
4315 INPUT#1, R, I
4320 NB=R:TS=I
4323 DIM AR(NB),AI(NB)
4325 FOR J=1 TO NB
4330 INPUT#1, R, I
4335 AR(J)=R:AI(J)=I
```

```
4340 NEXT J
4350 CLOSE#1
4393 GOTO 4995
4400 REM+++++++READ NEW TIME DATA+++++++++++++++
4405 OPEN NAMN$ FOR INPUT AS #1
4410 TS=R
4415 INPUT#1, R
4417 TS=R
4420 NB=R
4425 INPUT#1, R
4427 NB=R
4430 FOR J=1 TO NB
4435 Y(J)=R
4440 INPUT#1, R
4445 NEXT J
4450 CLOSE#1
4470 GOTO 4995
4995 RETURN
4997 REM ************************************************************
5000 REM @@@@@@  FFT SUBROUTINE   @@@@@@@@@@
5002 REM *** VAR. INPUT [A(NB),NB,N] ******
5003 REM *** VAR. OUT [AR(NB),AI(NB)] *****
5005 REM %%% "DIVIDE ALL ELEMENTS BY B" %%%%
5007 DIM AR(NB+5),AI(NB+5)
5008 HI=NB
5010 FOR J=1 TO NB
5020 A(J)=A(J)/NB
5030 NEXT J
5040 REM %%% "REORDER SEQUENCE" %%%%%%
5050 NBD=NB/2!
5060 NBM=NB-1
5070 J=1
5080 FOR L=1 TO NBM
5090 IF L>=J THEN GOTO 5130
5100 T=A(J)
5110 A(J)=A(L)
5120 A(L)=T
5130 K=NBD
5140 IF K>=J THEN GOTO 5180
5150 J=J-K
5160 K=K/2
5170 GOTO 5140
5180 J=J+K
5190 NEXT L
5191 FOR Z=1 TO 18
5192 HI=HI/2
5195 IF HI=1,THEN GOTO 5198
5196 NEXT Z
5198 NN=Z
5200 REM %%%"CALCULATE FFT" %%%%
5202 FOR Q=1 TO NB
5204 AR(Q)=A(Q):AI(Q)=0!
```

```
5206 NEXT Q
5210 PI=3.14159
5220 FOR M=1 TO NN
5225 REM PRINT "M=",M
5230 UR=1
5240 UI=0!
5250 ME=2^M
5255 K=ME/2
5260 WR=COS(PI/K)
5270 WI=-SIN(PI/K)
5280 FOR J=1 TO K
5290 FOR L=J TO NB STEP ME
5300 LPK=L+K
5310 TR=AR(LPK)*UR-AI(LPK)*UI
5320 TI=AR(LPK)*UI+UR*AI(LPK)
5325 REM PRINT L,LPK
5330 AR(LPK)=AR(L)-TR
5340 AI(LPK)=AI(L)-TI
5350 AR(L)=AR(L)+TR
5360 AI(L)=TI+AI(L)
5370 NEXT L
5372 PR=UR
5380 UR=UR*WR-UI*WI
5390 UI=PR*WI+WR*UI
5400 NEXT J
5410 NEXT M
5420 RETURN
5490 REM ************************************************************
6000 REM @@@@@@@@MAX/MIN PORTION @@@@@@@@@@@@@@@@@@@@@@@@@@@@@@
6005 REM @@@@ INPUT #### Y(J)-ARRAY TO FIND MAX/MIN OF ### @@@@
6007 REM @@@@ OUTPUT ### MN-MIN VAL. MAX-MAX VAL. OF ARRAY ### @@@@
6010 FOR J=1 TO NB
6015 IF J=1,THEN MN=Y(J):MX=Y(J):GOTO 6040
6020 IF Y(J)<MN,THEN MN=Y(J)
6030 IF Y(J)>MX,THEN MX=Y(J)
6040 NEXT J
6100 PRINT "MAX=",MX,"MIN=",MN
6105 PRINT "WOULD YOU LIKE TO INPUT YOUR OWN MAX AND MIN"
6108 REM!!!!!!USER CAN SET OWN MAX/MIN TO BE USED BY PLOTTING ROUTINE!!!!
6110 INPUT "1)YES 2)NO";MQ
6115 IF MQ=2,THEN GOTO 6490
6120 INPUT "MAX";MX
6130 INPUT "MIN";MN
6490 RETURN
6495 REM ************************************************************
7000 REM ***********GRAPHING SUBROUTINE ***********************
7005 REM @@@@@@ INPUT ## NP,Y(NP) ## @@@@@@@@@
7006 REM@@@@@@@@Y(I)=ARRAY FOR Y-AXIS@@@@@@@@@@@@@@@@@@
7007 REM@@@@@XVAR$=NAME OF X-VARIABLE@@@@@@@@@@
7008 REM@@@@@YVAR$=NAME OF Y-VARIABLE@@@@@@@@@@
7010 CLS:PRINT "INPUT MULT. FACTOR"
7013 INPUT "# OF FACTOR";NX:REM@@CONTRACTS AND EXPANDS THE X-AXIS@@@@@
```

```
7030 CLS:SCREEN 2
7040 LVX=LEN(XVAR$):LVY=LEN(YVAR$)
7050 RR=(25-LVY)/2:CC=(80-LVX)/2
7060 LINE (100,25)-(100,175):LINE-(600,175)
7070 LINE (95,100)-(105,100):LINE (95,25)-(105,25)
7080 LINE (350,170)-(350,180):LINE (600,170)-(600,180)
7090 LINL=16+LVX+LVY:HDH=(80-LINL)/2
7100 LOCATE 1,HDH
7120 PRINT "PLOT OF ";XVAR$;" VERSUS ";YVAR$
7150 LOCATE 21,CC:PRINT XVAR$
7160 FOR II=1 TO LVY STEP 1
7170 YV$=MID$(YVAR$,II,1)
7175 LOCATE RR,2
7180 PRINT YV$
7190 RR=RR+1
7200 NEXT II
7210 LOCATE 4,4
7220 PRINT USING "#.##^^^^";MXY
7230 LOCATE 13,4
7240 PRINT USING "#.##^^^^";HMY
7250 LOCATE 22,4
7260 PRINT USING "#.##^^^^";MNY
7270 LOCATE 23,40
7280 PRINT USING "#.##^^^^";HMX/NX
7282 LOCATE 23,13
7284 PRINT USING "#.##^^^^";MNX
7290 LOCATE 23,71
7300 PRINT USING "#.##^^^^";MXX/NX
7305 OI=100:OJ=175!-150!/(MXY-MNY)*(Y(1)-MNY)
7310 FOR I=101 TO 600 STEP 1
7320 J=175!-150!/(MXY-MNY)*(Y((I-98)/NX+1)-MNY)
7324 LINE (OI,OJ)-(I,J)
7325 REM PSET(I,J)
7327 OI=I:OJ=J
7330 NEXT I
7390 LOCATE 2,5
7400 INPUT "ENTER C TO CONTINUE";CC$
7420 ERASE Y
7490 RETURN
7495 REM ************************************************************
9000 REM ***THIS ROUTINE AVERAGES DATA ******
9002 REM @@@VAR.INPUT ## N-NO. OF DATA PTS.,Y(I)-AMPL./TIME ARRAY##@@@
9004 REM @@@VAR. OUT ###Y(N)-AVERAGED TIME DATA ###@@@@@
9005 US=0
9010 FOR I=1 TO N
9020 US=US+Y(I)
9030 NEXT I
9040 UA=US/N
9050 FOR J=1 TO N
9060 Y(J)=Y(J)-UA
9070 NEXT J
9500 RETURN
```

```
9505 REM ************************************************************
10000 REM @@@@@@@@TIME INPUT GATE SECTION @@@@@@@@@@@@@@@@@@@
10010 REM!!!!!!!!!THIS SUBROUTINE ZEROES ALL ARRAY VALUES NOT INSIDE!!!!!!!!!!
10020 REM!!!!!!!!!!!!!!!!!!!THE USER DEFINED GATE!!!!!!!!!!!!!!!!!!!!!!!!!
10021 REM!!!!NGST-DEFINES THE BEGINNING OF THE GATE!!!!!!
10022 REM!!!!NGEND-DEFINES THE END OF THE GATE!!!!!!!!!
10023 REM!!!!INITIALLY VALUES ARE INPUT IN SECONDS AND THEN CONVERTED!!!
10024 REM!!TO POINT NUMBER BY DEVIDING BY SAMPLE INTERVAL!!!!!
10095 CLS
10100 PRINT "WHAT GATE TIME GREATER"
10105 PRINT "THAN ",GST," DO YOU WANT?"
10107 PRINT "(IN SECONDS)"
10110 INPUT "GATE START=";NGST
10115 PRINT "WHAT END OF GATE TIME"
10117 GEND=N*TS
10120 PRINT "LESS THAN ",GEND," DO YOU"
10125 PRINT "WANT?"
10130 INPUT "GATE END=";NGEND
10132 NGST=NGST/TS:NGEND=NGEND/TS
10135 FOR I=1 TO NGST
10140 A(I)=0:Y(I)=0:REM@@@@@ZEROES ALL VALUES BEFORE GATE STARTS@@@@@@
10145 NEXT I
10150 FOR I=NGEND TO N
10155 A(I)=0:Y(I)=0:REM@@@ZEROES ALL VALUES PAST GATE END@@@@@@@@@@
10160 NEXT I
10990 RETURN
11000 REM **** ADD ZEROES TO T(J) ARRAY TO INCREASED N VALUE AS INPUT**
11001 PRINT "WOULD YOU LIKE TO INCREASE"
11002 PRINT "THE N VALUE (IE. THE NUMBER"
11003 PRINT "OF VALUES FOR FFT)."
11004 INPUT "1)YES 2)NO";NVCH:CLS:IF NVCH=2,THEN GOTO 11500
11005 PRINT "WHAT N VALUE DO YOU WANT"
11006 PRINT "THE NEW N VALUE MUST BE"
11007 PRINT "GREATER THAN THE OLD VALUE"
11008 PRINT "OLD N =";N
11010 INPUT "#      ";NPN
11015 NN=N+1
11020 FOR J=NN TO NPN
11025 T(J)=0:REM@@@@ADDS ZERO VALUED ARRAY MEMBERS@@@@@@@@@
11030 NEXT J
11035 N=NPN
11500 RETURN
13000 REM @@@@@ THIS ROUTINE TAKES DATA SETS AND @@@@@@@@@@@@
13002 REM @@@@@ AND MAKES THEM A POWER OF TWO @@@@@@@@@@
13004 REM@@@@@@@ALL EXTRA ARRAY VALUES ARE SET EQUAL TO ZERO@@@@@@
13008 IF N<=4096,THEN NB=4096
13010 IF N<=2048,THEN NB=2048
13015 IF N<=1024,THEN NB=1024
13020 IF N<=512,THEN NB=512
13025 IF N<=256,THEN NB=256
13030 IF N<=128,THEN NB=128
13035 IF N<=64,THEN NB=64
```

```
13040 FOR J=N TO NB
13045 T(J)=0:REM@@@@@@@EXTRA ARRAY VALUES SET EQUAL TO ZERO@@@@@@@@
13050 NEXT J
13090 N=NB:RETURN
13099 REM ************************************************************
15000 REM @@@@@@@@GENERAL RESPONSE SETUP @@@@@@@@@@@@
15001 IF MAE=0,THEN GOTO 15010
15002 IF NB<500,THEN DIM AMP(505):GOTO 15005
15003 DIM AMP(NB+1)
15005 GOTO 15099
15010 NAMF$="B:F"+MID$(NAM$,3):IP=3
15015 GOSUB 4000
15099 TTOL=TS*N
15100 FOR I=1 TO NB
15105 AMP(I)=TTOL*(AR(I)^2+AI(I)^2)^.5
15115 NEXT I
15118 IF ROC=2,THEN GOTO 15200
15119 IF ROC=4,THEN GOTO 15400
15120 IF ROC=3,THEN GOTO 15300
15200 REM !!!AMPLITUDE VS. FREQ.!!!!!!!
15203 DIM Y(NB)
15205 MNX=0:MXX=500/TTOL:HMX=.5*MXX
15210 FOR I=1 TO NB
15215 Y(I)=AMP(I)
15220 NEXT I
15225 GOSUB 6000:REM@@@@@@@@@FINDS MAX/MIN VALUES@@@@@@@@@@
15230 MXY=MX:MNY=MN:HMY=(MX+MN)/2!
15235 XVAR$="FREQ":YVAR$="AMPL"
15240 GOSUB 7000:REM@@@@PLOTS AMPLITUDE VS. FREQUENCY@@@@@@@@@
15295 GOTO 15990
15300 REM!!!!!!MOMENT CALCULATIONS !!!!!!!!!!
15305 NM=(NB-1)/2:REM@@@SETS CALCULATION OF MOMENTS UPPER VALUE@@@
15310 FT=1!/(TS*N):REM@@@@FREQUENCY DIFFERENTIAL@@@@@@@@@
15311 PRINT "WOULD YOU LIKE TO FILTER THE SIGNAL?"
15312 INPUT "1=YES 2=NO";FQ
15313 IF FQ=2,THEN NL=1:GOTO 15319
15314 INPUT "LOWER FREQUENCY (MHz)";LF
15315 INPUT "UPPER FREQUENCY (MHz)";UF
15316 NL=LF*1000000!/FT+1:NM=UF*1000000!/FT+1
15317 PRINT "NL=",NL,"NM=",NM:REM@@@SETS LOWER AND UPPER VALUE FOR FILTER@@
15318 PRINT "FT=",FT,"TS=",TS,"NM=",NM
15319 AM0=0!:AM1=0!:AM2=0!:AM4=0!
15320 FOR I=NL TO NM
15321 REM PRINT "I=",I
15325 AP=(AMP(I+1)+AMP(I))*FT/2!
15328 REM PRINT "AP=",AP
15330 AM0=AM0+AP
15332 REM PRINT "AM0=",AM0
15335 WW=(I-2)*FT+FT/2!
15338 REM PRINT "WW=",WW
15340 AM1=AM1+AP*WW
15342 REM PRINT "AM1=",AM1
```

```
15345 AM2=AM2+AP*WW^2
15348 REM PRINT "AM2=",AM2
15350 AM4=AM4+AP*WW^4
15351 REM PRINT "AM4=",AM4
15352 NEXT I
15355 A=AM0^.5
15360 B=AM1/AM0
15361 IF FQ=1 THEN GOTO 15375
15365 C=(AM2/AM0)^.5
15370 D=(AM4/AM2)^.5
15371 E=C/D
15375 PRINT "SQRT OF M0    =",A
15376 PRINT "M1 OVER M0    =",B
15377 PRINT "SQRT OF M2/M0=",C
15378 PRINT "SQRT OF M4/M2=",D
15379 PRINT "SWF3/SWF4     =",E
15380 PRINT "WOULD YOU LIKE TO STORE MOMENT CALCULATIONS ON DISK?"
15381 INPUT "1=YES 2=NO";NYM
15382 IF NYM=2 THEN GOTO 15395
15383 INPUT "WHAT WOULD YOU LIKE TO NAME THE FILE";MNM$
15384 NN$="B:"+MNM$+"M.DAT":OPEN NN$ AS #2 LEN=16
15385 FIELD #2, 4 AS AM$, 4 AS BM$, 4 AS CM$, 4 AS DM$
15386 RSET AM$=MKS$(A):RSET BM$=MKS$(B):RSET CM$=MKS$(C):RSET DM$=MKS$(E)
15387 PUT #2,1
15390 CLOSE #2
15395 INPUT "ENTER -C- TO CONTINUE";C$
15398 GOTO 15990
15400 REM !!!!!PHASE VS FREQ!!!!!!!!!!!!
15405 DIM Y(NB)
15410 FOR I=1 TO NB
15415 Y(I)=ATN(AI(I)/AR(I))
15420 NEXT I
15425 GOSUB 6000:REM@@@@@@@FINDS MAX/MIN@@@@@@@@@@@@@@
15430 MXY=MX:MNY=MN:HMY=(MX+MN)/2
15435 XVAR$="FREQ":YVAR$="PHASE"
15440 GOSUB 7000:REM@@@@@PLOTS PHASE ANGLE VS. FREQUENCY@@@@@@@@@@
15495 GOTO 15990
15990 REM MAE=0
15992 ERASE AMP
15995 RETURN
```

References

(1) R. M. Jones, *Mechanics of Composite Materials*, Scripta Book Company, Washington, D.C. 1975.

(2) T. K. O'Brien, "Stiffness Change as a Nondestructive Damage Measurement," in W. W. Stinchcomb Ed., *Mechanics of Nondestructive Testing,* Plenum Press, New York, (1980) pp. 101-122.

(3) K. L. Reifsnider, E. G. Henneke, and W. W. Stinchcomb, "The Mechanics of Vibrothermography," in W. W. Stinchcomb Ed., *Mechanics of Nondestructive Testing,* Plenum Press, New York, (1980) pp. 249-276.

(4) R. C. Stiffler and E. G. Henneke, II, "The Application of Low Frequency Acoustic Waves for Determining the Extensional and Flexural Stiffnesses in Composite Plates," (1985).

(5) Govada A. K., J. C. Duke Jr., E. G. Henneke II, and W.W. Stinchcomb, "A Study of the Stress Wave Factor Technique for the Characterization of Composite Materials," NASA Contracter Report 174870, 1985.

(6) H. Karaqulle, J. H. Williams, Jr. and S. S. Lee, "Application of Homomorphic Signal Processing to Stress Wave Factor Analysis," (1984).

(7) R. Talreja, A. Govada, and E. G. Henneke, II, "Quantitative Assessment of Damage Growth in Graphite Epoxy Laminates by Acousto-Ultrasonic Measurements" *Review of Progress in Quantitative Nondestructive Evaluation, Vol. 3B,* Eds. D. O. Thompson and D. E. Chementi, Plenum Press, New York, 1984, pp. 1099-1106.

(8) C. B. Scruby, R. J. Dewhurst, D. A. Hutchins and S. B. Palmer, "Laser Generation of Ultrasound in Metals" *Research Techniques in Nondestructive Testing, Vol. V,* Ed. R. S. Sharpe, Academic Press, London, 1982, pp. 281-327.

(9) C. J. Rebello and J. C. Duke, Jr., "Factors Influencing the Ultrasonic Stress Wave Factor Evaluation of Composite Material Structures," *Journal of Composites Technology and Research,*Vol. 8,No. 1, 1986, pp. 18-23.

(10) A. S. Sarrafzadeh-Khoee, J. C. Duke, Jr., M. T. Kiernan and E. G. Henneke, II, "A Study of the Stress Wave Factor Technique for Nondestructive Evaluation of Composite Materials," CCMS-86-02, 1986.

(11) PC-DAS User's Manual, General Research Corporation, McLean, Va., (1985).

(12) N. N. Hsu and F. R. Breckenridge, "Characterization and Calibration of Acoustic Emmision Sensors," *Materials Evaluation* 39 no. 1 (1979), pp. 60-68.

(13) S. L. McBryde and T. S. Hutchison, "Helium Gas Jet Spectral Calibration of Acoustic Emission Transducers and Systems," *Canadian Journal of Physics* 54 no. 17 (1976): pp. 1824-1830.

(14) D. E. Newland, *Random Vibration and Spectrum Analysis*, Longman Inc., New York, 1983.

(15) A. Vary and H. E. Kautz, "Transfer Function Concept for Ultrasonic Characterization of Material Microstructures," Reprint from CP-2383, a conference on *Analytical Ultrasonics in Materials Research and Testing,* (1984).

(16) W. W. Stinchcomb, K. L. Reifsnider, P. Yeung and J. Masters, "Effect of Ply Constraint on Fatigue Damage Development in Composite Material Laminates," *Fatigue in Composite Materials, ASTM STP 723,* (1981),pp. 64-84.

(17) E. G. Henneke II, J. C. Duke, Jr., W. W. Stinchcomb, A. Govada and A. Lemascon, "A Study of the Stress Wave Factor Technique for the Characteriztion of Composite Materials," NASA Contractor Report 3670, (1983).

(18) A. Vary and R. F. Lark, "Correlation of Fiber Composite Strength with the Ultrasonic Stress Wave Factor," NASA TM-78846, (1978).

(19) A. Vary, "Quantitative Ultrasonic Evaluation of Mechanical Properties of Engineering Materials," NASA TM-78905, (1978).

(20) Y. Pao and R. K. Kaul, "Waves and Vibrations in Isotropic and Anisotropic Plates," in G. Herrmann, ed., *R. D. Mindlin and Applied Mechanics*, Pergamon Press Inc., New York,1974, pp. 149-196.

(21) Instruction Manual Ultrasonic Analyzer Model 5052UA, Panametrics, Waltham, Mass.

The vita has been removed from the scanned document